ANALYSIS OF ASYNCHRONOUS FREQUENCY-HOP SPREAD-SPECTRUM MULTIPLE-ACCESS NETWORKS

by

Kyung-whoon Cheun

A dissertation submitted in partial fulfillment
of the requirements for the degree of
Doctor of Philosophy
(Electrical Engineering: Systems)
in The University of Michigan
1989

Doctoral Committee:

Associate Professor W.E. Stark, Chairperson
Professor D.L. Neuhoff
Professor D. Teichroew
Assistant Professor K.A. Winick

To

My Father, My Mother

My parents in law

My Wife

and to

Sungjin

ACKNOWLEDGEMENTS

I would like to express my deepest gratitude to Professor Stark, my thesis advisor. He provided me with enlightening discussions and comments on which this thesis and my knowledge on communications theory is based.

I would also like to thank my doctoral committee members, Professor Neuhoff, Professor Winick and Professor Teichroew for their invaluable comments on the thesis.

Most of all, I owe my utmost thanks to my parents who gave up many things in their lives so as to make mine a better one. And to my wife for overcoming the hardship of being a wife of an overstressed graduate student.

I would like to thank the following institutions for providing me with financial support throughout my four years of graduate study. The Pohang Steel Company of Korea, without whom my studies here may never have got off the ground, and The National Science Foundation (grant ECS 8451266), and the Hughes Aircraft Company.

TABLE OF CONTENTS

LIST OF FIGURES

Figure

LIST OF TABLES

Table

CHAPTER I

INTRODUCTION

Spread-Spectrum (SS) communications is a modulation technique where the modulated signal has much larger bandwidth than the minimum bandwidth needed to transmit the data. For example, the modulated signal could have bandwidth 100 khz when the information data rate is 100 bits/sec. The main advantages of using spread-spectrum systems over conventional *narrowband* systems are threefold [Vit 79b].

1. Ability to suppress interference.

2. Low Probability of Intercept (LPI).

3. Ability to make accurate ranging or time delay measurements.

The most important of these three is probably the interference suppression (rejection) capability where the interference source could be any combination of the following [Vit 79b].

1. Interference due to hostile opponents.

2. Interference due to other users (friendly) sharing the same spectrum in a network environment.

3. Interference due to multipath (self-jamming).

In this thesis we are interested in the capability of an SS communications system in rejecting interference of type (2).

The spreading of the bandwidth in an SS system is commonly done by one of the following two methods. The first, referred to as the Direct-Sequence Spread-Spectrum (DSSS) system [Sim 85], spreads the bandwidth by multiplying the information signal (with values $+1$ or -1) by a pseudorandom spreading sequence (with values $+1$ or -1) which has bandwidth much larger than that of the information signal. Since the spectrum of a product of two uncorrelated signals is given by the convolution of the spectrums of each signal, the resulting bandwidth will be approximately that of the spreading signal. The second technique for spreading the bandwidth of the transmitted signal is called the Frequency-Hop Spread-Spectrum (FHSS) technique and is adopted in this thesis as the spreading method. With today's technology, this method offers a larger bandwidth than the DSSS technique for a given information rate. FHSS communications systems will be described in detail in the next paragraph and in Chapter 2.

Spread-spectrum communications systems are almost always used with some kind of error correcting code. The gain one may obtain by employing error correcting codes in SS systems with interference is usually much larger than that in standard narrowband communications systems.

The discussion in this chapter contains standard terminology in the FHSS Multiple-Access (FHSS-MA) field that will be precisely defined in Chapter 2 where a detailed description of the channel, and user (transmitter-receiver pair) models used for the analyses are given. Mathematical descriptions of the problems will be given in the corresponding chapters. It is suggested that readers not familiar with FHSS-MA

networks read Chapter 2 first.

In a standard Frequency-Hop Spread-Spectrum (FHSS) communications system, a given bandwidth W_{ss} is divided into q equal width sub-bands called *frequency slots* or simply slots. For every n channel symbols to be transmitted, the transmitter chooses one of the q slots for transmission in some pseudorandom fashion. Hence the frequency used by the system *hops* among the q available slots as a function of time and hence the name frequency hopping. FHSS communications systems were originally developed because of their ability to provide reliable communications in the presence of hostile jammers and in fading/multipath environment and also because of their Low Probability of Intercept (LPI) property [Sch 77] [Sim 85].

Recently, the application of FHSS systems to Multiple-Access (MA) networks, where many users share a single physical channel without central coordination, has been the focus of interest of many researchers [Pur 81] [Ger 82] [Pur 87b] [Heg 88] [Kim 89]. This method of sharing a given physical channel among many users is called Frequency-Hop Spread-Spectrum Multiple-Access (FHSS-MA) communications. A FHSS-MA network [Pur 87b] is formed simply when many users employing FHSS modulation over the same spectrum coexist. Though FHSS-MA systems can be just as bandwidth efficient as traditional narrowband ALOHA MA system in the sense that, for a given bandwidth it can achieve the same throughput [Kim 87], the main reason for applying FHSS techniques to MA networks is to take advantage of the interference and fading/multipath rejection capabilities of the FHSS system. Hence the major application of FHSS-MA networks are probably in constructing survivable networks for military communications. Other advantages of Spread-Spectrum Multiple-Access (SSMA) networks in general are the capture effect [Pur 87b] which refers to the ability of a receiver to lock on to one transmission when there are sev-

eral overlapping transmissions addressed to it and the fact that SSMA networks offer greater flexibility than traditional multiple-access systems. For example, the number of users sharing the network can be increased very easily and the the performance of the network degrades gracefully as the number of users in the network is increased. Also, unlike traditional techniques (e.g. Time division multiple-access, Frequency division multiple-access) a SSMA network can operate without network timing or a system controller.

The objective of this thesis is to provide a more accurate analysis of the modulation (demodulation) and coding aspects of FHSS-MA networks than are presently available, especially for asynchronous FHSS-MA (AFHSS-MA) networks where the hopping patterns of different users are not synchronized. We also consider different schemes that enhance the performance of an AFHSS-MA networks and analyze them.

In this chapter we will cite some of the previous work on Frequency-Hop Spread-Spectrum Multiple-Access (FHSS-MA) networks and give a brief summary of the problems we consider. We will comment on the significance of these problems and related work done by other researchers. A summary of the results is also given in this chapter.

1.1 Previous Work

In this section we will briefly cite some of the previous key results in FHSS-MA networks theory. In [Ger 82], Geraniotis and Pursley derived the probability of a hop being hit by another user in the network in a FHSS-MA network for memoryless and Markov hopping patterns. In [Pur 86] error probabilities and local throughput were derived for an asynchronous frequency-hop packet radio network for slotted

and unslotted ALOHA network protocols with error control coding. By using an information theoretic approach [Heg 85], Hegde and Stark showed the existence of an optimal number of users in the network. This number maximizes the total reliable information transmitted through the network. They also derived the probability distribution of the number of hits in a block of m symbols in a FHSS-MA network and showed that the error resulting from assuming that the hits are independent from hop to hop is negligible[Heg 88]. In [Kim 87] asymptotic performance of Reed-Solomon codes for slotted FHSS-MA network was derived both with and without perfect side-information and concatenated coding schemes with random inner codes were considered. In [Mad 88] similar analyses were done for unslotted FHSS-MA networks assuming perfect side-information. It was also shown that when perfect side-information is available, the asymptotic performance of FHSS-MA networks is insensitive to both the distribution of packet lengths and to whether or not transmission is slotted. Convolutional coding for SSMA networks was considered in [Pur 85] and an upper bound on the packet error probability was derived for the case when hard decisions are made. Many researchers have also considered the network protocols for spread-spectrum multiple-access networks [Wie 86] [Ray 81] [Pur 87b]. This will not be discussed in this thesis.

1.2 Problems

In this section we discuss the problems considered in this thesis and previous work done by other researchers on these problems. More detailed descriptions are given at the beginning of each chapter.

1.2.1 Error Probability

The first problem we consider is that of computing the uncoded probability of bit error in an AFHSS-MA network where one binary symbol is transmitted per hop using Binary Frequency Shift Keying (BFSK) modulation. Most of the work done on FHSS-MA up to now assumes that the probability of bit error whenever a hop is hit by multiple-access interference in a FHSS-MA networks is 1 when M-ary ($M > 2$) Frequency Shift Keying (MFSK) is used and $\frac{1}{2}$ when BFSK is used. These approximations are used simply because there are no better bounds or approximations available. Recently there has been some interest in deriving more accurate approximations to the probability of error for an AFHSS-MA network when one symbol is transmitted per hop and BFSK with noncoherent detection is used. In [Kel 88], an exact expression for the probability of error was derived when a hop is hit by one interfering user and Monte Carlo simulations were performed when a hop is hit by more than two users (up to four). In [Ger 88], approximations to the probability of error were developed by assuming that the frequency separation between the BFSK tones is large enough so that the nonorthogonality of the interfering tones (due to the asynchronocity of the hopping patterns) can be neglected. But in practice, it would be advantageous to use the minimum frequency separation because for a given bandwidth, this would allow a larger number of slots to be used and thus decrease the probability that a hop is hit by other interfering users. In [Sho 88], an exact expression for the probability of error *given* the initial phases, delays, power levels and the data bits of the interfering tones was derived. But in most practical AFHSS-MA systems, it is natural to assume that most of these quantities are random and thus the expression for the error probability given in [Sho 88] must be averaged over these variables to give the average error probability. This averaging involves two K'-fold

integrations for the initial phases and delays and a K'-fold summation for the data bits of the interfering tones where K' is the number of interfering users in the frequency slot. This is a nontrivial task even for moderate values of K'. In short, these result do not provide a sufficiently accurate or numerically tractable expressions for the probability of error.

In Chapter 3 we derive an analytical expression for the probability of error based on a general model for the AFHSS-MA network provided in Chapter 2. This expression will yield exact error probability when orthogonal BFSK is employed and an approximation when nonorthogonal BFSK is employed. This expression is also easier to evaluate than the one provided in [Ger 88]. We also describe an efficient simulation technique to verify that our results agrees with simulation results. We compare our results to the case when approximations in [Ger 88] are made and show that the latter gives optimistic results. Using our result, we compute various performance measures for FHSS-MA networks and find that assuming that the probability of error is $\frac{1}{2}$ whenever a hop is hit results in excessively pessimistic estimates of coded system performance and analyses based on this assumption have lead to misleading results. For example, the excessively pessimistic analysis of the hard decisions receiver under this assumption lead to the claim that, using perfect side-information to erase the hops that were hit (and make hard decisions on the hop that were not hit) would outperform simple hard decisions. Our results show that, in fact, simple hard decisions significantly outperforms the system using perfect side-information.

1.2.2 Viterbi Ratio Thresholding

Since for most error correcting codes, the erasure correcting capability of the code is roughly twice that of its error correcting capacity, it follows that if we can devise a

way to single out those hops that were highly corrupted (probability of error close to $\frac{1}{2}$) and erase the symbols corresponding to those hops, we can expect an increase in performance. In Chapter 4 we consider Viterbi Ratio Thresholding (VRT) [Vit 82] [Vit 85] to provide an alternate way of providing information about the quality of the channel to the side-information as defined in Chapter 2. Using VRT to obtain information about the channel for FHSS-MA networks was first considered in [Kel 88] where simulations were done to estimate the channel statistics when a hop is hit by a small number of interfering users (< 4). We use the technique developed in Chapter 3 to derive the resulting channel statistics when VRT is used. We provide simulation results to confirm that our results agrees with the simulation results in this case also. We consider two different forms of VRT and compare the results with various forms of side-information and conclude that VRT provides a very simple means of obtaining reliable information about the quality of the channel that significantly improves the performance of the system.

1.2.3 Binary Error Correcting Codes in Generating Side-Information for Slow FHSS-MA networks

In Chapter 5 we consider slow FHSS-MA networks where more than one code symbol is transmitted in each hop. The widely used assumption is that when a hop is hit, all the symbols in the hop are hit. Here we attack the problem of finding the probability that l out of the n symbols transmitted in a hop are actually hit when the hop itself is hit. Using this result, we consider a concatenated coding scheme where a set of k data symbols to be transmitted in a hop is encoded using an (n, k) binary code. Bounded distance decoding is used to decode this code, which corrects up to a predetermined number of errors and with high probability, outputs an erasure when

the number of errors exceeds this value. The idea here is similar to VRT in that instead of assuming that a hop is highly corrupted whenever it is hit and erasing the corresponding symbols, we estimate the actual level of corruption of a given hop and erase the symbols in the hop accordingly. We compare the performance of this system to a system employing the test pattern scheme proposed in [Pur 87a] and a system with perfect side-information. Numerical results show that this scheme performs much better than the test pattern scheme with the same system parameters, especially for low signal-to-noise ratios. It also performs better than the system using perfect side-information to erased the symbols transmitted in a hop that was hit. We also consider the case when the channel is further corrupted by Rayleigh fading and show that we obtain a performance better than both the systems using test patterns and perfect side-information.

CHAPTER II

SYSTEM MODEL AND PERFORMANCE MEASURES

In this chapter we provide a detailed description of the AFHSS-MA network model that will be used in the following chapters and the performance measures used to compare different schemes. For our purposes, a radio communications network will consist of K users. Associated with each user is a transmitter and a receiver which desire to communicate. Communication is accomplished by transmitting signals in a common spectrum. The signal received at any receiver consists of a weighted and delayed sum of the K transmitted signals plus additive white Gaussian noise.

First we describe the models for the hopping patterns used in FHSS-MA networks and the mechanism for hits at the hop level. We then look at hits at the waveform level and derive an expression for the outputs of the matched filters when binary frequency shift keying and noncoherent detection is used with Markov hopping patterns and the hop is hit by K' interfering users. This is followed by definitions of various forms of side-information. In the last section we introduce channel capacity and normalized throughput which will be used as performance measures to compare different schemes.

2.1 Hopping Patterns

In a FHSS-MA network, the available bandwidth W_{ss} [Hz] is divided into q sub-bands referred to as (frequency) slots as shown in Fig. 2.1. Each slot is of bandwidth $\frac{W_{ss}}{q}$ and the *center frequency* of each slot, denoted by F_l, $l = 1, \cdots, q$, is the frequency of the Radio Frequency (RF) carrier of the signal transmitted in the frequency slot. That is, the l-th frequency slot is the frequency range $\left[F_l - \frac{W_{ss}}{2q}, F_l + \frac{W_{ss}}{2q}\right]$ with center frequency F_l. We denote the set of available center frequencies by $\mathsf{F}_c = \{F_l : l = 1, \cdots, q\}$. In the following discussions we will use the terms center frequency and frequency slot interchangeably. It is assumed that a user transmitting in the l-th slot emits negligible power outside the l-th slot.

A user in the network consists of a transmitter which intends to communicate with its corresponding receiver but not with other receivers in the network. The q available frequency slots are shared among K actively communicating users. Each user in the network is assigned a *hopping pattern* which is a doubly infinite pseudorandom sequence with elements in F_c denoted by $\mathbf{h} = \{h_i\}_{i=-\infty}^{i=+\infty}$ with $h_i \in \mathsf{F}_c$. Without loss of generality, we assume that each user has a clock with period T_h. The k-th user chooses a new center frequency for transmission at the beginning of each clock cycle, i.e., at multiples of T_h, using a frequency hopper. The hopping pattern then designates the center frequency to be used by the transmitter at any time interval $(m \cdot T_h, (m+1)T_h]$ referred to as the m-th hop interval, where m is any integer. That is, if $h_m = F_l$, the transmitter uses center frequency F_l in the time interval $(mT_h, (m+1)T_h]$ to transmit data. The time spent on a particular frequency slot (T_h) is referred to as the *hop duration* or the *dwell interval.* We denote the set of hopping patterns assigned to the K users in the network by $\{\mathbf{h}^k\}_{k=1}^K$ where $\mathbf{h}^k = \{h_i^k\}_{i=-\infty}^{i=+\infty}$ denotes the hopping

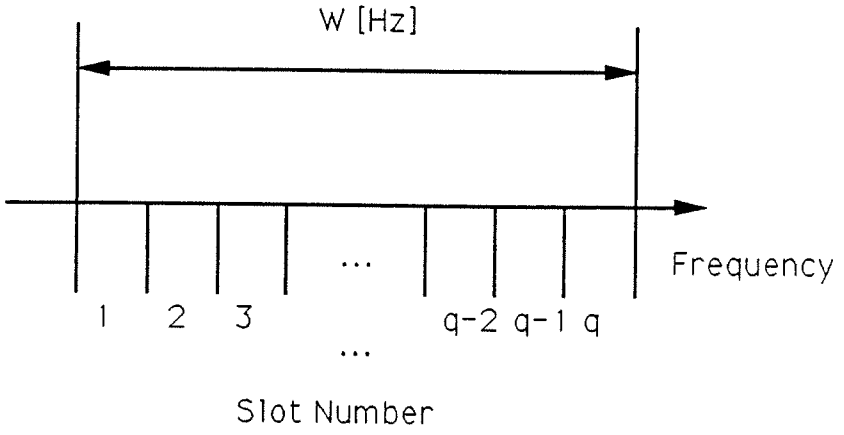

Figure 2.1: Division of the available bandwidth into q frequency slots.

pattern assigned to the k-th user.

For many FHSS radio networks, the hopping patterns are generated using cryptographic techniques and are not even available to the system engineer. In these cases, it is useful to model the hopping patterns as a sequence of random variables. We will adopt this model here. We will assume that the hopping patterns of different users are mutually independent and have the same statistics. The most widely used models for the hopping patterns are memoryless (independent) hopping patterns and Markov hopping patterns. In the memoryless hopping pattern model, $\{h_i^k\}$ is a sequence of independent and identically distributed (i.i.d.) random variables with a uniform distribution on F_c. In the Markov hopping pattern model, the conditional distribution of h_i^k given h_{i-1}^k is a uniform distribution on $\mathsf{F}_c - \{h_{i-1}^k\}$ for any given i, i.e., the system never uses the same center frequency for two consecutive hops. Fig. 2.2 shows an example of the memoryless and the Markov hopping patterns.

We can categorize FHSS-MA systems into the following two different schemes. In one scheme, the hopping patterns of the users in the network are synchronized so that the transition from one frequency slot to the next frequency slot of all the users in the network are aligned as seen by each of the receivers. When this is true, we say that the system is synchronized at the hop level, and the network is referred to as a Synchronous FHSS-MA (SFHSS-MA) network. In the second scheme referred to as the Asynchronous FHSS-MA (AFHSS-MA) network, the transitions from hop to hop are not synchronized at each of the receivers. In practical systems the second scheme is usually employed since in many cases, achieving this kind of synchronization is very difficult except for some special cases. For example, SFHSS-MA is possible when a number of mobile users transmit to a single base station and the base station in turn broadcasts the data back to the mobile stations.

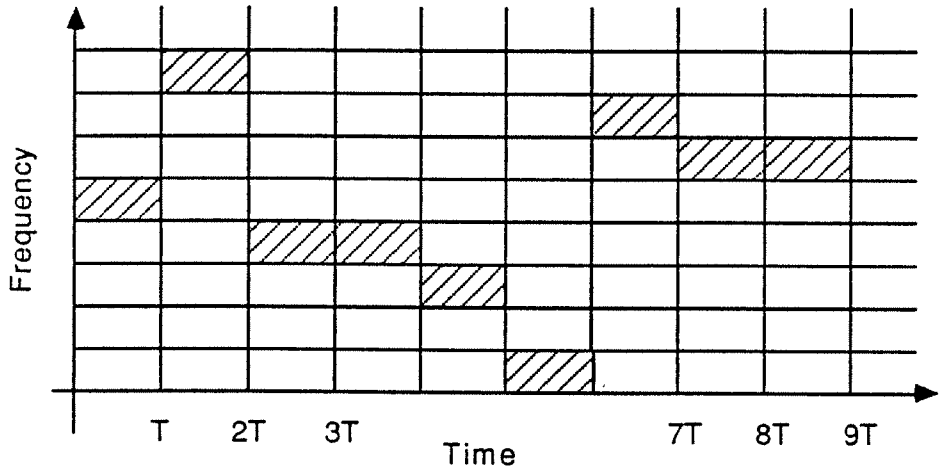

Example of a Memoryless Hopping Pattern

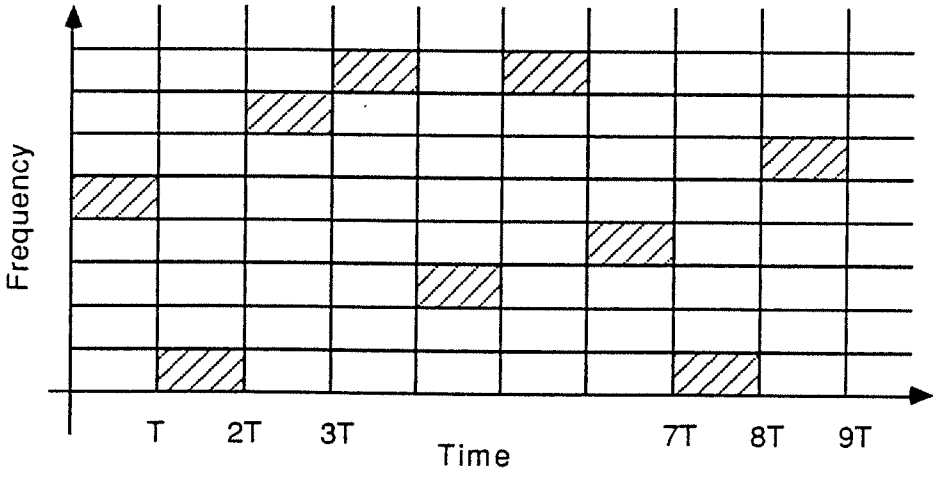

Example of a Markov Hopping Pattern

Figure 2.2: Example of memoryless and Markov hopping patterns.

Whenever two or more users simultaneously transmit in a particular frequency-slot for a nonzero time interval, we say that a *hit* has occurred. Consider a given receiver (say the first receiver) and assume that the signal transmitted by the first transmitter (the transmitter with which the first receiver wishes to communicate) is at center frequency F_l during the time interval $(mT_h + \tau_1', (m+1)T_h + \tau_1']$ (the m-th hop) as seen by the first receiver, where τ_1' is the propagation delay between transmitter one and receiver one. It is usually assumed that $\{\tau_k' \bmod T_h\}_{k=2}^{K}$ which denotes the propagation delays modulus the hop duration between the transmitter k and receiver one are mutually independent and uniformly distributed in $(0, T_h]$. We will adopt this assumption in this thesis. First let us consider the case where a hop is hit by a particular user (say j) in the network. A hit by this user j can be categorized into the following three different types. We say that the m-th hop of the first user is hit from the left if the signal at the receiver of the first user due to user j uses the center frequency F_l for the subinterval $(mT_h + \tau_1', (m+1)T_h + \tau_1' + t']$ and that it is hit from the right if user j uses the center frequency F_l for the subinterval $(mT_h + \tau_1' + t'', (m+1)T_h + \tau_1']$ where $0 < t', t'' < T$. We denote these events by H_L^m and H_R^m respectively and note that for memoryless hopping, the events H_L^m and H_R^m are independent. When a hop is hit from the left or from the right only, as described above, we say that the hit is a *partial* hit. Finally a hit is categorized as a *full* hit if the hop is hit from the left *and* from the right by user j. The probability of partial and full hits are denoted by p_p and p_f. The probability of a hop being hit by a particular user in the network denoted by $p_h = p_p + p_f$ is given by [Ger 82]

$$p_h = \begin{cases} \frac{1}{q}(2 - \frac{1}{q}) & : \text{asynchronous hopping} \\ \frac{1}{q} & : \text{synchronous hopping} \end{cases} \tag{2.1}$$

when memoryless (independent) hopping patterns are employed, and

$$p_h = \begin{cases} \frac{2}{q} & : \text{asynchronous hopping} \\ \frac{1}{q} & : \text{synchronous hopping} \end{cases} \tag{2.2}$$

when Markov hopping patterns are employed. These results are rather obvious for the synchronous cases and the asynchronous Markov hopping case. For the asynchronous memoryless hopping case, p_h can easily be derived as follows.

$$\begin{aligned} p_h &= Pr\{H_L \cup H_R\} \\ &= Pr\left\{H_L \cap \overline{H}_R\right\} + Pr\left\{H_R \cap \overline{H}_L\right\} + Pr\{H_L \cap H_R\} \\ &= \frac{1}{q}(1 - \frac{1}{q}) \times 2 + \frac{1}{q^2} \\ &= \frac{1}{q}(2 - \frac{1}{q}). \qquad \square \end{aligned}$$

In the above equations, $\overline{H}_R$ denotes the complement of the event H_R and simlarily for $\overline{H}_L$.

An example of hopping patterns when there are two asynchronous users in the network is shown in Fig. 2.3. It is easy to see that for the asynchronous Markov hopping pattern case, the probability that a frequency slot used by one user is shared with another user for the entire hop duration is zero. Hence for asynchronous Markov hopping patterns $p_f = 0$ and hence $p_p = p_h$. On the other hand for asynchronous independent hopping patterns, a hit may be either a full hit or a partial hit. The probabilities p_f and p_p for independent hopping patterns can easily be seen to be [Ger 85]

$$\begin{aligned} p_p &= \frac{2}{q}\left(1 - \frac{1}{q}\right) \\ p_f &= \frac{1}{q^2}. \end{aligned} \tag{2.3}$$

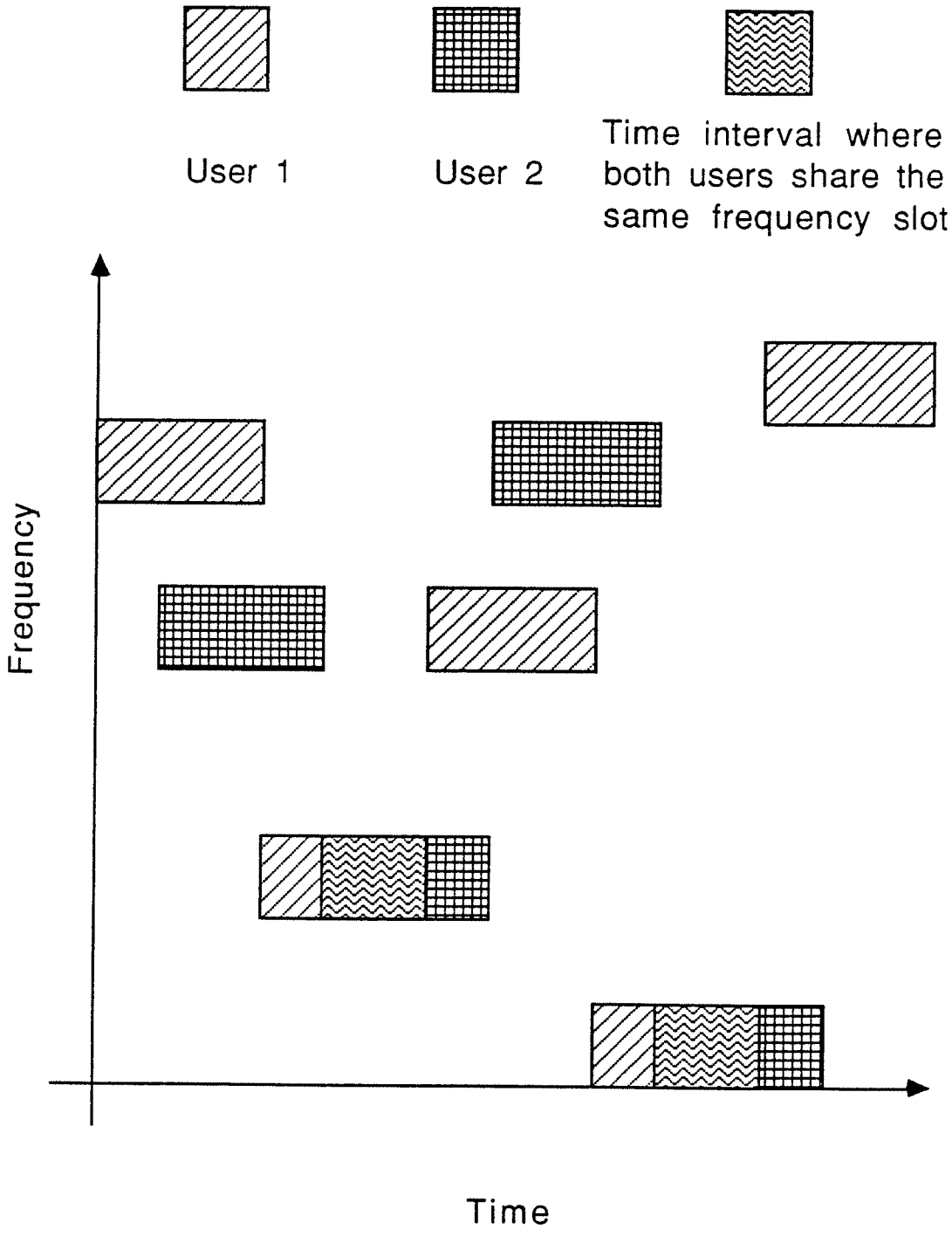

Figure 2.3: Example of hopping patterns in a network with two users.

Using the above expressions for p_h and the independence of hopping patterns, we can write the probability that a particular hop is hit by at least one other user when there are a total of K active users in the network, denoted by P_{hit} as

$$P_{hit} = 1 - (1 - p_h)^{K-1}. \tag{2.4}$$

2.2 User-Channel Model: One Symbol Per Hop

In this section we provide a detailed description of the transmitter-receiver pair, the channel, and the interference at the waveform level when one binary channel symbol is transmitted in each hop. Using this, we derive an expression for the output of the matched filters when binary frequency shift keying, noncoherent detection, and Markov hopping patterns are employed. The extension of the argument to the more general case when one M-ary channel symbol is transmitted per hop is straightforward.

Each user in the network consists of a FHSS user transmitting one binary symbol in each hop duration and a receiver that is perfectly synchronized (locked on) to the hopping pattern of the corresponding transmitter, i.e., the receiver knows the center frequency of the received signal of the corresponding transmitter at each time instant.

We assume that Markov hopping patterns are employed. Assuming Markov hopping patterns not only simplifies the analysis but also simplifies numerical computations. As we will see later, this is mainly due to the fact that when Markov hopping patterns are used, all the hits are partial hits ($p_f = 0$) and no full hits occur. Also in later chapters, it will be shown that the results obtained by assuming Markov hopping patterns provide close approximations to the results for independent hopping patterns.

In Fig. 2.4, we show the block diagram of the models for the transmitters and the channel, and Fig. 2.5 is the block diagram of the model for the receivers. Fig. 2.4 together with Fig. 2.5 make up a general model of an AFHSS-MA network with K active users sharing a common physical channel. We assume that each receiver hears the transmissions of all active users in the network but only wishes to communicate with the transmitter to which it is synchronized. All the users are assumed to be identical except possibly for the output power and have mutually independent hopping sequences with the same statistics.

Since different users may be located at different sites and different users may have different power, the power level of different users as seen by a receiver may be different. The attenuated and delayed signals of the users are added along with Additive White Gaussian Noise (AWGN), possibly corrupted by fading/multipath and presented to the receivers for detection and decoding. The receivers demodulate and decode independently of each other, i.e., there is no cooperation among the users. Also there may be some kind of side-information about the channel available to the receivers to aid the decoding process. Side-information will be discussed in detail in Section 2.4. The transmitted signals of other users as seen by a specific receiver, say the first receiver, may be considered as just another form of channel corruption mechanism. The users other than the one intended (i.e., the one that it is synchronized to) are called *interfering users* and the interference due to the interfering users is called the *multiple-access interference*. Hence the channel model for the first user can be simplified as shown in Fig. 2.6. The (channel) coder and the decoder in Figs. 2.4-2.5 provides error protection against interference due to other users in the network and AWGN.

The modulator/demodulator is assumed to be Binary Frequency Shift Keying

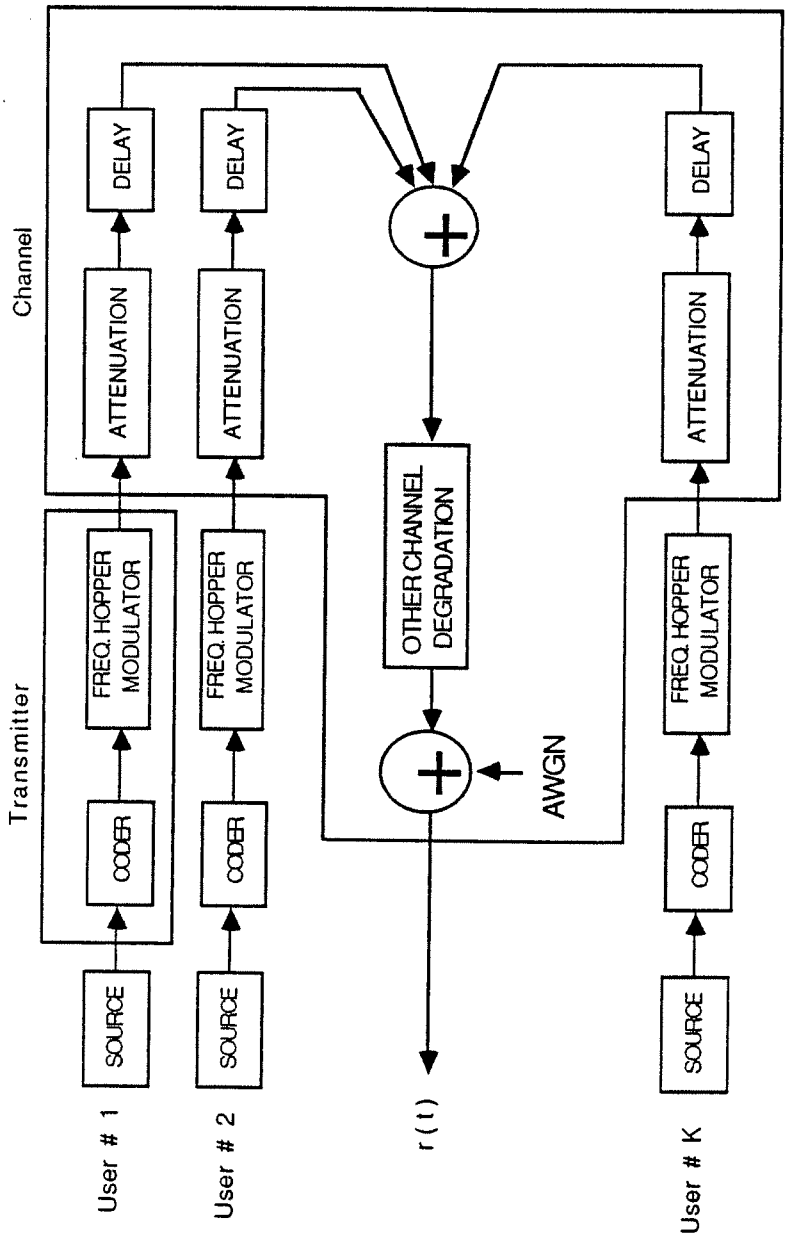

Figure 2.4: Block diagram of the transmitters and the channel of an AFHSS-MA network.

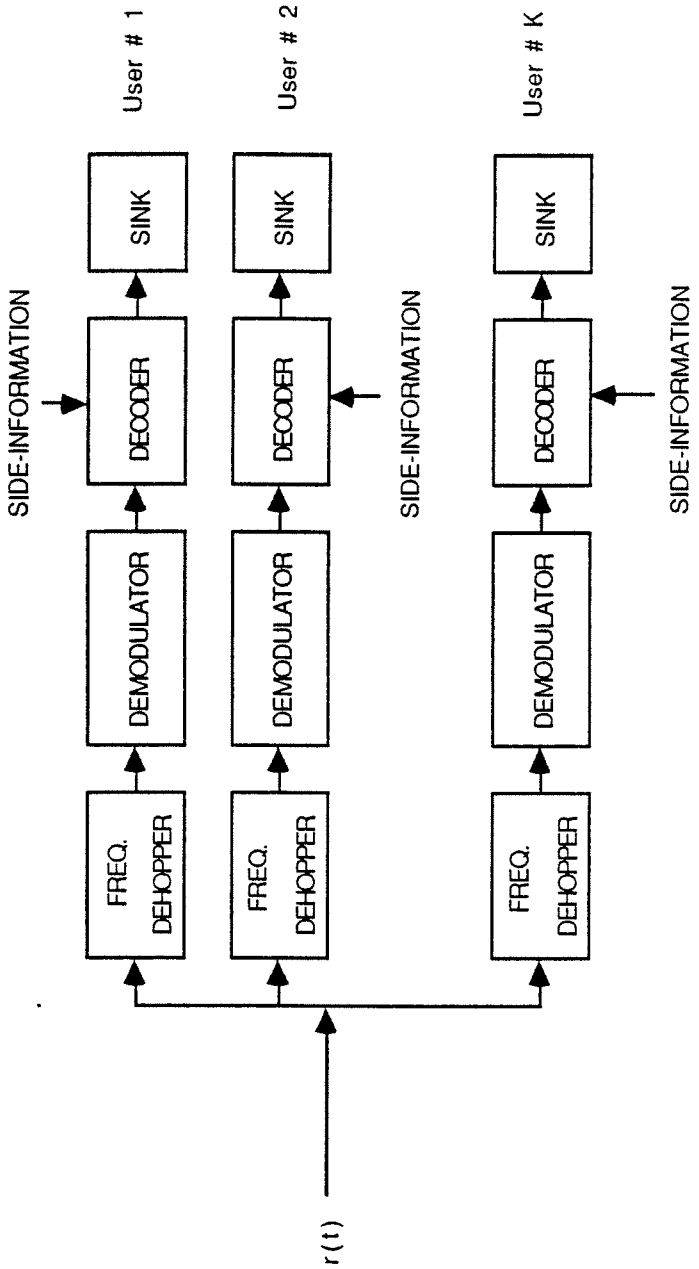

Figure 2.5: Block diagram of the receivers of an AFHSS-MA network.

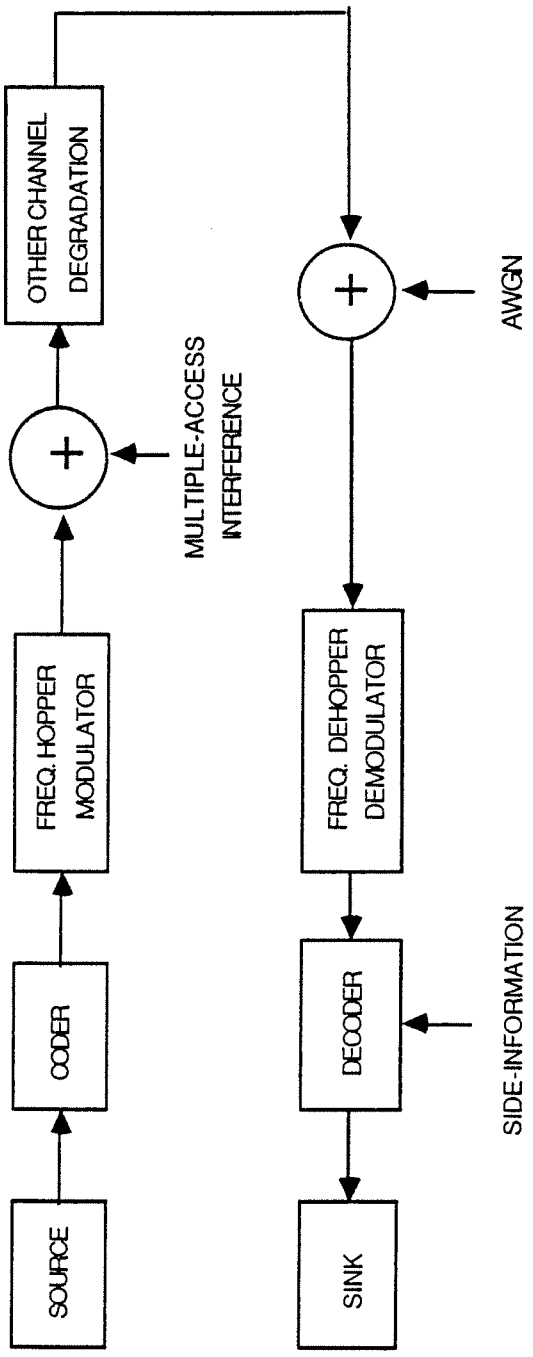

Figure 2.6: Simplified channel model.

(BFSK) modulation with noncoherent demodulation. Noncoherent demodulation is usually used in FHSS systems since it is generally very difficult to acquire an accurate approximation to the signal phase during the short hop duration. Let $f_j^k \in \mathsf{F}_c$ be the center frequency of the j-th frequency hop of the k-th user. Let $b_j^k \in \{-1, 1\}$ denote the j-th data bit of the k-th user. Also let $\varphi_j^k \in (-\pi, \pi]$ be the initial phase of the k-th user for the j-th hop and $\Gamma(t)$ be the shaping waveform for the BFSK tones. For simplicity, we assume that $\Gamma(t) = 1$ for $0 < t < T_h$ and zero otherwise. Then using standard complex notation to represent real signals, the transmitted signal of the k-th users for the j-th hop in the time interval $(jT_h, (j+1)T_h]$ can be written as

$$s_k(t) = \Gamma(t - jT_h) \exp[i2\pi(f_j^k + b_j^k \Delta f)t + \varphi_j^k]$$

where $2\Delta f$ is the frequency separation between the two tones corresponding to b_j^k and $i = \sqrt{-1}$. The signal actually transmitted is given by the real part of $s_k(t)$. For now, we assume that the only interference added to the transmitted signal other than multiple-access interference is the AWGN.

At the first receiver, the received signal is first passed through a band-pass Radio Frequency (RF) filter to attenuate any other signal that might be present outside the spread-spectrum band. Then for the j-th hop of the first transmitter using center frequency f_j^1, the signal is then multiplied by a sinusoidal tone from a local oscillator with frequency $f_j^1 - f_{IF}$ using a multiplier circuit, where f_{IF} is called the Intermediate Frequency (IF). The multiplier together with the circuitry to track the hopping pattern of the corresponding transmitter, is usually called the *dehopper*. The resulting signal is same as the signal out of the RF filter except that now, the center frequency of the j-th hop is located at f_{IF}. The signal output from the multiplier is then fed through the IF filter which is a band-pass filter with center frequency f_{IF}

and bandwidth $\frac{W_{ss}}{q}$. Finally, the noncoherent demodulator makes decisions based on this signal. All other receivers in the network will operate in the same fashion except that they will follow the hopping patterns of the corresponding transmitters.

Now,the signal seen at the output of the IF filter of the first receiver during the j-th hop interval denoted by $r_j(t)$ can be written as shown below given that there are $K'+1$ users sharing the frequency slot (i.e., from the first receiver's point of view, the hop is hit by K' interfering users.)

$$\begin{aligned} r_j(t) &= \sum_{k=1}^{K'+1} \Gamma(t - jT_h)\alpha_k s_k(t - \tau_j^k) + z(t) \\ &= \sum_{k=1}^{K'+1} \Gamma(t - jT_h)\alpha_k \exp\left(i2\pi(f_{IF} + b_j^k \Delta f)(t - \tau_j^k) + i\varphi_j^k\right) + z(t) \end{aligned}$$

where $\tau_j^k \in (-T_h, T_h]$ is the delay of the beginning of the transmission of the k-interfering users with respect to the beginning of transmission of the j-th hop of the first user *mod* T_h. The term $z(t)$ denotes the complex white Gaussian noise process with two sided power spectral density $\frac{N_0}{2}$ and the amplitudes of the signals out of the IF filter due to the k-th tranmitter as seen by the first receiver are denoted by $\alpha_k > 0$. Also, without loss of generality, the propagation delay from the first transmitter to the first receiver was normalized to zero. We also define the normalized delay of the k-th user with respect to the first user for the j-hop as $p_j^k = \frac{\tau_j^k}{T_h}$. Fig. 2.7 shows the hop j-th hop for the first user being hit by three interfering users with different delays, amplitudes, and data bits.

For detection of the signals, we employ the noncoherent demodulator that is optimal when only AWGN is present. The demodulator for the first transmitter is given by Fig. 2.8 [Pro 83] where

$$r_1(t) = \Gamma(t - jT_h)\exp[-i2\pi(f_{IF} + \Delta f)t]$$

$$r_{-1}(t) = \Gamma(t - jT_h)\exp[-i2\pi(f_{IF} - \Delta f)t].$$

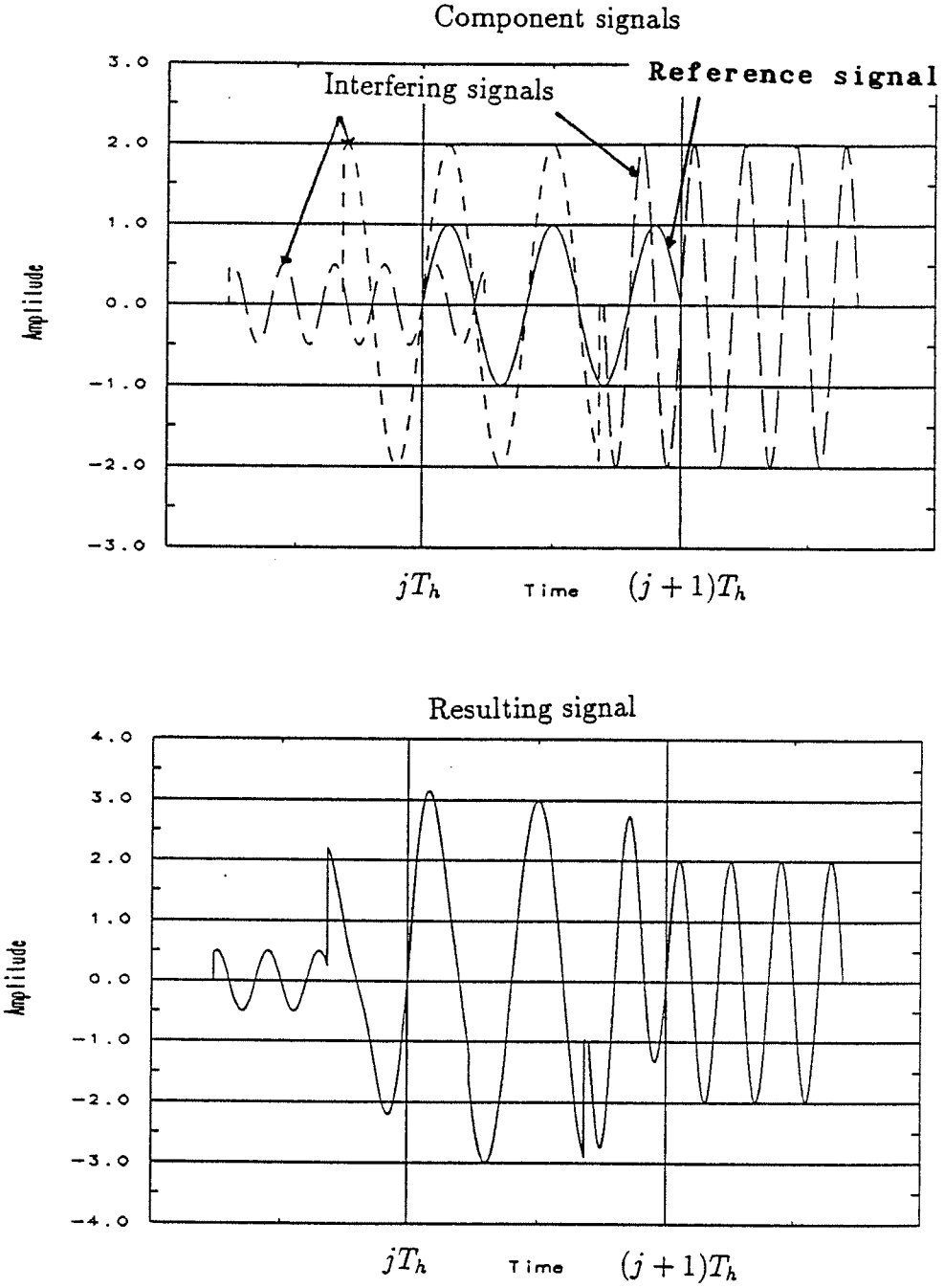

Figure 2.7: Delay Model.

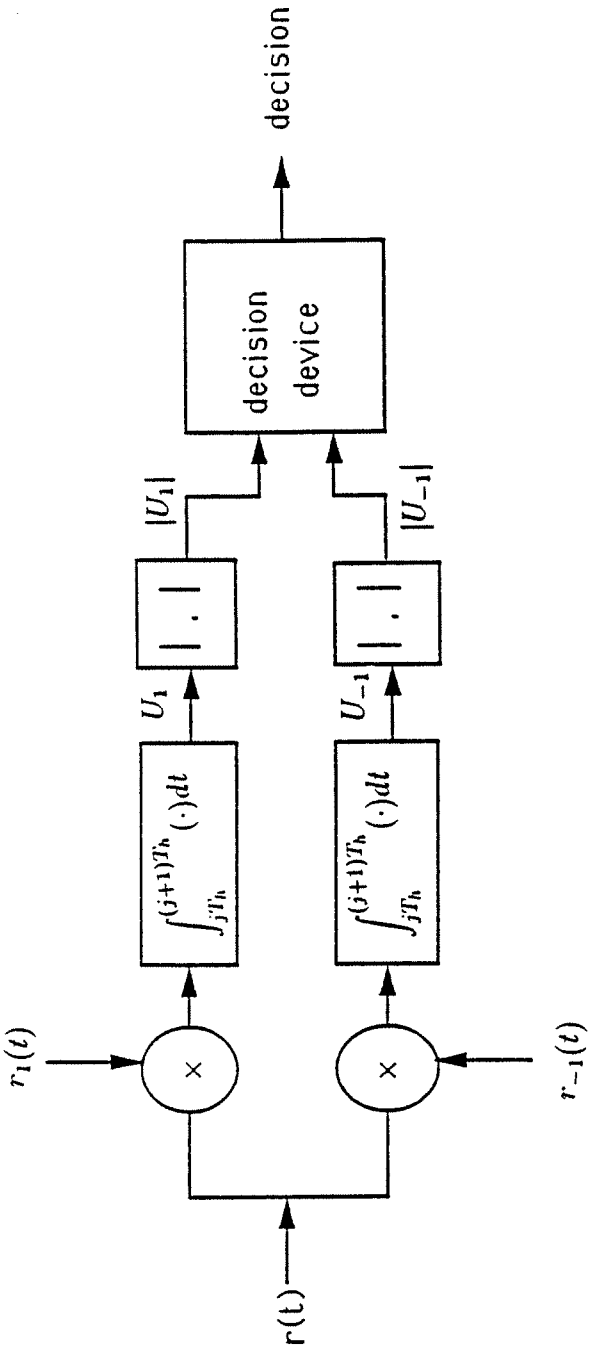

Figure 2.8: Noncoherent demodulator.

The decision variables are $|U_1|$ and $|U_{-1}|$ which are obtained from the received signal $r(t)$ by first multiplying $r_j(t)$ by $r_1(t)$ and $r_{-1}(t)$ respectively and integrating over the hop duration and taking the magnitude. Hence the outputs of the integrators (Fig. 2.8) U_1 and U_{-1} are given by

$$\begin{aligned} U_1 &= \int r_j(t) r_1(t) dt \\ U_{-1} &= \int r_j(t) r_{-1}(t) dt. \end{aligned}$$

Hence U_1, U_{-1} can be written as follows given that $b_j^1 = +1$ (Note that we dropped the subscript j and use k as the subscript).

$$\begin{aligned} U_1 &= z_1 + \sqrt{\frac{E_b}{N_0}} e^{i\varphi_1} + \sqrt{\frac{E_b}{N_0}} \sum_{k=2}^{K'+1} \left(\frac{\alpha_k}{\alpha_1}\right) e^{-i2\pi f_{IF} \tau_k} e^{i\varphi_k} a_k(1, p_k, b_k) \\ U_{-1} &= z_{-1} + \rho \sqrt{\frac{E_b}{N_0}} e^{i\varphi_1} + \sqrt{\frac{E_b}{N_0}} \sum_{k=2}^{K'+1} \left(\frac{\alpha_k}{\alpha_1}\right) e^{-i2\pi f_{IF} \tau_k} e^{i\varphi_k} a_k(-1, p_k, b_k) \end{aligned}$$

where z_1 and z_{-1} are complex Gaussian random variables with $E\{z_1 z_1^*\} = 1$, $E\{z_{-1} z_{-1}^*\} = 1$, $E\{z_1 z_{-1}^*\} = \rho^*$ (x^* denotes the complex conjugate of x) and $\frac{E_b}{N_0}$ is the signal-to-noise ratio of the first user with $E_b = \frac{\alpha_1^2 T_h}{2}$. The term ρ is the complex correlation coefficient between the two BFSK tones defined as $\rho = e^{-i2\pi\Delta f T_h} \frac{\sin(2\pi\Delta f T_h)}{2\pi\Delta f T_h}$. The terms $a_k(l, p_k, b_k)$, $l \in \{1, -1\}$ are complex functions of p_k and b_k. If we let $A_k(l, p_k, b_k)$ and $\theta_k(l, p_k, b_k)$ be the magnitude and the phase of $a_k(l, p_k, b_k)$, then simple analysis shows that they can be written as follows.

$$A_k(l, p_k, b_k) = \delta(l, b_k)\hat{q}_k + \delta(l, -b_k)\hat{q}_k \frac{\sin 2\pi\zeta\hat{q}_k}{2\pi\zeta\hat{q}_k} \tag{2.5}$$

and

$$e^{\theta_k(l, p_k, b_k)} = sgn(p_k)\delta(l, b_k) e^{isgn(l)\pi p_k} + -sgn(p_k)\delta(l, -b_k) \tag{2.6}$$

where $\delta(x, y)$ is the Kronecker delta function defined to be 1 if $x = y$ and 0 otherwise. The function $sgn(x)$ returns the sign of the number x (i.e. $sgn(x) = +1$ if $x \geq 0$ and

$sgn(x) = -1$ if $x < 0$), $\hat{q}_k = 1 - |p_k|$ and $\zeta = \frac{T_h}{\Delta f}$. Hence

$$U_1 = z_1 + \sqrt{\frac{E_b}{N_0}} e^{i\varphi_1} + \sqrt{\frac{E_b}{N_0}} \sum_{k=2}^{K'+1} e^{-i\{2\pi f_{IF}\tau_k + \theta_k(1,p_k,b_k)\}} e^{i\varphi_k} A'_k(1, p_k, b_k)$$

$$U_{-1} = z_{-1} + \rho\sqrt{\frac{E_b}{N_0}} e^{i\varphi_{-1}} + \sqrt{\frac{E_b}{N_0}} \sum_{k=2}^{K'+1} e^{-i\{2\pi f_{IF}\tau_k + \theta_k(-1,p_k,b_k)\}} e^{i\varphi_k} A'_k(-1, p_k, b_k). \quad (2.7)$$

where

$$A'_k(l, p_k, b_k) = \left(\frac{\alpha_k}{\alpha_1}\right) A_k(l, p_k, b_k), \quad l \in \{-1, +1\}.$$

The decision device in Fig. 2.8 makes decisions about the transmitted binary symbols based on $|U_1|$ and $|U_{-1}|$. For example, the decision device may simply make hard decisions by deciding that a '+1' was transmitted if $|U_1| > |U_{-1}|$ and a '-1' was transmitted if $|U_1| \leq |U_{-1}|$. In this case, the resulting channel from the transmitted binary symbol to the decision outputs can be modeled as a Binary Symmetric Channel (BSC) (Fig. 2.9) with some transition probability p. On the other hand, if the decision device makes decisions or erasures based on some rule, e.g., Viterbi ratio thresholding, then the resulting channel can be modeled as a Binary Symmetric Errors and Erasure Channel (BSEEC) with error and erasure probabilities p_e and p_x as shown in Fig. 2.10 if the rule is *symmetric*. Both BSC and the BSEEC belong to a class of channels called the discrete memoryless channels. Discrete memoryless channels will be discussed in Section 2.5.1. Chapters 3 and 4 will be concerned with deriving expressions for these probabilities.

2.3 User-Channel Model: Multiple Symbols Per Hop

In this section we describe the case when multiple binary symbols are transmitted in each hop duration. This type of FHSS-MA system is generally referred as *slow* FHSS-MA system. We denote the number of symbols transmitted in a hop by n (Fig. 2.11). The model for the users and the channel are same as the one given in

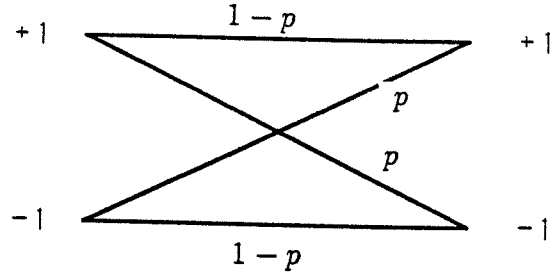

Figure 2.9: BSC.

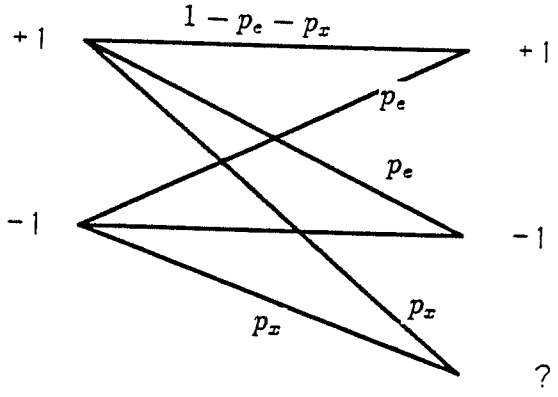

Figure 2.10: BSEEC.

the previous section except that now n binary symbols are transmitted in each hop.

A major difference between analyzing an AFHSS-MA network where one channel symbol is transmitted per hop and a slow AFHSS-MA network is that for the first system. when a hop is hit, the symbol corresponding to the hop is always subject to multiple-access interference whereas in a slow AFHSS-MA network, symbols within a hop may not be subject to multiple-access interference (referred to as a symbol hit as opposed to a hop hit) even though the hop itself is hit as shown in Fig.2.12. Also within a hop, the symbol hits are not independent from each other which complicates the analysis. The statistics of hits for a slow AFHSS-MA network employing Markov hopping patterns will be derived in Chapter 5.

2.4 Side-Information and Quantization

In this section we will define what we mean by *side-information*. We will introduce various forms of side-information and discuss the increase in complexity needed to obtain this information. We will also discuss how the outputs of the noncoherent detector could be quantized to yield various amounts of information about the quality of the channel.

It is generally very difficult to give a clear cut definition of what side-information is. In this thesis, we will define side-information to be any form of information about the quality of the channel other than that obtainable by processing the outputs of the matched filters of the noncoherent demodulator, i.e., $|U_1|$ and $|U_{-1}|$. The most popular form of side-information considered in FHSS-MA networks is the information as to whether a particular hop was hit or not. This form of side-information is usually referred to as *perfect* side-information. Previous results [Pur 86] [Kim 89] indicated

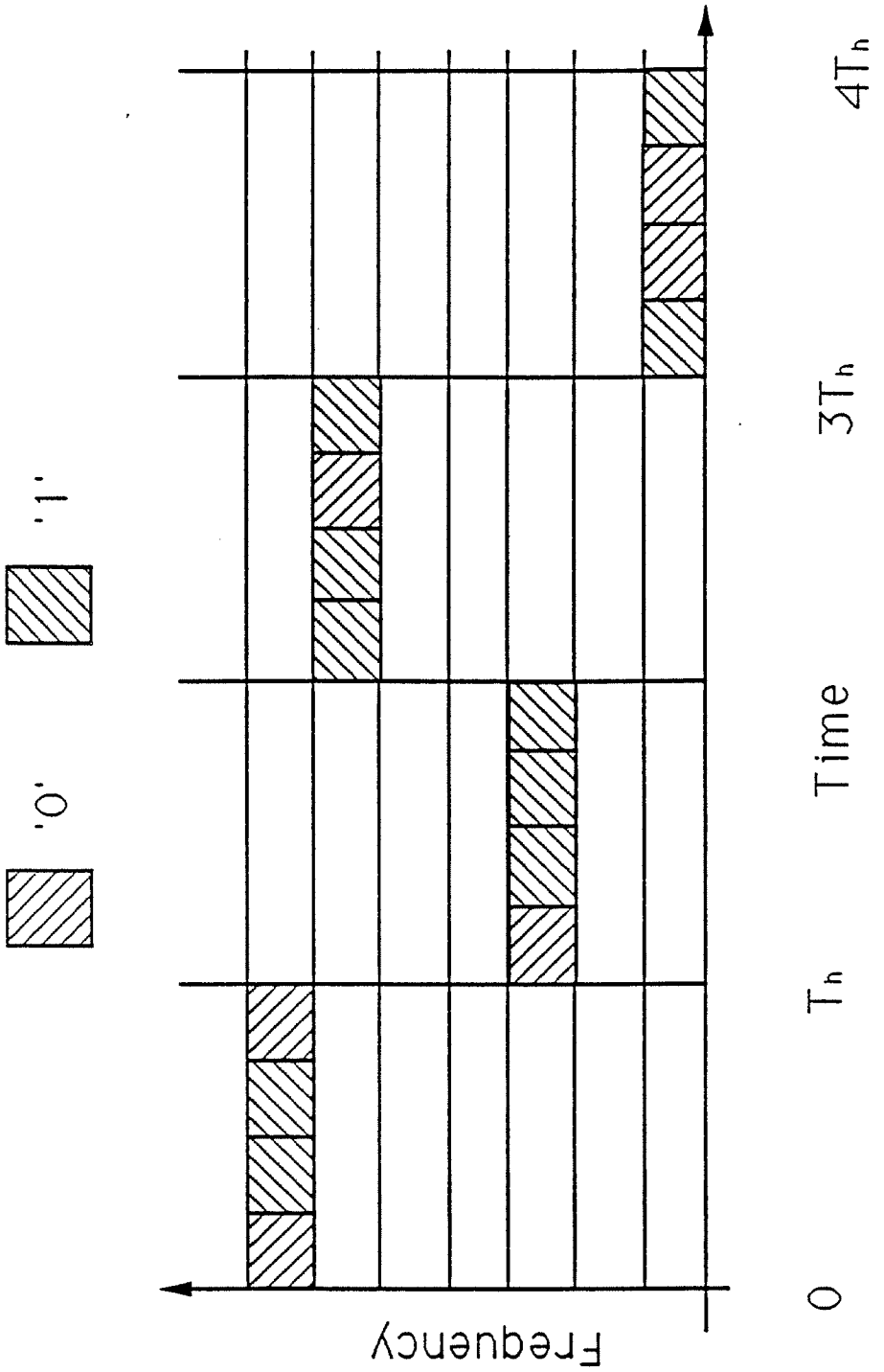

Figure 2.11: Slow FHSS system transmitting n=4 bits per hop.

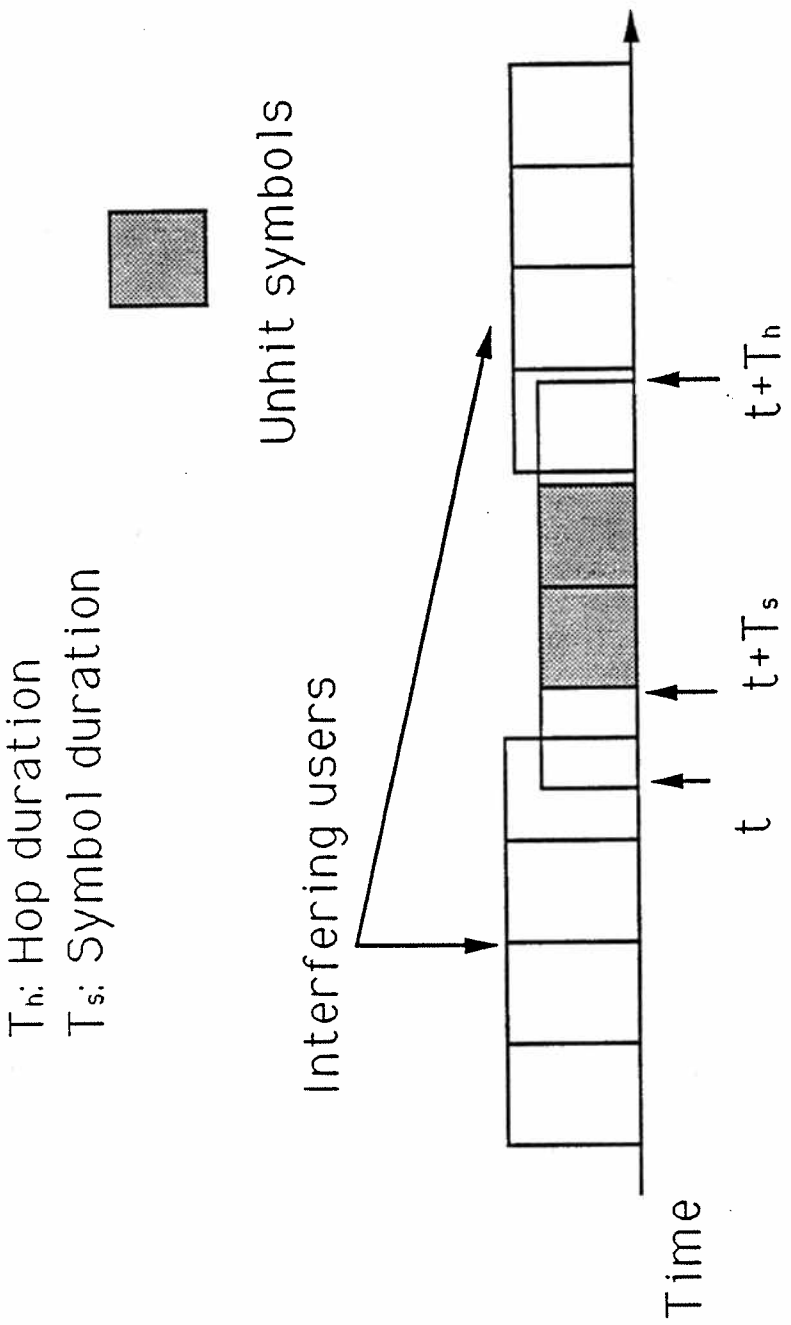

Figure 2.12: Hits in a slow AFHSS-MA network

that using this form of side-information to erase the symbol transmitted in a hop that was hit can greatly improve the performance of a coded FHSS-MA networks. The idea behind trying to acquire and use this form of side-information is that when a hop is hit, the hit is usually detrimental and it is advantageous to erase the symbols corresponding to the hop to make use of the larger erasure correcting capability of the forward error correcting codes which is roughly twice the error correcting capability. One way for a receiver to obtain perfect side-information is for the receiver to track the hopping patterns of all the users in the network. Another way is to detect perfectly (if it is possible) whether a frequency slot to be used is also being used by other users by measuring the energy in the frequency slot just before hopping to that frequency slot and just after leaving that frequency slot. The first method is usually expensive to implement and the second method is usually not very reliable unless the signal-to-noise ratio is very large. Although obtaining the (perfect) side-information is usually difficult and/or expensive, the improvement in the performance when using this information to erase the hops that were hit shown in previous works justified the effort. We will show in this thesis that in reality, the previous results on using perfect side-information to erase the symbols that were hit based on the assumption that the probability of error is $\frac{1}{2}$ whenever a hop is hit are misleading. In fact, when all the hops that were hit are erased, the performance will degrade considerably below that of a system that simply chooses the largest of the matched filters as its estimate, i.e., makes hard-decisions. Of course we do not have to erase the symbols corresponding to the hops that were hit. For example, it is possible to make Maximum Likelihood (ML) decisions based on the code words with perfect side-information available to the decoder. If the receiver is tracking the hopping patterns of all the users in the network to obtain this information, the receiver also has knowledge of exactly how

many interfering users hit a specific hop. This is a much more detailed information than that provided by perfect side-information, and it is also possible for a receiver to make ML decision on the code symbols with this side-information available to the receiver.

On the other hand, without using side-information, we can obtain information about the quality of the channel (the quality of the channel for a hop) by processing the outputs of the matched filter of the noncoherent detector as in Viterbi ratio thresholding. The Viterbi ratio thresholding technique offers a method of more finely quantizing the output of the noncoherent detector than the simple hard-decisions, which is a two level quantizer. This method of obtaining information about the channel is usually much easier to implement. It will be shown in Chapter 4 that Viterbi ratio thresholding provides quality information about the channel to the decoder and improves the performance of the network over simple hard decisions.

2.5 Performance Measures

In this section we introduce some of the performance measures that will be used in later Chapters. We will introduce Discrete Memoryless Channels (DMC) and show how the AFHSS-MA channel can be closely modeled as a DMC. We then derive the channel capacity for various DMCs that will arise in the analysis of an FHSS-MA channels. Finally we introduce the normalized throughput as a measure of information flow in a network.

2.5.1 Discrete Memoryless Channel

A communications channel is called a Discrete Memoryless Channel (DMC) [Vit 79a] if it is characterized by a discrete input alphabet $\mathbf{X}$, a discrete output

alphabet $\mathbf{Y}$, and a set of conditional probabilities of $p_{Y|X}(y|x)$ where the input to the channel is denoted by X and the output of the channel is denoted by Y. Also, the output letter of the channel must depend only on the corresponding input so that for an input sequence of of length N_i denoted by $\mathbf{x} = (x_1, \cdots, x_{N_i})$, the conditional probability of the corresponding output sequence $\mathbf{y} = (y_1, \cdots, y_{N_i})$ may be expressed as

$$p_{N_i}(\mathbf{y}|\mathbf{x}) = \Pi_{n=1}^{N_i} p(y_n|x_n).$$

The BSC and the BSEEC are examples of a DMC.

In an AFHSS-MA network it is clear that the channel has discrete input and output alphabets with corresponding transition probabilities given that some sort of quantization is done at the receiver. It can be shown [Heg 88] that the asynchronous FHSS-MA channel actually has memory and hence the memoryless condition is not satisfied. But it is also shown in [Heg 88] that the memory is very weak for realistic values of q and hence a DMC approximation of asynchronous FHSS-MA channels is very accurate.

2.5.2 Channel Capacity

First let us define a quantity C' for a DMC which is the maximum of the mutual information between the input X and the output Y (written as $I(X;Y)$) over all possible input distributions. That is

$$C' = \max_{q_X} I(X;Y) \tag{2.8}$$

where q_X denotes the distribution of X and for discrete input and output alphabets, the mutual information $I(X;Y)$, is given by

$$I(X;Y) = \sum_y \sum_x p(y|x) q_X(x) \log \frac{p(y|x)}{\sum_{x'} p(y|x') q_X(x')}. \tag{2.9}$$

The channel capacity of a communications channel, denoted by C, is defined to be the maximum data rate at which reliable (i.e., arbitrarily small probability of error) communications is possible over the channel. The channel coding theorem for the DMC [Gal 68] states that, for any DMC, there exists a code of rate r [bits/channel use] such that reliable communication is possible provided that

$$r < C'$$

where C' is given by (2.8). The converse of the channel coding theorem states that for any DMC , there exists no code that provides reliable communications with rate greater than C'. Hence, $C = C'$ and the channel capacity for a DMC is given by (2.8).

The channel capacities of BSC (C_{BSC}) and BSEEC (C_{BSEEC}) (figs. 2.9-2.10) can easily be shown to be the following [Gal 68].

$$C_{BSC} = 1 + (1-p)\log_2(1-p) + p\log_2 p, \tag{2.10}$$

$$C_{BSEEC} = p_c \log_2\left(\frac{2p_c}{1-p_x}\right) + p_e \log_2\left(\frac{2p_e}{1-p_x}\right) \tag{2.11}$$

where $p_c = 1 - p_e - p_x$. Let us consider a DMC with binary input and 4-ary output as shown in Fig.2.13. It will be shown in Chapter 4 that this is the resulting channel when 4-level Viterbi ratio thresholding is employed. The channel capacity for this channel denoted by C_4 can be computed to be the following using (2.8) and (2.9) [Che 88a].

$$\begin{aligned} C_4 &= p_c \log_2\left(\frac{2p_c}{p_c+p_e}\right) + p_{cx}\log_2\left(\frac{2p_{cx}}{p_{cx}+p_{ex}}\right) \\ &+ p_{ex}\log_2\left(\frac{2p_{ex}}{p_{cx}+p_{ex}}\right) + p_e \log_2\left(\frac{2p_e}{p_c+p_e}\right). \end{aligned} \tag{2.12}$$

When side-information is available, the channel capacity can be written as [Mce 84]

$$C = \max_{q_X} I(X; Y, S) \tag{2.13}$$

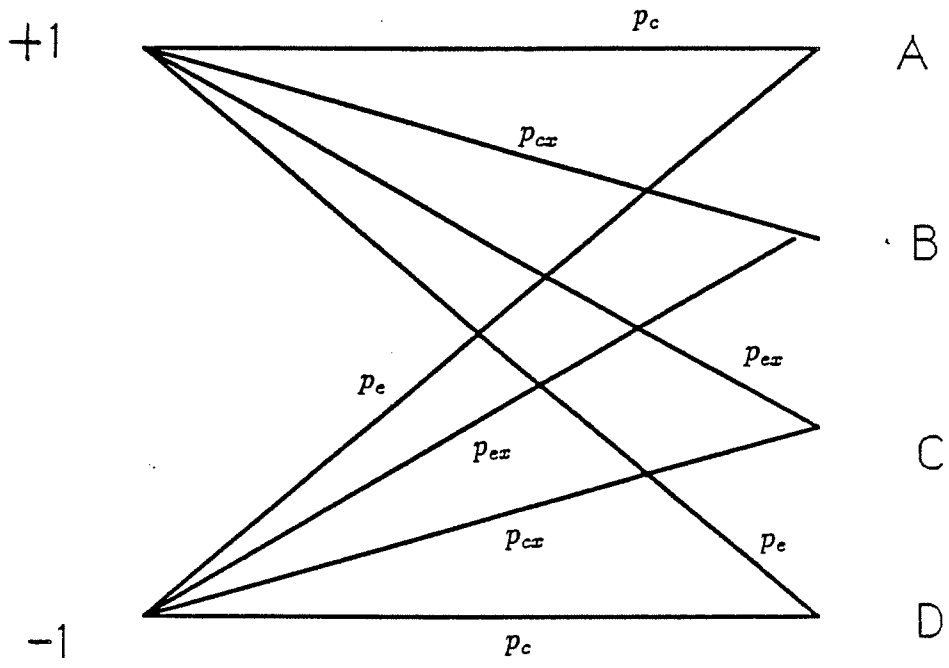

Figure 2.13: Binary input 4-ary output DMC.

where the random variable S denotes side-information. The mutual information $I(X;Y,S)$ is given by $I(X;Y,S) = E_S\{I(X;Y|S)\}$ where E_S denotes the expectation over the random variable S,

$$I(X;Y|s) = \sum_y \sum_x p(y|x,s) q_X(x) \log \frac{p(y|x,s)}{\sum_{x'} p(y|x',s) q_X(x')} \tag{2.14}$$

and s is a particular outcome of the random variable S. When perfect side-information is available, the channel of an AFHSS-MA channel, with the receiver making hard decisions can be modeled as a BSC whose transition probability is a function of $S \in \{H, \overline{H}\}$ where H denotes the event that the hop is hit and $\overline{H}$ denotes the complement of H. Hence using (2.11) and (2.12) the channel capacity C_{PSI}, can be written as [Mce 84]

$$C_{PSI} = I(X;Y|H)P_{hit} + I(X;Y|\overline{H})(1 - P_{hit}) \tag{2.15}$$

where $I(X;Y|H)$ is given by (2.10), $p = \frac{p'}{P_{hit}}$ and

$$p' = \sum_{K'=1}^{K-1} \begin{pmatrix} K-1 \\ K' \end{pmatrix} P(K')\, p_h^{K'}\, (1-p_h)^{K-1-K'}$$

where $P(K')$ is the probability of error given that the hop is by K' interfering users. The mutual information when the hop is not hit $I(X;Y|\overline{H})$, is given by (2.10) with $p = P(0)$. Similarly, when side-information as to the number of interfering users hitting the hop is available, the channel capacity, C_{NUM} can be written as follows

$$C_{NUM} = \sum_{K'=0}^{K} I(X;Y|H^{K'}) \begin{pmatrix} K-1 \\ K' \end{pmatrix} p_h^{K'} (1-p_h)^{K-i-K'} \tag{2.16}$$

where $H^{K'}$ denotes the event that the hop is hit by K' interfering users and $I(X;Y|H^{K'})$ is given by (2.10) with $p = P(K')$.

2.5.3 Throughput

A network is a collection of users operating over a common channel. During the normal operation of a network, there exists a large number of potential users of which only a small subset will try to communicate at a given time. The information to be transmitted by a user is grouped into *packets* before transmission and the transmission is successful only if the packet is received error free. A network is referred to as a *slotted network* if the transmission of the packets between users are synchronized and unslotted if the transmission of the packets are not synchronized. Achieving this synchronocity of packets is generally much easier than achieving synchronization at the hop level. We assume that the transmission of packets are synchronized throughout the thesis.

A useful measure of performance of a network is the throughput W defined as

$$W = (1 - P_p) \cdot K \tag{2.17}$$

where the factor P_p is the probability of incorrectly transmitting a packet across the network where a packet is simply defined to be a fixed number of data bits considered to be a unit of information to be sent over the network. The throughput measures the average number of packets successfully transmitted over the network. In order to make fair comparisons we need to normalize the throughput over the bandwidth and time needed to transmit the packet. We define the normalized throughput w as follows [Pur 86]

$$w = \frac{W \cdot r}{q} \tag{2.18}$$

where r [bits/channel use] is the rate of the code used if any.

When a code that achieves channel capacity is employed, the normalized through-

put can be written as

$$w = \frac{C \cdot K}{q}. \tag{2.19}$$

2.6 Review of Problems

In this section we will look at the problems that will be considered in the following chapters. In Chapter 3, our main goal is to compute the average probability that $|U_1|$ is greater than $|U_{-1}|$ for the first user given that a '+1' was transmitted in a given hop and the hop is hit by a given number of users. That is, we would like to compute the average error probability where the averaging is over the delays, the data bits, the initial phases of the interfering users.

In Chapter 4 we consider the use of Viterbi ratio thresholding [Vit 82] [Vit 85] as a means of quantizing the output of the detector to more than 2 levels provided by hard decisions. In this case, the computation of the channel statistics involves evaluation of the probabilities of the form $Pr\{|U_1| > \theta|U_{-1}|\}$ for some $\theta > 1$. This can easily be done using the same techniques used in Chapter 3. The analysis in Chapter 3 and Chapter 4 will be carried out using the techniqus of spherically symmetric random variables.

In Chapter 5 we consider slow AFHSS-MA networks. Here the main concern is the computation of the probability that a certain number of symbol hits will occur given that a hop is hit. This is important because for an asynchronous, slow FHSS-MA network, when a hop is hit by a small number of interfering users, there is high probability that not all the symbols in the hop will be hit since the hit may be a partial hit. Also it is easy to show that for practical systems when a hop is hit, with high probability it will be hit by a small number of users, usually less than three.

CHAPTER III

PROBABILITY OF ERROR IN AN AFHSS-MA NETWORK

In this chapter, we will derive an expression for the probability of error for an AFHSS-MA network when one binary symbol is transmitted per hop using BFSK modulation with noncoherent detection and when Markov hopping patterns are employed. This expression will yield the exact probability of error when orthogonal BFSK is employed and an approximation when nonorthogonal BFSK is employed. Most of the previous work on AFHSS-MA employing BFSK assume error probability of $\frac{1}{2}$ [Pur 87a] (referred to as the $\frac{1}{2}$-*approximation*) whenever a hop is hit by multiple-access interference. Our results indicate that the $\frac{1}{2}$-approximation is an excessively pessimistic assumption and using this assumption in analyzing the performance of AFHSS-MA networks transmitting one symbol per hop has yielded misleading results.

Before we can derive an expression for the probability of error, we need to introduce the concept of spherically symmetric random vectors and present some known results. Most of the results on spherically symmetric random vectors used in our analysis are due to Lord [Lor 54] and Bird [Bir 85].

3.1 Spherically Symmetric Random Vectors

In this section, we summarize some of the basic results on spherically symmetric random vectors obtained in [Lor 54] [Bir 85]. For a rigorous derivation of the results, the reader is referred to these references.

Let $\mathbf{X}$ be a d-dimensional absolutely continuous random vector with probability density function (pdf) $p(\mathbf{x})$ where $\mathbf{x}$ denotes a realization of $\mathbf{X}$. Then the characteristic function of $\mathbf{X}$ denoted by $\Phi(\mathbf{s})$ is defined as

$$\Phi(\mathbf{s}) = \int \exp(i\mathbf{x} \cdot \mathbf{s}) p(\mathbf{x}) d\mathbf{x} \tag{3.1}$$

where the integration is over the support set of $\mathbf{X}$, $\mathbf{s}$ is a d-dimensional vector in $\Re^d$ (the d-dimensional Eucledian space) and $\mathbf{x} \cdot \mathbf{s}$ denotes the inner product of the vectors $\mathbf{x}$ and $\mathbf{s}$. It is easily seen that $\Phi(\mathbf{s})$ can also be written as follows.

$$\Phi(\mathbf{s}) = E\{\exp(i\mathbf{X} \cdot \mathbf{s})\}.$$

Hence if $\mathbf{X}$ is a sum of n independent random vectors, i.e., $\mathbf{X} = \sum_{i=1}^{n} \mathbf{X}_i$ where the addition of vectors is componentwise, then the characteristic function of $\mathbf{X}$ can be decomposed as follows

$$\Phi(\mathbf{s}) = \Phi_1(\mathbf{s}) \cdots \Phi_n(\mathbf{s}) \tag{3.2}$$

where $\Phi_i(\mathbf{s})$ is the characteristic function of $\mathbf{X}_i$. This process can be reversed to find the pdf of $\mathbf{X}$ when the characteristic function is known, by using the following inversion formula

$$p(\mathbf{x}) = (2\pi)^{-d} \int \exp(-i\mathbf{x} \cdot \mathbf{s}) \Phi(\mathbf{s}) d\mathbf{s} \tag{3.3}$$

where the integration is over $\Re^d$.

A random vector $\mathbf{X}$ is said to spherically symmetric if $p(\mathbf{x})$ is a function of the magnitude of the random vector $R = |\mathbf{X}|$ only, i.e., $p(\mathbf{x}) = f(r)$ where r is a

realization of R. From now on, we assume $\mathbf{X}$ to be spherically symmetric. The infinitesimal volume $d\mathbf{x}$ of (3.1) is given by

$$d\mathbf{x} = r^{d-1} dr d\Sigma_d$$

where Σ_d is the surface of the d-dimensional unit sphere. Also if we let s be the magnitude of the vector $\mathbf{s}$, then

$$\mathbf{x} \cdot \mathbf{s} = rs\cos(\theta)$$

where θ is the angle between $\mathbf{x}$ and $\mathbf{s}$. Thus

$$\Phi(\mathbf{s}) = \int_0^\infty r^{d-1} f(r) dr \int \exp(irs\cos(\theta)) d\Sigma_d \tag{3.4}$$

where the inner integral is over Σ_d and thus the value of the inner integral is independent of the direction of $\mathbf{s}$ and is a function of r and s only. Hence we note that for a spherically symmetric random vector, the characteristic function $\Phi(\mathbf{s})$ is a function of s only, i.e., $\Phi(\mathbf{s}) = \Phi(s)$. From now on the characteristic function Φ will refer to $\Phi(s)$ with the scalar argument s. The inner integral of (3.4) can be evaluated by converting to polar coordinates $(r, \theta_1, \cdots, \theta_{d-1})$ where $\theta_1, \cdots, \theta_{d-2} \in (0, \pi]$ and $\theta_{d-1} \in (0, 2\pi]$ and using the fact that $\Sigma_d = 2\pi^{\frac{1}{2}d}/\Gamma(\frac{1}{2}d)$ where the Gamma function $\Gamma(\cdot)$ is defined as [Abr 72]

$$\Gamma(z) = \int_0^\infty t^{z-1} e^{-t} dt$$

and $\Gamma(n+1) = n!$ for integer values of n. Thus,

$$\Phi(s) = (2\pi)^{\frac{1}{2}d} s^{-\frac{1}{2}d+1} \int_0^\infty r^{\frac{1}{2}d} J_{\frac{1}{2}d-1}(rs) f(r) dr \tag{3.5}$$

where $J_\nu(\cdot)$ denotes the Bessel function of the first kind defined as [Abr 72]

$$J_\nu(z) = \frac{1}{\pi}\int_0^\pi \cos(z\sin(\theta) - \nu\theta) d\theta - \frac{\sin(\nu\pi)}{\pi}\int_0^\infty e^{z\sinh(t) - \nu t} dt.$$

Since $\Phi(\cdot)$ is a function of s only we may obtain the following formula for $f(r)$ by applying similar procedures to (3.3).

$$f(r) = (2\pi)^{-\frac{1}{2}d} r^{-\frac{1}{2}d+1} \int_0^\infty s^{\frac{1}{2}d} J_{\frac{1}{2}d-1}(rs)\Phi(s)ds. \tag{3.6}$$

If we define a probability function $p(r)$ such that $p(r)dr$ denotes the probability $Pr\{r < |\mathbf{X}| \leq r + dr\}$ then $p(r)$ is the pdf for $|\mathbf{X}|$ where $f(r)$ is the pdf for X. We note that

$$\begin{aligned} p(r) &= f(r) r^{d-1} \Sigma_d \\ &= \frac{2\pi^{\frac{1}{2}d} r^{d-1} f(r)}{\Gamma(\frac{1}{2}d)} \end{aligned}$$

since $r^{d-1}\Sigma_d$ is the surface area of a sphere with radius r in d-dimensions. By defining Λ_α as [Jah 45]

$$\Lambda_\alpha(z) = \Gamma(\alpha+1)(\frac{1}{2}z)^{-\alpha} J_\alpha(z)$$

it can be shown that

$$\Phi(s) = \int_0^\infty p(r) \Lambda_{\frac{1}{2}d-1}(rs) dr \tag{3.7}$$

and

$$p(r) = 2^{-\frac{1}{2}d+1} \left\{ \Gamma(\frac{1}{2}s) \right\}^{-1} \int_0^\infty (rs)^{\frac{1}{2}d} J_{\frac{1}{2}d-1}(rs)\Phi(s)ds. \tag{3.8}$$

Let us denote the cumulative distribution function (CDF) of $R = |\mathbf{X}|$ to be

$$F(r) = \int_0^r p(u)du.$$

Then it can be shown that the following relations hold between the CDF and the characteristic function of the random vector $\mathbf{X}$.

$$\Phi(s) = 2^{\frac{1}{2}d-2} \Gamma\left(\frac{1}{2}s\right) s^{2-\frac{1}{2}d} \int_0^\infty r^{1-\frac{1}{2}d} J_{\frac{1}{2}d}(rs) F(r) dr \tag{3.9}$$

and

$$F(r) = 2^{-\frac{1}{2}d+1} \left\{ \Gamma(\frac{1}{2}s) \right\}^{-1} r^{\frac{1}{2}d} \int_0^\infty s^{\frac{1}{2}d-1} J_{\frac{1}{2}d}(rs)\Phi(s)dr. \tag{3.10}$$

For the special cases of $d = 2, 3$, equations (3.7) and (3.10) are simplified as follows.

When $d = 2$,

$$\begin{aligned} \Phi(s) &= \int_0^\infty J_0(rs)p(r)dr \\ F(r) &= r\int_0^\infty J_1(rs)\Phi(s)ds. \end{aligned} \tag{3.11}$$

When $d = 3$

$$\begin{aligned} \Phi(s) &= \int_0^\infty \left(\frac{\sin(rs)}{rs}\right) p(r)dr \\ F(r) &= \left(\frac{2r}{\pi}\right)\int_0^\infty \left(\frac{\sin(rs)}{rs} - \cos(rs)\right)\Phi(s)ds. \end{aligned} \tag{3.12}$$

The relations (3.11) and (3.12) between the characteristic function and the distribution functions of a spherically symmetric random vector are useful when the characteristic function of the random vector is relatively easy to compute (usually applying (3.2)) but the distribution function is not. This is exactly the case in the study of the probability of error in AFHSS-MA networks. Next we will present some known results on the characteristic function of a spherically symmetric random vector that simplifies its evaluation in many cases.

In the following argument, we will show that given a d-dimensional spherically symmetric random vector $\mathbf{X}$, the characteristic function $\Phi(s)$ of $\mathbf{X}$ projected onto a subspace of dimension $q \leq d$ passing through the origin is identical to that of the original vector $\mathbf{X}$. Clearly the projection results in another spherically symmetric random vector with pdf

$$p_q(x'_1, \cdots, x'_q) = \int p_d(x_1, \cdots, x_d)dx''_1 \cdots dx''_{d-q}$$

in Cartesian coordinates $(x_1, \cdots, x_d)$ where $(x'_1, \cdots, x'_q)$ as the coordinates in the space of projection and $x''_i \in \{x_1, \cdots, x_d\}$. The characteristic function of the pro-

jected vector is written as

$$\begin{aligned}\Phi_q(s_1,\cdots,s_q) &= \int p_q(x'_1,\cdots,x'_q)e^{i(s_1x'_1+,\cdots,+s_qx'_q)}dx'_1\cdots dx'_q \\ &= \int p_d(x_1,\cdots,x_d)e^{i(s_1x'_1+,\cdots,+s_qx'_q)}dx'_1\cdots dx'_d,\end{aligned}$$

that is

$$\Phi_q(s_1,\cdots,s_q) = \Phi_d(s_1,\cdots,s_q,0,\cdots,0) \tag{3.13}$$

where Φ_d is the characteristic function of the original d-dimensional random vector. Now, since the projected random vector is also spherically symmetric, both sides of (3.13) are functions of only $s = \sqrt{s_1^2+\cdots+s_q^2}$ and hence

$$\Phi_q(s) = \Phi_s(s) \tag{3.14}$$

Now consider a random vector $\mathbf{Y}$ which is a sum of m statistically independent and spherically symmetric random vectors, $\mathbf{W}_i$. Then by (3.2) we know that the characteristic function of $\mathbf{Y}$ is given as

$$\Phi_{\mathbf{Y}}(\mathbf{s}) = \Pi_{i=1}^{m}\Phi_{\mathbf{W}_i}(s) \tag{3.15}$$

where $\Phi_{\mathbf{W}_i}(s)$ is the characteristic function of $\mathbf{W}_i$. Hence the characteristic function of $\mathbf{Y}$ is a function of s only and this implies that the sum of independent and spherically symmetric random vectors is also a spherically symmetric random vector.

The expression that is directly needed in computing the probability of error of an AFHSS-MA network is that of the magnitude of one 2-dimensional spherically symmetric random vector being greater than that of another, independent, 2-dimensional spherically symmetric random vector. Let U_1 and U_{-1} be two statistically independent, 2-dimensional spherically symmetric random vectors. Denote the characteristic functions of U_1 and U_{-1} and their magnitudes by $\Phi_1(s)$, $\Phi_{-1}(s)$ and r_1, r_{-1} respec-

tively. Then the probability of r_{-1} being greater than r_1 may be written as follows

$$\Pr(r_1 < r_{-1}) = \int_0^\infty \Pr(r_1 < r_{-1}|r_{-1})p(r_{-1})dr_{-1}.$$

From (3.11) we know that

$$\Pr(r_1 < r_{-1}|r_{-1}) = r_{-1}\int_0^\infty J_1(r_{-1}s)\Phi_1(s)ds.$$

Combining these two expressions we have

$$\Pr(r_1 < r_{-1}) = \int_0^\infty \Phi_1(s)\int_0^\infty r_{-1}p(r_{-1})J_1(r_{-1}s)dr_{-1}ds. \tag{3.16}$$

By differentiating the expression for $\Phi(s)$ in (3.11) we find that

$$\int_0^\infty r_{-1}p(r_{-1})J_1(r_{-1}s)dr_{-1} = -\frac{d\Phi_{-1}(s)}{ds}.$$

Hence we have an expression for $\Pr(r_1 < r_{-1})$ in terms of the characteristic functions of U_1 and U_{-1}.

$$\Pr(r_1 < r_2) = -\int_0^\infty \Phi_1(s)\frac{d\Phi_{-1}(s)}{ds}ds. \tag{3.17}$$

This concludes the summary of important results on spherically symmetric random vectors.

3.2 Derivation of an Expression for the Probability of Error

In this section, we will use the background developed in Chapter 2 and the previous section on spherically symmetric random vectors to derive an expression for the probability of error in an AFHSS-MA network when one binary symbol is transmitted per hop using BFSK signalling and Markov hopping patterns.

The following is some notation that will be used in this chapter. Let N be the number of different power levels as seen by the first receiver, which we call power level groups. The number of users in each power level group is denoted by $\overline{K}_i$,

$i = 1, \cdots, N$. Let $\mathbf{K} = (\overline{k}_1, \cdots, \overline{k}_N)$ be the interference pattern vector with each component $\overline{k}_i$ representing the number of interfering users from each power level group that hit the hop under consideration and let $\boldsymbol{\alpha} = (\alpha_1, \cdots, \alpha_{K'+1})$ where α_k denotes the amplitude of the signal due to the k-th user.. Obviously $\sum_{i=1}^{N} \overline{K}_i = K-1$ and $\sum_{i=1}^{N} \overline{k}_i = K'$ where K is the number of active users in the network and K' is the number of interfering users sharing the slot.. We also define the vectors $\mathbf{p}$ and $\mathbf{b}$ to be $\mathbf{p} = (p_1, \cdots, p_{K'+1})$, $\mathbf{b} = (b_1, \cdots, b_{K'+1})$ where p_k and b_k are the normalized delay and the data bits of the k-th user as defined in Chapter 2.

First we will derive an expression for the probability of error conditioned on the delays ($\mathbf{p}$), the data bits ($\mathbf{b}$) and the power levels ($\mathbf{K}$) given that a hop is hit by K' interfering users using the fact that the outputs of the integrators of the matched filters are spherically symmetric. We will then average this over the appropriate random variables to obtain the average probability of error.

We consider the probability of error for the first user transmitting on a slot with center frequency f_1. A total of $K'+1$ users are assumed to be sharing the slot. Under the model described in Chapter 2, the outputs of the integrators of the matched filters given that a '+1' was transmitted were shown to be given by (2.7) which is repeated here,

$$\begin{aligned} U_1 &= z_1 + \sqrt{\frac{E_b}{N_0}} e^{i\varphi_1} + \sqrt{\frac{E_b}{N_0}} \sum_{k=2}^{K'+1} e^{-i\{2\pi f_{IF}\tau_k + \theta_k(1,p_k,b_k)\}} e^{i\varphi_k} A'_k(1, p_k, b_k) \\ U_{-1} &= z_{-1} + \rho\sqrt{\frac{E_b}{N_0}} e^{i\varphi_1} + \sqrt{\frac{E_b}{N_0}} \sum_{k=2}^{K'+1} e^{-i\{2\pi f_{IF}\tau_k + \theta_k(-1,p_k,b_k)\}} e^{i\varphi_k} A'_k(-1, p_k, b_k). \end{aligned}$$

We assume that the initial phases of the users are i.i.d. with a uniform distribution on $(-\pi, \pi]$. Then conditioned on $\mathbf{p}$, $\mathbf{b}$ and $\mathbf{K}$, the terms $2\pi f_{IF}\tau_k + \theta_k(l, p_k, b_k)$ and $A'_k(l, p_k, b_k)$, $l \in \{+1, -1\}$, are constants and the phase terms $e^{-i\{2\pi f_{IF}\tau_k + \theta_k(l,p_k,b_k)\}} e^{i\varphi_k}$ may be replaced by $e^{i\varphi'_k(l)}$ where $\{\varphi'_k(l) mod(\pi)\}$ are i.i.d. and uniformly distributed

in $(-\pi, \pi]$ for $l \in \{+1, -1\}$ since we need only consider the phase terms $mod(\pi)$. Hence the expressions for U_1 and U_{-1} can be simplified as follows

$$\begin{aligned} U_1 &= z_1 + \sqrt{\frac{E_b}{N_0}} e^{i\varphi_1} + \sum_{k=2}^{K'+1} e^{i\varphi_k'(1)} A_k'(1, p_k, b_k) \\ U_{-1} &= z_{-1} + |\rho| \sqrt{\frac{E_b}{N_0}} e^{i\varphi_1'} + \sum_{k=2}^{K'+1} e^{i\varphi_k'(-1)} A_k'(-1, p_k, b_k). \end{aligned} \tag{3.18}$$

where $\varphi_1' = \theta(\rho) + \varphi_1$ where $\theta(\rho)$ denotes the phase of ρ. Now it is clear that U_1 and U_{-1} are sums of independent and spherically symmetric complex random variables and hence they themselves are spherically symmetric conditioned on $\mathbf{p}$, $\mathbf{b}$ and $\mathbf{K}$. Since the noncoherent detector chooses the largest of $|U_1|$ and $|U_{-1}|$ as its estimate, the probability of error conditioned on $\mathbf{p}$, $\mathbf{b}$, $\mathbf{K}$ can be written as follows

$$\begin{aligned} P_e(\mathbf{p}, \mathbf{b}, \mathbf{K}) &= \Pr\{|U_{-1}| > |U_1| \mid b_1 = +1, \mathbf{p}, \mathbf{b}, \mathbf{K}\} \Pr\{b_1 = +1\} \\ &+ \Pr\{|U_1| > |U_{-1}| \mid b_0 = -1, \mathbf{p}, \mathbf{b}, \mathbf{K}\} \Pr\{b_1 = -1\}. \end{aligned}$$

If we assume that the data bits of the first user are equi-probable, then $P_e(\mathbf{p}, \mathbf{b}, \mathbf{K})$ can be simplified to

$$P_e(\mathbf{p}, \mathbf{b}, \mathbf{K}) = \Pr\{|U_{-1}| > |U_1| \mid b_1 = +1, \mathbf{p}, \mathbf{b}, \mathbf{K}\}.$$

We note from (3.18) and (2.7) that $|U_1|$ and $|U_{-1}|$ are not statistically independent since the noise terms z_1 and z_{-1} are correlated. But Theorem 3.1 given below shows that $|U_1|$ and $|U_{-1}|$ are statistically independent given $\mathbf{p}, \mathbf{b}, \mathbf{K}$, when orthogonal BFSK is employed, i.e., when $|\rho| = 0$. Before we can prove Theorem 3.1, we first need to establish the following Lemma.

Lemma III.1 *Let X and Y be two independent and identically distributed random variables with uniform distribution on $(-\pi, \pi]$. Then $V = (X + Y) mod(\pi)$ and $W = (X + c) mod(\pi)$ are independent where c is a constant.*

proof

It is easy to show that V has a uniform distribution on $(-\pi, \pi]$. Also,

$$\Pr\{V \leq v | W = w\} = \Pr\{(c' + Y) mod(\pi) \leq v\}$$

where $c' = w - c$ is a constant. Since $(c' + Y) mod(\pi)$ has a uniform distribution on $(-\pi, \pi]$,

$$\Pr\{V \leq v | W = w\} = \Pr\{V \leq v\}. \quad \square$$

Using this Lemma we may prove the following Theorem.

Theorem III.1 *The decision variables* $|U_1|$ *and* $|U_{-1}|$ *are statistically independent given* $\mathbf{p}, \mathbf{b}, \mathbf{K}$ *when* $|\rho| = 0$.

proof

When $|\rho| = 0$, U_1 and U_{-1}, given $\mathbf{p}, \mathbf{b}, \mathbf{K}$ can be written as follows.

$$\begin{aligned} U_1 &= z_1 + \sqrt{\frac{E_b}{N_0}} e^{i\varphi_1} + \sum_{k=2}^{K'+1} e^{i\varphi_k'(1)} A_k'(1, p_k, b_k) \\ U_{-1} &= z_{-1} + \sum_{k=2}^{K'+1} e^{i(\varphi_k'(1)+c_k)} A_k'(-1, p_k, b_k) \end{aligned}$$

where c is a constant. Hence, we can write

$$\begin{aligned} U_1 e^{-i\varphi_1} &= z_1' + \sqrt{\frac{E_b}{N_0}} + \sum_{k=2}^{K'+1} e^{i(\varphi_k'(1)-\varphi_1)} A_k'(1, p_k, b_k) \\ U_{-1} &= z_{-1} + \sum_{k=2}^{K'+1} e^{i(\varphi_k'(1)+c_k)} A_k'(-1, p_k, b_k) \end{aligned}$$

where $z_1' = z_1 e^{-i\varphi_1}$. Now using Lemma 3.1, we see that $(\varphi_k'(1) - \varphi_1) mod(\pi)$ and $(\varphi_k'(1) + c_k) mod(\pi)$ are independent for $k = 1, \cdots, K' + 1$. Hence, $U_1 e^{-i\varphi_1}$ and U_{-1} are independent. Also, since $|U_1| = |U_1 e^{-i\varphi_1}|$, $|U_1|$ and $|U_2|$ are independent. $\square$

To make the analysis tractable for the case when $|\rho| > 0$, we make the assumption that $|U_1|$ and $|U_{-1}|$ are independent for these cases and use (3.17). Hence the

probability of error is written as follows (an approximation when $|\rho| > 0$.)

$$P_e(\mathbf{p}, \mathbf{b}, \mathbf{K}) = -\int_0^\infty \Phi_1(s) \frac{d\Phi_{-1}(s)}{ds} ds.$$

Let $\overline{\Phi}_1(s)$ and $\overline{\Phi}_{-1}(s)$ to be

$$\begin{aligned} \overline{\Phi}_1(s) &= \Pi_{k=2}^{K'+1} J_0\left(A'_k(1, p_k, b_k)s\right) \\ \overline{\Phi}_{-1}(s) &= \Pi_{k=2}^{K'+1} J_0\left(A'_k(-1, p_k, b_k)s\right) \end{aligned}$$

which are the characteristic functions of the contributions of the multiple-access interferences on the decision variables U_1, U_{-1}. Let $J_n(\cdot)$ denotes the Bessel function of the first kind of integer order n defined by [Abr 72]

$$J_n(z) = \frac{1}{\pi} \int_0^\pi \cos(z \sin(\theta) - n\theta) d\theta.$$

Then $\Phi_1(s)$ and $\Phi_{-1}(s)$ can easily shown to be the following using the fact that the characteristic function of the projection of a spherically symmetric random vector is identical to that of the original vector and (3.2).

$$\begin{aligned} \Phi_1(s) &= e^{-\frac{s^2}{4}} J_0\left(\sqrt{\frac{E_b}{N_0}} s\right) \overline{\Phi}_1(s) \\ \Phi_{-1}(s) &= e^{-\frac{s^2}{4}} J_0\left(|\rho| \sqrt{\frac{E_b}{N_0}} s\right) \overline{\Phi}_{-1}(s). \end{aligned} \tag{3.19}$$

Hence $\frac{d\Phi_{-1}(s)}{ds}$ can be computed to be

$$\begin{aligned} \frac{d\Phi_{-1}(s)}{ds} &= -e^{-\frac{s^2}{4}} \left[\left(\frac{s}{2} J_0\left(|\rho| \sqrt{\frac{E_b}{N_0}} s\right) + |\rho| \sqrt{\frac{E_b}{N_0}} J_1\left(|\rho| \sqrt{\frac{E_b}{N_0}} s\right) \right) \overline{\Phi}_{-1}(s) \right. \\ &\quad \left. - J_0\left(|\rho| \sqrt{\frac{E_b}{N_0}} s\right) \frac{d\overline{\Phi}_{-1}(s)}{ds} \right]. \end{aligned}$$

Now if we further define $\overline{\Phi}_{1,-1}(s)$ as

$$\begin{aligned} \overline{\Phi}_{1,-1}(s) &= \overline{\Phi}_1(s) \left[\left(\frac{s}{2} J_0\left(|\rho| \sqrt{\frac{E_b}{N_0}} s\right) + |\rho| \sqrt{\frac{E_b}{N_0}} J_1\left(|\rho| \sqrt{\frac{E_b}{N_0}} s\right) \right) \overline{\Phi}_{-1}(s) \right. \\ &\quad \left. - J_0\left(|\rho| \sqrt{\frac{E_b}{N_0}} s\right) \frac{\overline{\Phi}_{-1}(s)}{ds} \right], \end{aligned}$$

then $P_e(\mathbf{p}, \mathbf{b}, \mathbf{K})$ can be written as

$$P_e(\mathbf{p}, \mathbf{b}, \mathbf{K}) = \int_0^\infty e^{-\frac{s^2}{2}} J_0\left(\sqrt{\frac{E_b}{N_0}}s\right) \overline{\Phi}_{1,-1}(s)ds. \tag{3.20}$$

Straightforward computation yields

$$\frac{d\overline{\Phi}_{-1}(s)}{ds} = -\sum_{k=2}^{K'+1} A'_k(-1, p_k, b_k) J_1(A'_k(-1, p_k, b_k)s) \Pi_{i\neq k} J_0(A'_i(-1, p_i, b_i)s).$$

Hence $\overline{\Phi}_{1,-1}(s)$ is given by

$$\begin{aligned}
\overline{\Phi}_{1,-1}(s) &= \left[\frac{s}{2} J_0\left(|\rho|\sqrt{\frac{E_b}{N_0}}s\right) + |\rho|\sqrt{\frac{E_b}{N_0}} J_1\left(|\rho|\sqrt{\frac{E_b}{N_0}}s\right)\right] \\
&\times \Pi_{k=2}^{K'+1} \left[J_0\left(A'_k(1, p_k, b_k)s\right) J_0\left(A'_k(-1, p_k, b_k)s\right)\right] \\
&+ J_0\left(|\rho|\sqrt{\frac{E_b}{N_0}}s\right) \sum_{k=2}^{K'+1} A'_k(-1, p_k, b_k) J_1\left(A'_k(-1, p_k, b_k)s\right) J_0\left(A'_k(1, p_k, b_k)s\right) \\
&\times \Pi_{i\neq k} \left[J_0\left(A'_i(1, p_i, b_i)s\right) J_0\left(A'_i(-1, p_i, b_i)s\right)\right].
\end{aligned} \tag{3.21}$$

This together with (3.20) gives the desired expression for the probability of error conditioned on $\mathbf{p}$, $\mathbf{b}$ and $\mathbf{K}$.

3.2.1 Averaging over the Random Variables

In this section, we consider the case when the data bits b_k's and the delays p_k's are random variables. In this case, we need to average (3.20) over $\mathbf{p}$ and $\mathbf{b}$ and evaluate $P_e(\mathbf{K}) = E_{\mathbf{p},\mathbf{b}}\{P_e(\mathbf{p}, \mathbf{b}, \mathbf{K})\}$ which can be written as

$$\begin{aligned}
E_{\mathbf{p},\mathbf{b}}\{P_e(\mathbf{p}, \mathbf{b}, \mathbf{K})\} &= E_{\mathbf{p},\mathbf{b}}\left\{\int_0^\infty e^{-\frac{s^2}{2}} J_0\left(\sqrt{\frac{E_b}{N_0}}s\right) \overline{\Phi}_{1,-1}(s)\right\} ds \\
&= \int_0^\infty e^{-\frac{s^2}{2}} J_0\left(\sqrt{\frac{E_b}{N_0}}s\right) E_{\mathbf{p},\mathbf{b}}\{\overline{\Phi}_{1,-1}(s)\} ds.
\end{aligned} \tag{3.22}$$

We assume that b_k's are i.i.d. and are equally likely to be '+1' or '−1'. We also assume that p_k's are i.i.d. and uniformly distributed on $(-1, +1]$ and that p_k's and b_k's are also independent. These naturally arising assumptions are usually made in the analysis of AFHSS-MA networks [Ger 88].

Now, under these assumptions we can write $E_{\mathrm{p,b}}\{\overline{\Phi}_{1,-1}(s)\}$ as follows using the fact that the expectation of products of independent random variables is the product of the expectations of the individual random variables.

$$\begin{aligned} E_{\mathrm{p,b}}\{\overline{\Phi}_{1,-1}(s)\} &= \left[\frac{s}{2}J_0\left(|\rho|\sqrt{\frac{E_b}{N_0}}s\right)+|\rho|\sqrt{\frac{E_b}{N_0}}J_1\left(|\rho|\sqrt{\frac{E_b}{N_0}}s\right)\right] \\ &\times \Pi_{k=2}^{K'+1}\left[E_{p,b}\left\{J_0\left(A'_k(1,p,b)s\right)J_0(A'_k(-1,p,b)s)\right\}\right] \\ &+ J_0\left(|\rho|\sqrt{\frac{E_b}{N_0}}s\right) \\ &\times \sum_{k=2}^{K'+1} E_{p,b}\left\{A'_k(-1,p,b)J_1\left(A'_k(-1,p,b)s\right)J_0\left(A'_k(1,p,b)s\right)\right\} \\ &\times \Pi_{i\neq k}\left[E_{p,b}\left\{J_0\left(A'_i(1,p,b)s\right)J_0\left(A'_i(-1,p,b)s\right)\right\}\right] \end{aligned} \tag{3.23}$$

where we dropped the dependence of p_k's and b_k's on k in the notation. Now if we group the product and the summation into groups of equal power levels, we have

$$\begin{aligned} E_{\mathrm{p,b}}\{\overline{\Phi}_{1,-1}(s)\} &= \left[\frac{s}{2}J_0\left(|\rho|\sqrt{\frac{E_b}{N_0}}s\right)+|\rho|\sqrt{\frac{E_b}{N_0}}J_1\left(|\rho|\sqrt{\frac{E_b}{N_0}}s\right)\right] \\ &\times \Pi_{i=1}^{N}\left[E_{p,b}\left\{J_0(A'_i(1,p,b)s)J_0(A'_i(-1,p,b)s)\right\}\right]^{\overline{k}_i} \\ &+ J_0\left(|\rho|\sqrt{\frac{E_b}{N_0}}s\right) \\ &\times \sum_{i=1}^{N}\Big[\overline{k}_i E_{p,b}\left\{A'_i(-1,p,b)J_1(A'_i(-1,p,b)s)J_0(A'_i(1,p,b)s)\right\} \\ &\times \left(E_{p,b}\left\{J_0(A'_i(1,p,b)s)J_0(A'_i(-1,p,b)s)\right\}\right)^{\overline{k}_i-1} \\ &\times \Pi_{j\neq i}^{N}\left(E_{p,b}\left\{J_0(A'_j(1,p,b)s)J_0(A'_j(-1,p,b)s)\right\}\right)^{\overline{k}_j}\Big] \end{aligned} \tag{3.24}$$

where the subscript of A' now denotes the power level group.

Equation (3.24) with equation (3.22) yields the desired general expression for the average probability of error given that a hop is hit by an interference vector $\mathbf{K}$.

We observe that for each point s we choose in our numerical integration of (3.22), we need to numerically compute the expectations

$$E_{p,b}\left\{A'_i(-1,p,b)J_1(A'_i(-1,p,b)s)J_0(A'_i(1,p,b)s)\right\} \tag{3.25}$$

and

$$E_{p,b}\left\{J_0(A_i'(1,p,b)s)J_0(A_i'(-1,p,b)s)\right\} \tag{3.26}$$

for each power level i for a given signal-to-noise ratio. We will see in the numerical results section that the evaluation of these two expressions dominate the computational complexity needed to evaluate the probability of error. But we note that the expectations (3.25) and (3.26) do not depend on K' which implies that once we have computed these expectations, the probability of error for different K's may be evaluated very quickly. This simplicity is a result of the fact that the network is assumed to employ Markov hopping patterns [Ger 88].

It is worthwhile at this point to see how this expression would be simplified if all the users in the network had the same power level as seen by the first receiver, as in a satellite network. If we set $\alpha_k = \alpha_1$ for all $k = 1, 2, \cdots K$, then $E_{\mathrm{p,b}}\{\overline{\Phi}_{1,-1}(s)\}$ simplifies to

$$\begin{aligned} E_{\mathrm{p,b}}\{\overline{\Phi}_{1,-1}(s)\} &= \left[\frac{s}{2}J_0\left(|\rho|\sqrt{\frac{E_b}{N_0}}s\right) + |\rho|\sqrt{\frac{E_b}{N_0}}J_1\left(|\rho|\sqrt{\frac{E_b}{N_0}}s\right)\right] \\ &\times \left[E_{p,b}\left\{J_0(A(1,p,b)s)J_0(A(-1,p,b)s)\right\}\right]^{K'} \\ &+ J_0\left(|\rho|\sqrt{\frac{E_b}{N_0}}s\right) \\ &\times \cdot K' \cdot E_{p,b}\left\{A(-1,p,b)J_1(A(-1,p,b)s)J_0(A(1,p,b)s)\right\} \\ &\times \left[E_{p,b}\left\{J_0(A(1,p,b)s)J_0(A(-1,p,b)s)\right\}\right]^{K'-1} \end{aligned} \tag{3.27}$$

where we further dropped the dependence of A on the power level. If we simplify the problem by assuming that orthogonal BFSK is employed, i.e., $|\rho| = 0$, then $E_{\mathrm{p,b}}\{\overline{\Phi}_{1,-1}(s)\}$ further simplifies to

$$\begin{aligned} E_{\mathrm{p,b}}\{\overline{\Phi}_{1,-1}(s)\} &= \frac{s}{2}\left[E_{p,b}\left\{J_0(A'(1,p,b)s)J_0(A'(-1,p,b)s)\right\}\right]^{K'} \\ &+ K' \cdot E_{p,b}\left\{A'(-1,p,b)J_1(A'(-1,p,b)s)J_0(A'(1,p,b)s)\right\} \\ &\times \left[E_{p,b}\left\{J_0(A'(1,p,b)s)J_0(A'(-1,p,b)s)\right\}\right]^{K'-1} \end{aligned} \tag{3.28}$$

and (3.22) gives the exact probability of error in this case. We may simply replace the $A'(l,p,b)$'s in the above equation with $A(l,p,b)$ to account for the case when all users have the same power level and orthogonal BFSK is used. In these cases we may compute $P_e(\mathbf{K}) = P_e(K')$, the probability of error for a hop given that the hop is hit by K' users with the same power as the first user using (3.22) and thus compute the average probability of error P_e for the first user using

$$P_e = \sum_{K'=0}^{K-1} \binom{K-1}{K'} p_h^{K'} (1-p_h)^{(K-K')} P_e(K'). \tag{3.29}$$

For the general case, the average probability of error for the first user may be written as [Ger 88]

$$\begin{aligned} P_e &= E_{\mathbf{K}}\{P_e(\mathbf{K})\} \\ &= \sum_{\overline{k}_1=0}^{\overline{K}_1} \cdots \sum_{\overline{k}_N=0}^{\overline{K}_N} P_e(\mathbf{K}) \ \Pi_{i=1}^{N} \left\{ \binom{\overline{K}_i}{\overline{k}_i} p_h^{\overline{k}_i} (1-p_h)^{\overline{K}_i - \overline{k}_i} \right\} \\ &= \int_0^\infty e^{-\frac{s^2}{2}} J_0\left(\sqrt{\frac{E_b}{N_0}} s\right) \\ &\times \left[\sum_{\overline{k}_1=0}^{\overline{K}_1} \cdots \sum_{\overline{k}_N=0}^{\overline{K}_N} E_{\mathbf{p},\mathbf{b}}\left\{\overline{\Phi}_{1,-1}(s)\right\} \Pi_{i=1}^{N} \left\{ \binom{\overline{K}_i}{\overline{k}_i} p_h^{\overline{k}_i} (1-p_h)^{\overline{K}_i - \overline{k}_i} \right\} \right] ds. \end{aligned} \tag{3.30}$$

3.2.2 Nonorthogonal BFSK Signalling

Here we discuss the reason for considering non-orthogonal FSK where $|\rho| > 0$. As described below, the basic idea behind using non-orthogonal FSK in AFHSS-MA networks is to provide a trade-off between the number of errors caused by the background noise and the number of errors caused by multiple-access hits.

If we assume that the error probability is $\frac{1}{2}$ whenever a hop is hit, the fact that the system performance will be dominated by multiple-access interference rather than background noise for sufficiently large signal-to-noise ratios leads to the following

idea. If we use non-orthogonal FSK instead of orthogonal FSK ($|\rho| = 0$), we will be able to increase the number of slots available to the network for a given fixed bandwidth since the spacing between the BFSK tones decrease and hence the bandwidth required for a frequency slot decreases. This in effect reduces p_h. This is done at the cost of higher quiescent error probability since increasing $|\rho|$ increases the error probability when the hop is not hit [Pro 83]. These two competing factors will result in an optimum $|\rho|$ that minimizes the average error probability and since the multiple-access hits are far more detrimental than the quiescent errors with the $\frac{1}{2}$-approximation, the optimal $|\rho|$ will be greater than zero. In general this optimum $|\rho|$ will depend on the number of users in the network and the signal-to-noise ratio. Now if we define μ to be

$$\mu = \frac{\Delta f}{\Delta f_{ortho}}$$

where Δf is the frequency separation employed and $\Delta f_{ortho} = \frac{1}{2T_h}$ is the minimum frequency separation needed for the tones to be orthogonal. Then the resulting number of slots available is simply given by

$$q = \left\lfloor \frac{q_{ortho}}{\mu} \right\rfloor \geq q_{ortho}$$

where q_{ortho} is the number of slots available when $\Delta f = \Delta f_{ortho}$ and $\lfloor x \rfloor$ denotes the largest integer not exceeding x. Thus with Markov hopping patterns, p_h decreases from $\frac{2}{q_{ortho}}$ to $\frac{2}{q}$ as we decrease the frequency separation from Δf_{ortho} to Δf.

Though this is an interesting idea, and it can be shown that with the $\frac{1}{2}$-approximation, the gain achieved by using $|\rho| > 0$ can be as high as two orders of magnitude when coding is employed, it will be shown in the numerical results section that if we use the results developed in this chapter for the probability of error, we see that the gain achieved by using non-orthogonal signalling is practically negligible.

3.2.3 Independent Hopping Patterns

Up to now, we have considered Markov hopping patterns to simplify the analysis and obtain numerically easy to compute results and also since for practical values of q, it is expected to provide a close approximation to the performance of a system using independent hopping patterns. In this subsection we will briefly discuss the changes that should be made in order to consider independent hopping patterns and derive an upper bound and a lower bound on the average probability of error. Using these bounds, it will be shown in the numerical results section that for practical values of q, the probability of error when Markov patterns are assumed is a very good approximation to the probability of error when independent hopping patterns are assumed. First let us define the following parameters

- K_1 = The number of interfering users causing partial hits.
- K_2 = The number of interfering users causing full hits to tone '+1'.
- K_3 = The number of interfering users causing full hits to tone '−1'.
- K_4 = The number of interfering users causing partial hits to both tones

and $K' = K_1 + K_2 + K_3 + K_4$. Also let p'_k, $k = 1, \cdots, K'+1$ be i.i.d. and uniform in $(-1, 0)$, then the outputs of the matched filters U_1^i and U_{-1}^i can be written as

$$\begin{aligned} U_1^i &= \sqrt{\frac{E_b}{N_0}} e^{i\varphi_1} + \sum_{k_1=0}^{K_1} e^{i\varphi'_{k_1}(1)} A'_{k_1}(1, p_k, b_k) \\ &+ \sum_{k_2=0}^{K_2} e^{i\varphi'_{k_2}(1)} A'_{k_2}(1, 0, 1) \\ &+ \sum_{k_4=0}^{K_4} e^{i\varphi'_{k_4}(1)} \left[A'_{k_4}(1, p'_{k_4}, b^{(1)_{k_4}}) + A'_{k_4}(1, (1+p'_{k_4}), b^2_{k_4}) \right] \\ &+ z_1 \end{aligned}$$

$$
\begin{aligned}
U_{-1}^{i} &= |\rho|\sqrt{\frac{E_b}{N_0}}e^{i\varphi_1'} + \sum_{k_1=0}^{K_1} e^{i\varphi_{k_1}'(-1)} A_{k_1}'(2, p_{k_1}, b_{k_1}) \\
&+ \sum_{k_3=0}^{K_3} e^{i\varphi_{k_3}'(-1)} A_{k_3}'(-1, 0, -1) \\
&+ \sum_{k_4=0}^{K_4} e^{i\varphi_{k_4}'(-1)} \left[A_{k_4}'(-1, p_{k_4}', b_{k_4}^{(1)}) + A_{k_4}'(-1, (1+p_{k_4}'), b_{k_4}^{(2)})\right] \\
&+ z_{-1}
\end{aligned}
$$

where as before $A_k'(l, p_k, b_k) = \left(\frac{\alpha_k}{\alpha_1}\right)\sqrt{\frac{E_b}{N_0}}A_k(l, p_k, b_k)$ and $b_k^{(i)}$, $i \in \{+1, -1\}$ are independent and equally likely to be '-1' or '$+1$'. The phase terms are defined similarly as before. Now, if we define $\overline{\Phi}_1(s)$ and $\overline{\Phi}_{-1}(s)$ as

$$
\begin{aligned}
\overline{\Phi}_1(s) &= \Pi_{k_1=0}^{K_1} J_0(A_{k_1}'(1, p_{k_1}, b_{k_1})s)\Pi_{k_2=0}^{K_2} J_0(A_{k_2}'(1, 0, 1)s) \\
&\times \Pi_{k_4=0}^{K_4} J_0\left[(A_{k_4}'(1, p_{k_4}', b_{k_4}^{(1)})s) + A_{k_4}'(1, (1+p_{k_4}'), b_{k_4}^{(2)})s)\right] \\
\overline{\Phi}_{-1}(s) &= \Pi_{k_1=0}^{K_1} J_0(A_{k_2}'(1, p_{k_1}, b_{k_1})s)\Pi_{k_3=0}^{K_3} J_0(A_{k_2}'(-1, 0, -1)s) \\
&\times \Pi_{k_4=0}^{K_4} J_0\left[(A_{k_4}'(-1, p_{k_4}', b_{k_4}^{(1)})s) + A_{k_4}'(-1, (1+p_{k_4}'), b_{k_4}^{(2)})s)\right]
\end{aligned}
$$

then the characteristic functions of U_1 and U_{-1} are again given by

$$
\begin{aligned}
\Phi_1(s) &= e^{-\frac{s^2}{4}} J_0\left(\sqrt{\frac{E_b}{N_0}}s\right)\overline{\Phi}_1(s) \\
\Phi_{-1}(s) &= e^{-\frac{s^2}{4}} J_0\left(|\rho|\sqrt{\frac{E_b}{N_0}}s\right)\overline{\Phi}_{-1}(s).
\end{aligned}
$$

From this point on we can go through similar steps as before and use the results for averaging over K_i's from [Ger 88] and find the average probability of error for the first user. Instead of doing this let us consider an upper bound and a lower bound on the probability of error when independent hopping patterns are assumed. If we can show that the upper bound and the lower bound are tight and also that the probability of error when Markov hopping patterns are assumed falls in between these bounds then we will have in effect shown that the probability of error when

Markov hopping patterns are assumed is a good approximation to the probability of error when independent hopping patterns are assumed. Let us consider a very simple bound where we assume that whenever a hop is overlapped by an interfering user for its entire duration (full hit), the probability error is 1 or 0 resulting in an upper bound and a lower bound respectively. Then it is easy to see that the average probability of error when all the users have the same power level will be upper bounded as

$$\begin{aligned} P_e &\leq \sum_{K'=0}^{K-1} \binom{K-1}{K'} p_p^{K'} (1-p_p-p_f)^{K-1-K'} P_e(K') \\ &+ \left[1-(1-p_f)^{K-1}\right] \end{aligned}$$

and lower bounded as

$$P_e \geq \sum_{K'=0}^{K-1} \binom{K-1}{K'} p_p^{K'} (1-p_p-p_f)^{K-1-K'} P_e(K')$$

where p_p and p_f are the probability of partial and full hits given by (2.3) and $P_e(K')$ is the probability of error given that the hop is hit by K' partial hits which has already been computed. Numerical results shows that for all K, the probability of error when Markov hopping patterns are assumed is indeed a good approximation to the probability of error when independent hopping patterns are assumed.

3.2.4 Asymptotic Performance

It is also possible to consider the asymptotic average error probability as $K,\ q \to \infty$ but with $\frac{K}{q} = \lambda$ fixed as in [Kim 89]. Let us first define $F(s)$, $E_1(s)$, and $E_2(s)$ as follows.

$$\begin{aligned} F(s) &= e^{-\frac{s^2}{2}} J_0\left(\sqrt{\frac{E_b}{N_0}}s\right)\left[\frac{s}{2}J_0\left(|\rho|\sqrt{\frac{E_b}{N_0}}s\right) + |\rho|\sqrt{\frac{E_b}{N_0}}J_1\left(|\rho|\sqrt{\frac{E_b}{N_0}}s\right)\right] \\ E_1(s) &= E_{p,b}\left\{J_0(A'_k(1,p,b)s)J_0(A'_k(-1,p,b)s)\right\} \\ E_2(s) &= E_{p,b}\left\{A'_k(-1,p,b)J_1(A'_k(-1,p,b)s)J_0(A'_k(1,p,b)s)\right\}. \end{aligned}$$

Then we can show that the average probability of error when all the users have the same power level may be written as

$$P_e(K) = \sum_{K'=0}^{K-1} \binom{K-1}{K'} p_h^{K'}(1-p_h)^{(K-K')} \times \int_0^\infty \left[F(s)E_1(s)^{K'} + J_0\left(|\rho|\sqrt{\frac{E_b}{N_0}}s\right) K'E_2(s)E_1^{K'-1} \right] ds.$$

Straightforward analysis shows that

$$\lim_{K,q\to\infty,\, \frac{K}{q}=\lambda} P_e(K) = \int_0^\infty e^{-2\lambda(1-E_1(s))} \left[F(s) + 2\lambda J_0\left(|\rho|\sqrt{\frac{E_b}{N_0}}s\right) E_2(s) \right] ds.$$

Unfortunately it is not practical to numerically evaluate this expression since the integrand does not converge to zero fast enough. But numerical computations of the throughput show that the probability of error as a functions of λ remains essentially unchanged for $q \geq 100$. It is also possible to derive an expression for the case when the signal-to-noise ratio tends to infinity (i.e., negligible background noise), but the resulting integral converges quite slowly and thus is not practical to compute numerically.

3.3 Simulation

In order to verify that our results are correct, we carry out Monte Carlo simulations to estimate the error probability of a AFHSS-MA system when a hop is hit by a given number of interfering users. We consider the case when orthogonal BFSK is employed and all the users have the same power at the receiver.

The simulation can be done most easily by using (2.7) with $\rho = 0$. For each simulation point, we generate the random variables $\{\varphi_k\}$, $\{p_k\}$, $\{b_k\}$ and the Gaussian noise variables z_1 and z_{-1} and simply count the number of events that satisfies the condition that $|U_{-1}| > |U_1|$. It turns out that this method of simulation (which is

essentially the Monte Carlo method of integration [Kuo 72]) is very efficient and we can estimate $Pr(|U_1| < |U_{-1}|)$ for $K' = 1, \cdots, 20$ in less than six hours on an Appllo DN4000 workstation counting 20,000 errors for each data point. Of course, $K' \leq 5$ would be sufficient in most cases since the probability of error is very close to $\frac{1}{2}$ when $K' > 5$ in practical situations.

3.4 Numerical Results

In this section we will provide numerical results for the probability of error for an AFHSS-MA network using the expressions developed in previous sections. We will also provide the results for the channel capacity and the associated throughput of the network. We will compare our results to the $\frac{1}{2}$-approximation and the approximation made in [Ger 88]. Basically the assumption made in [Ger 88] is that in equation (2.5),

$$A_k(1, p_k, -1) = A_k(-1, p_k, +1) = 0.$$

That is, an interfering tone corresponding to the data bit of '+1' does not affect the output of the matched filter corresponding to the data bit of '−1'. We will refer to this approximation as the 'Geraniotis' approximation'. The case when there are two different power levels as seen by the receiver will also be considered as well as for the case when the signalling is nonorthogonal.

First, let us consider orthogonal BFSK with $\Delta f = \frac{1}{2T_h}$, that is, the case when $\rho = 0$ with the minimum separation between the tones. We use (3.20) to compute the error probability of a given hop as a function of the normalized delay p when the hop is hit by one interfering user of the same power level with the data bit of the interfering user as a parameter. For signal-to-noise ratio equal to 11dB, this is shown in Fig. 3.1 for $p > 0$ along with simulation results where 10,000 errors were collected for each data point. Obviously the error probability is symmetric about

$p = 0$ since it is only a function of $|p|$. We see that our results coincide very closely with the simulation results. Figs. 3.2-3.6 are the plots for the error probability computed using (3.22) and Geraniotis' approximation compared to the simulation results where 20,000 errors were collected for each data point for $K' = 1, \cdots, 5$ and $\frac{E_b}{N_0} =$ 8, 11, 13, 16 and 19dB. Orthogonal BFSK with $\Delta f = \frac{1}{2T_b}$ is assumed and the power levels of all the users are assumed to be the same. We observe that Geraniotis' approximation gives optimistic results, especially for small number of users which usually dominate the average error probability. These probabilities for $\frac{E_b}{N_0} = 11$dB are tabulated in Table 3.1.

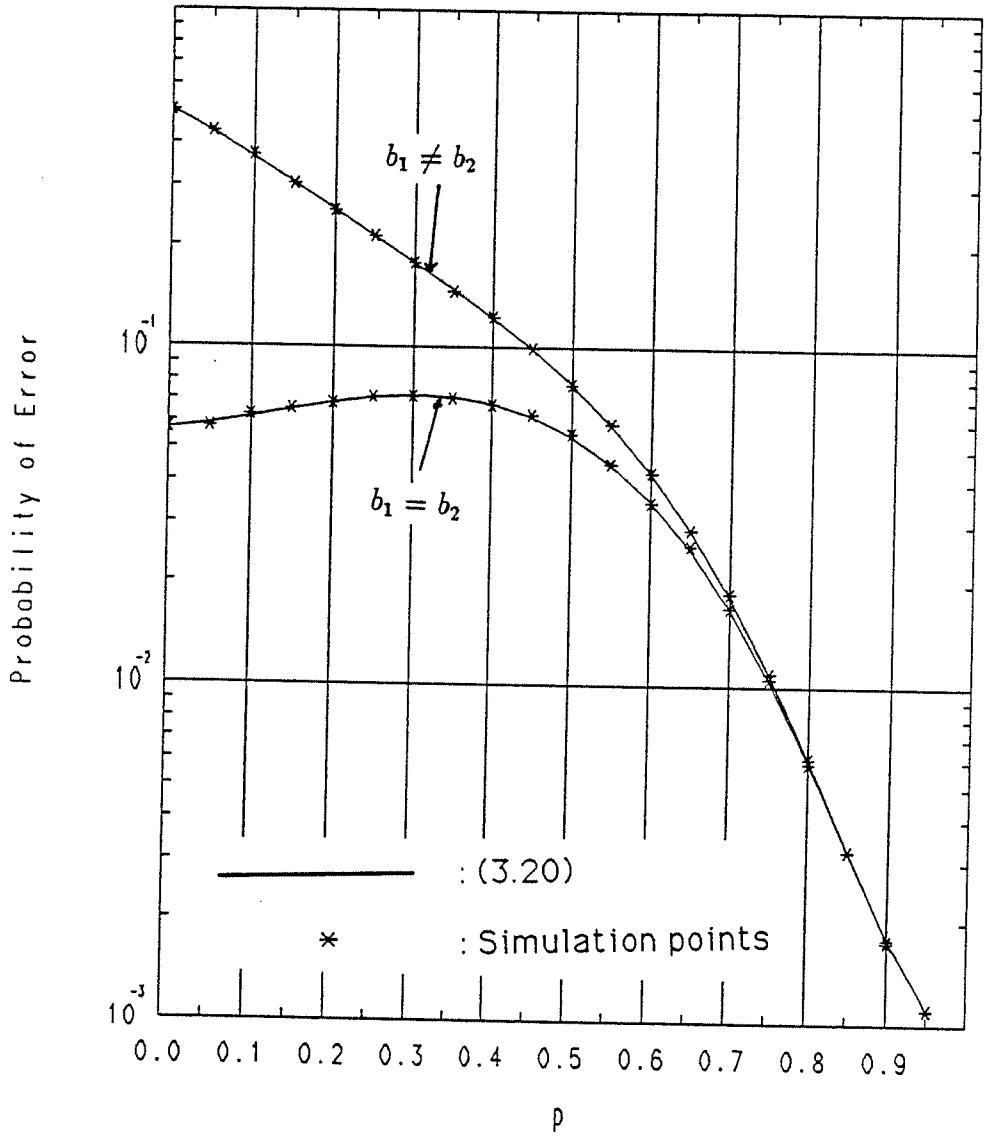

Figure 3.1: Probability of error as a function of the normalized delay with one interfering tone with equal power $\frac{E_b}{N_0}$=11dB.

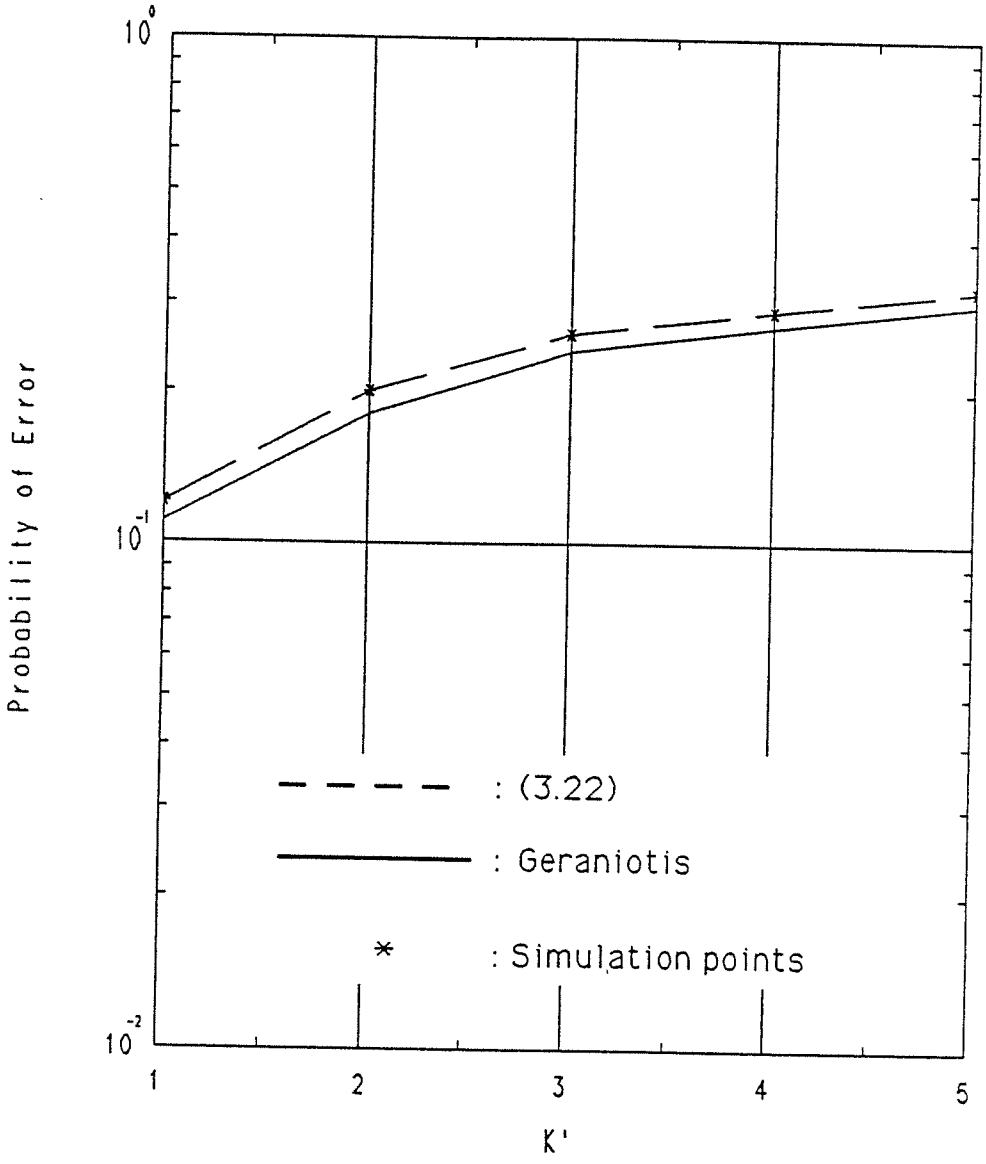

Figure 3.2: Probability of error versus the number of interfering tones for $\frac{E_b}{N_0}$=8dB. All users have same power.

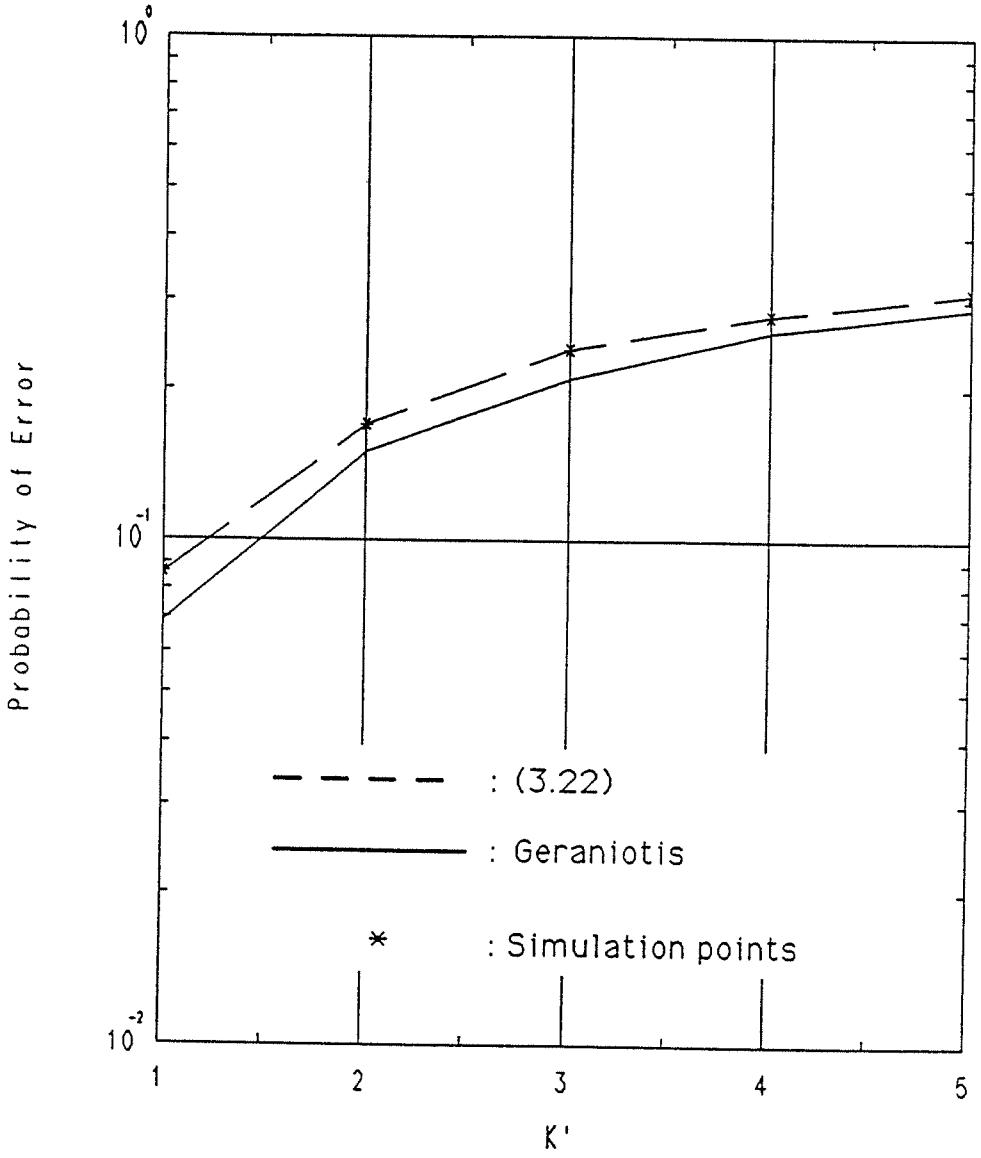

Figure 3.3: Probability of error versus the number of interfering tones for $\frac{E_b}{N_0}$=11dB. All users have same power.

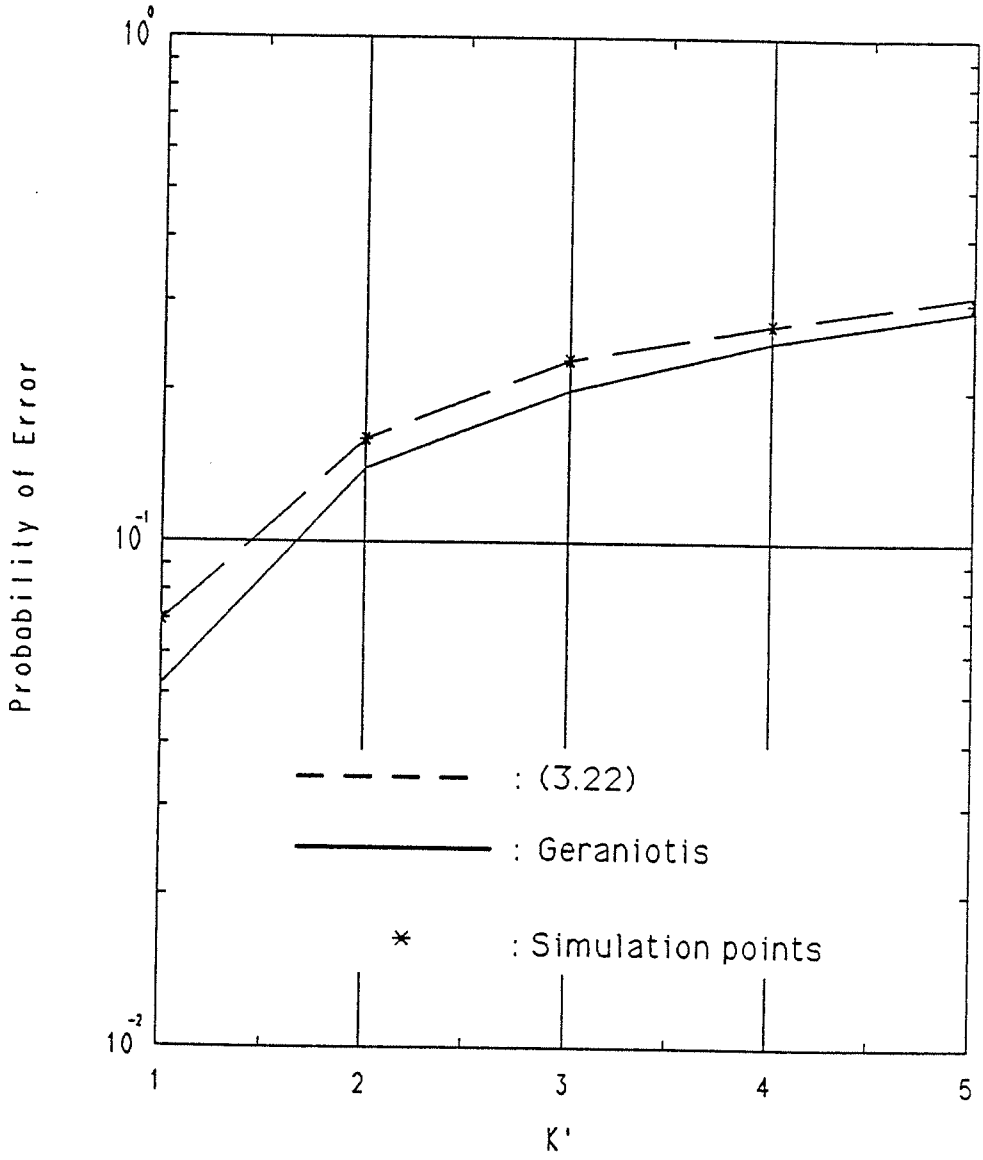

Figure 3.4: Probability of error versus the number of interfering tones for $\frac{E_b}{N_0}$=13dB. All users have same power.

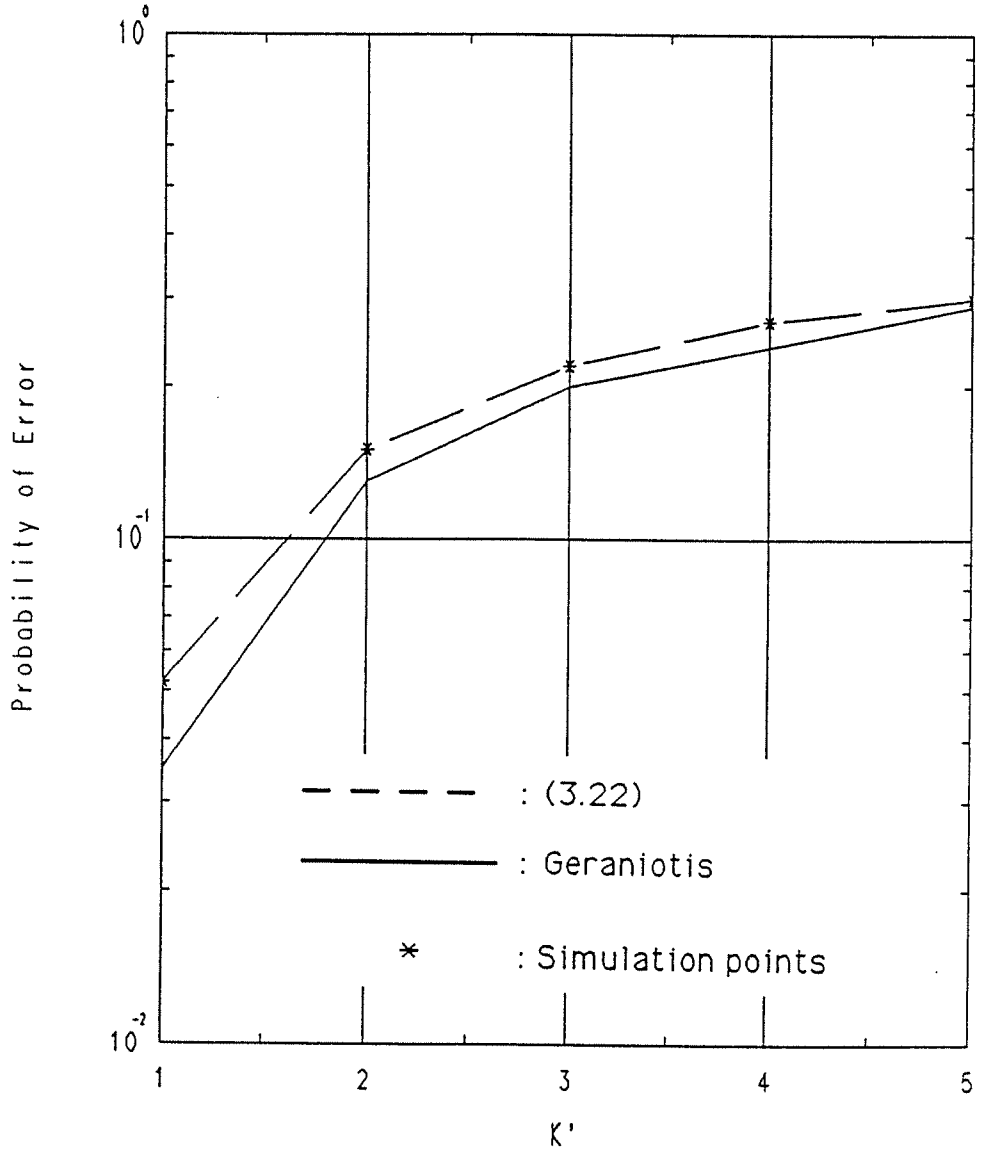

Figure 3.5: Probability of error versus the number of intertering tones for $\frac{E_b}{N_0}$=16dB. All users have same power.

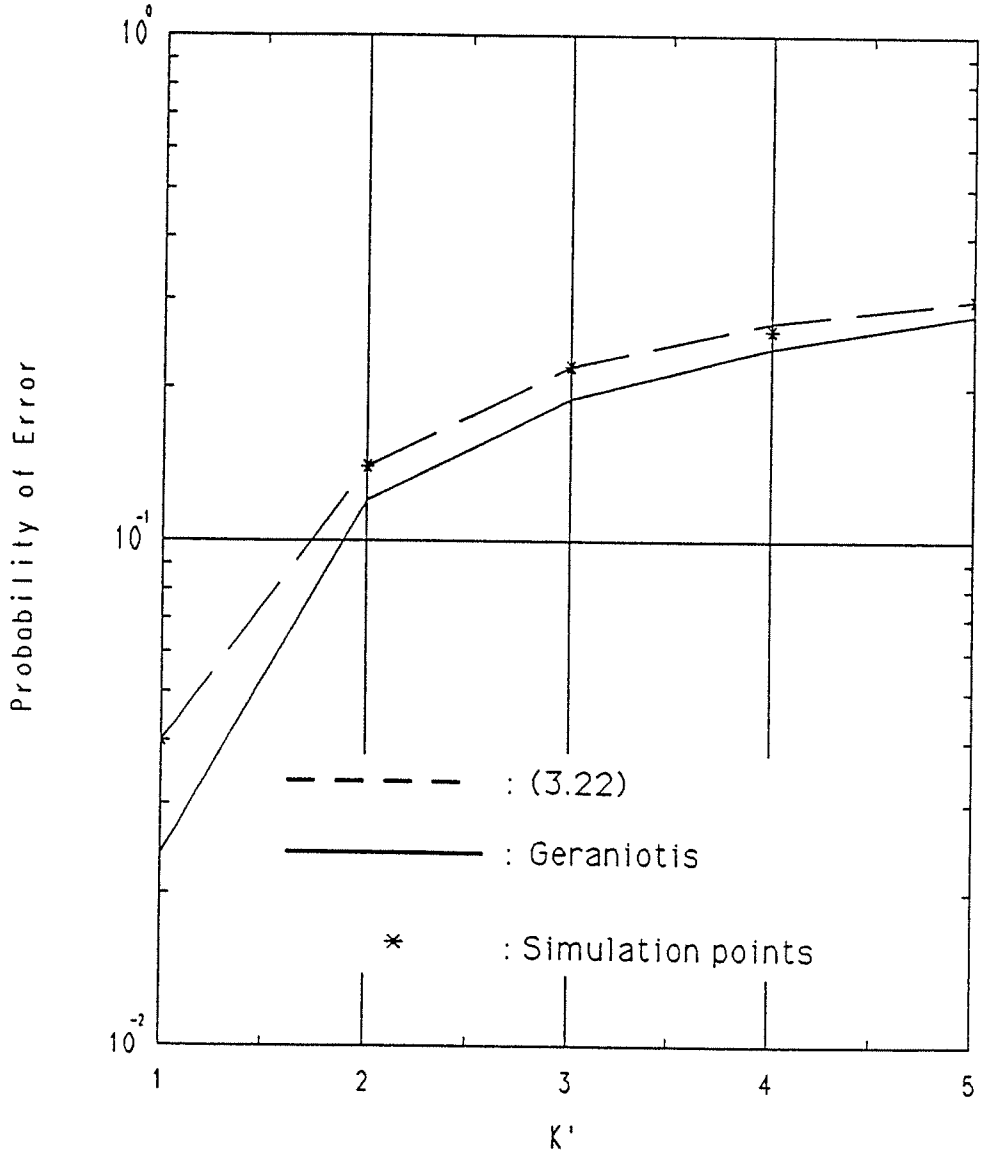

Figure 3.6: Probability of error versus the number of interfering tones for $\frac{E_b}{N_0}$=19dB. All users have same power.

K'	Geraniotis'	Equation (3.22)	Simulation
1	6.88e-2	8.59e-2	8.62e-2
2	0.15	0.17	0.17
3	0.21	0.24	0.24
4	0.26	0.28	0.28
5	0.29	0.31	0.31

Table 3.1: Comparison of Geraniotis' approximation and (3.22). $\frac{E_b}{N_0}$=11dB.

The difference between Geraniotis' results and those computed using (3.20) and the simulation results may seem small, but when coding is employed, small differences in the channel statistic is usually amplified by orders of magnitude. Hence it is very important that we compute the channel statistics accurately. We also notice that the exact error probabilities are much smaller than $\frac{1}{2}$. Since we have established that the expressions developed in this chapter gives correct results, from here on, we will only consider our results and that of Geraniotis' and compare them to the results under the $\frac{1}{2}$-approximation.

Now let us use (3.29) to look at the average probability of error for a hop given that there are K active users in the network and orthogonal BFSK is employed. Let the number of available slots q be 100. In Figs. 3.7-3.11 we show the average error probability of a hop under Geraniotis' and the $\frac{1}{2}$-approximations and the exact values developed in this chapter for different signal-to-noise ratios. We note that there could be up to an order of magnitude difference between the exact results and the $\frac{1}{2}$-approximation. With error correction coding, the difference would be further amplified.

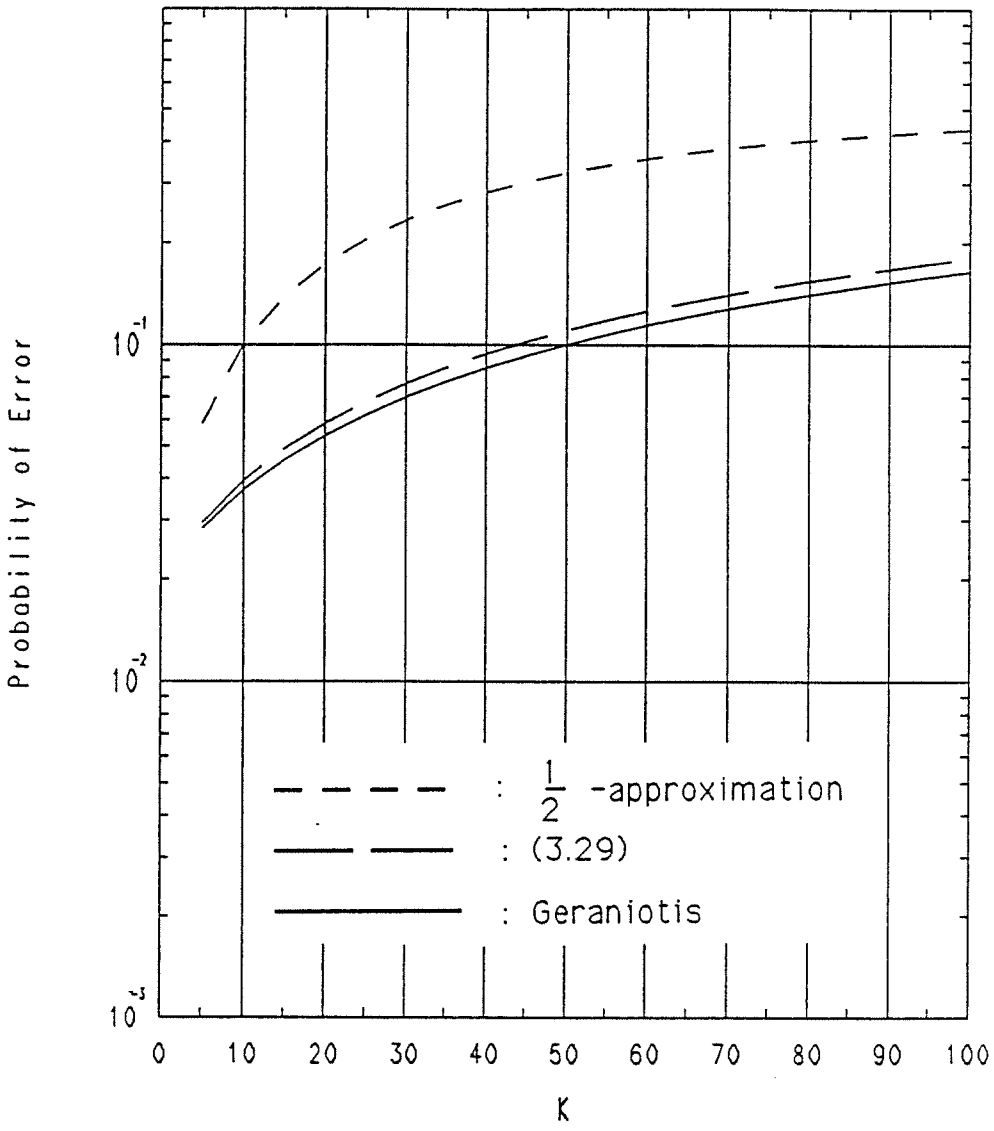

Figure 3.7: Average probability of error given that there are K users in the network with the same power level. $\frac{E_b}{N_0}$=8dB. $q = 100$.

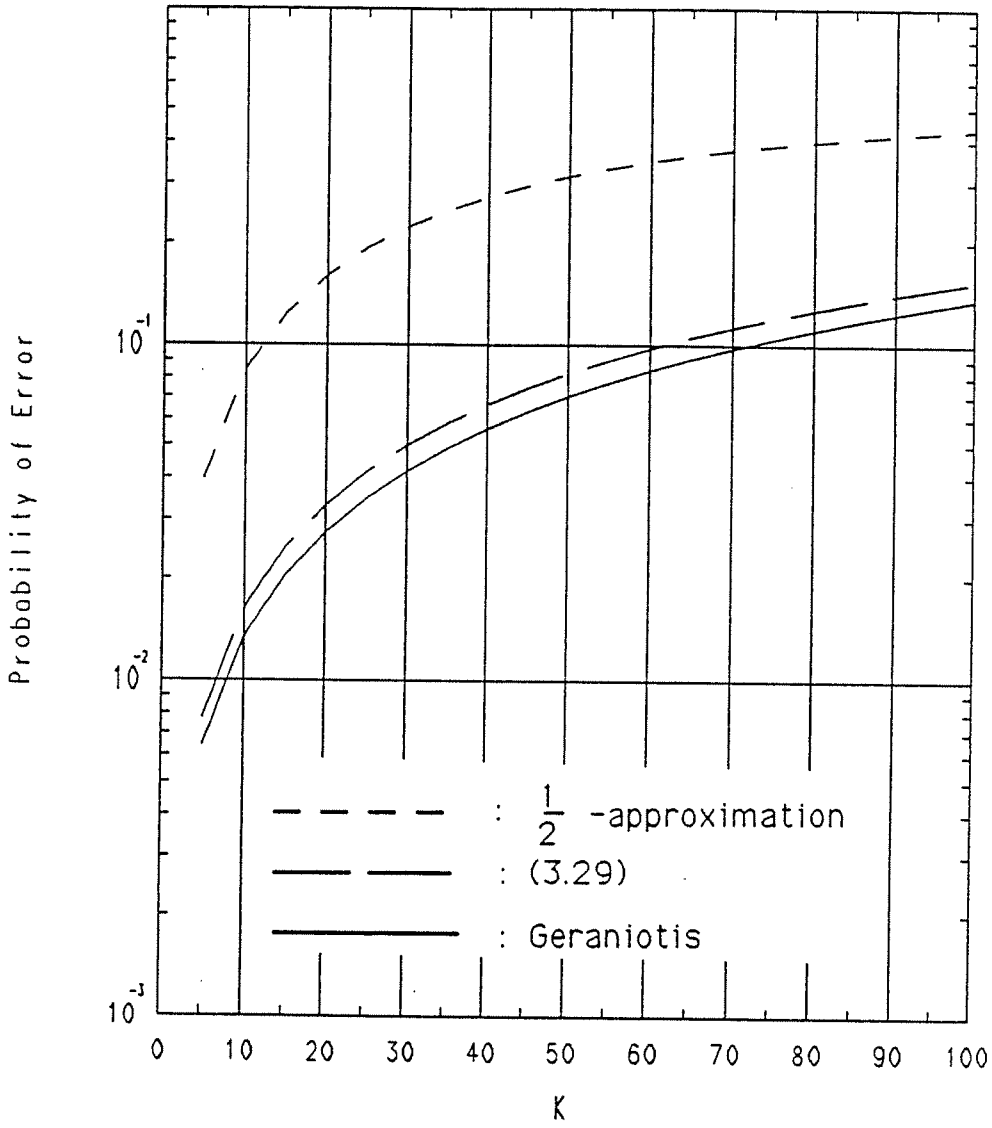

Figure 3.8: Average probability of error given that there are K users in the network with the same power level. $\frac{E_b}{N_0}$=11dB. $q = 100$.

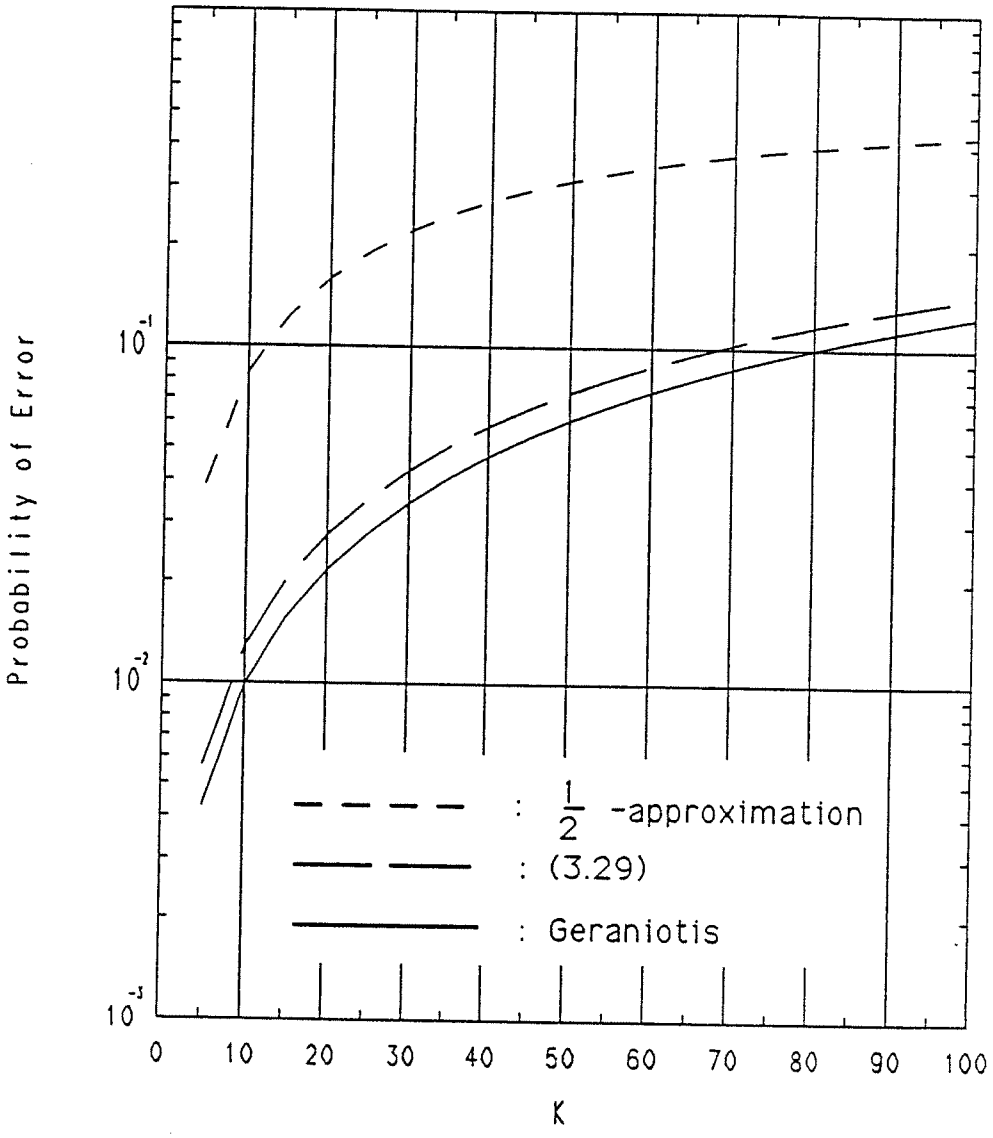

Figure 3.9: Average probability of error given that there are K users in the network with the same power level. $\frac{E_b}{N_0}$=13dB. $q = 100$.

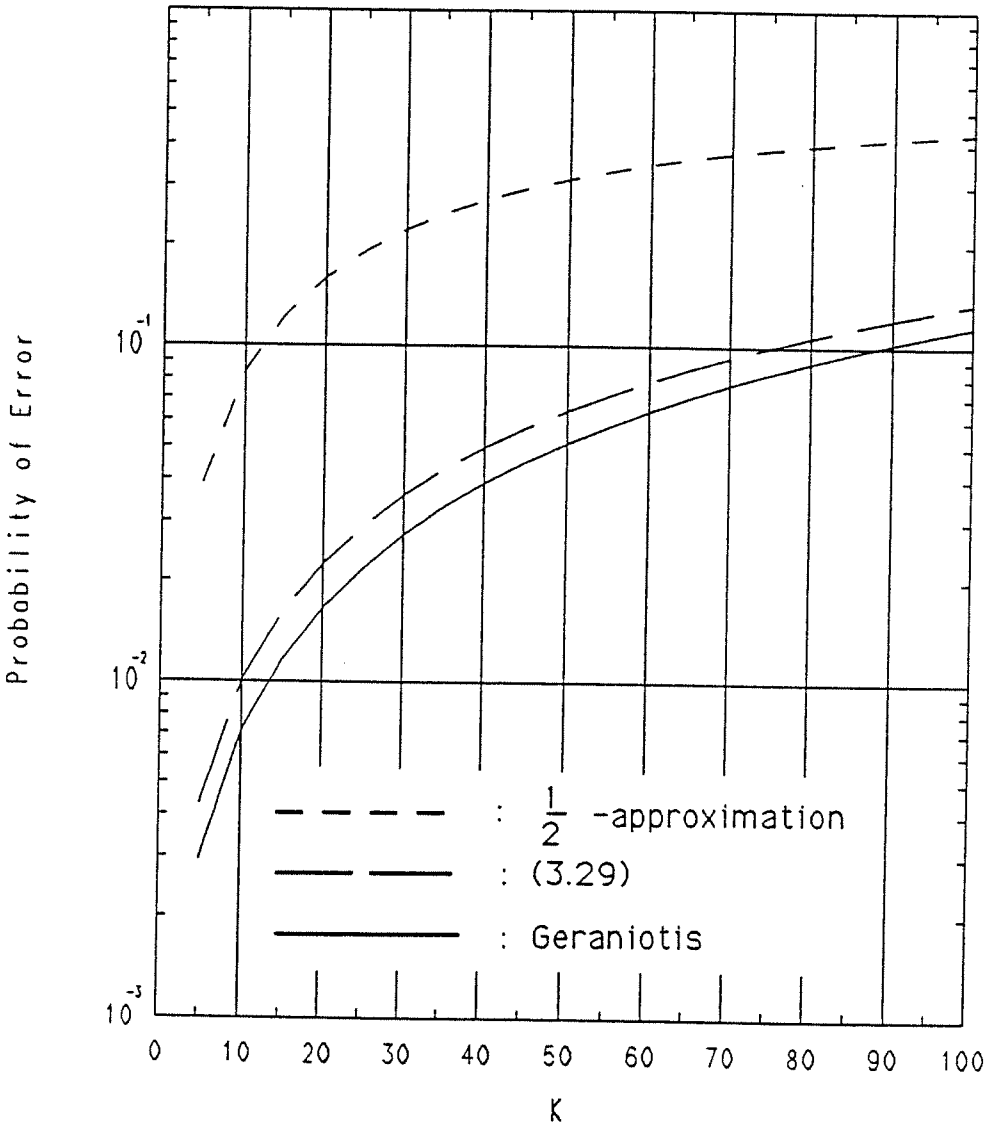

Figure 3.10: Average probability of error given that there are K users in the network with the same power level. $\frac{E_b}{N_0}$=16dB. $q = 100$.

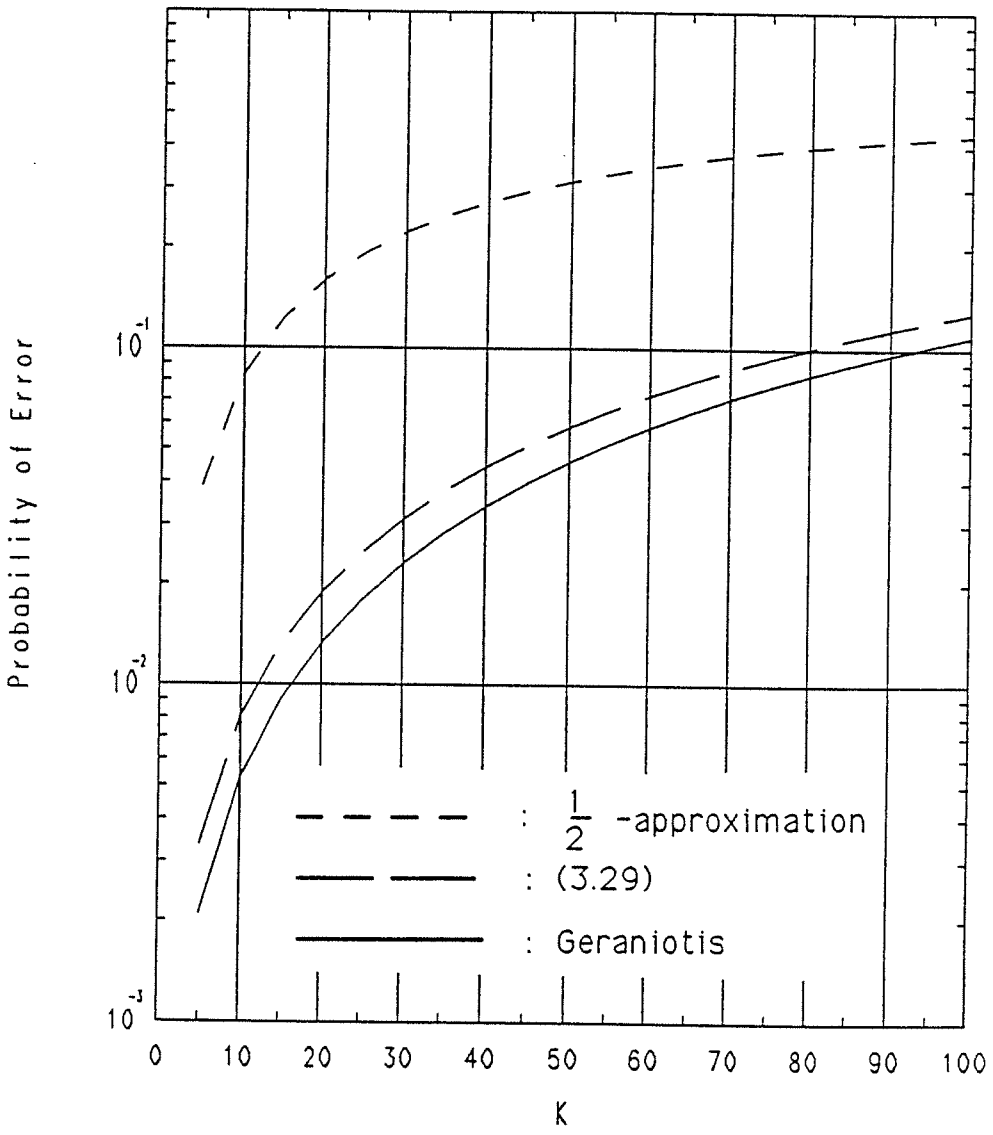

Figure 3.11: Average probability of error given that there are K users in the network with the same power level. $\frac{E_b}{N_0}$=19dB. $q = 100$.

This fact that the actual average probability of error is much less than that computed using the $\frac{1}{2}$-approximation leads to very interesting results. For example, we will see that using perfect side-information to erase the hops that were hit results in very poor performance. Much worse than simple hard decisions. Fig. 3.12 and 3.13 shows the channel capacity and the associated throughput computed using the results from Section 2.5 for a system using perfect side-information to erase the symbols of the hop that were hit and a system that simply makes hard decision for $\frac{E_b}{N_0}$=8, 19dB. We note that contrary to previous results, the system that simply makes hard decisions without side-information actually does much better than the system using perfect side-information to erase the symbols corresponding to the hops that were hit. This can be explained by recalling that the probability of error when a hop is hit by a small number of interfering users (which are usually the most probable cases) is much lower than $\frac{1}{2}$. Hence it turns out that if we erase all the symbols corresponding to the hops that were hit and make hard decision on the symbols that were not hit, we will in fact be throwing away many reliable symbols.

Next, we consider the case where there are two different power level groups P_1 and P_2 as seen by the first receiver. We take P_1 to have the same power as the first user, i.e., $\alpha^{(1)} = \alpha_1$ where $\alpha^{(i)}$ denotes the amplitude of the tone corresponding to the i-th power level group. We consider two cases where $\alpha^{(2)} = 0.5$, $\alpha^{(2)} = 1.5$, i.e., the other group either has 1.76dB more or 3dB less power than the reference user. We tabulate the results obtained using (3.30) for $K = 11$ and $K = 21$ and various combinations of $\overline{K}_1, \overline{K}_2$ in Table 3.2 for $\frac{E_b}{N_0}$ =11dB. Also included in the table are the $\frac{1}{2}$-approximation and the results when equal power among the users is assumed. We note that the errors resulting from these approximations are quite large and again they will further be amplified with coding.

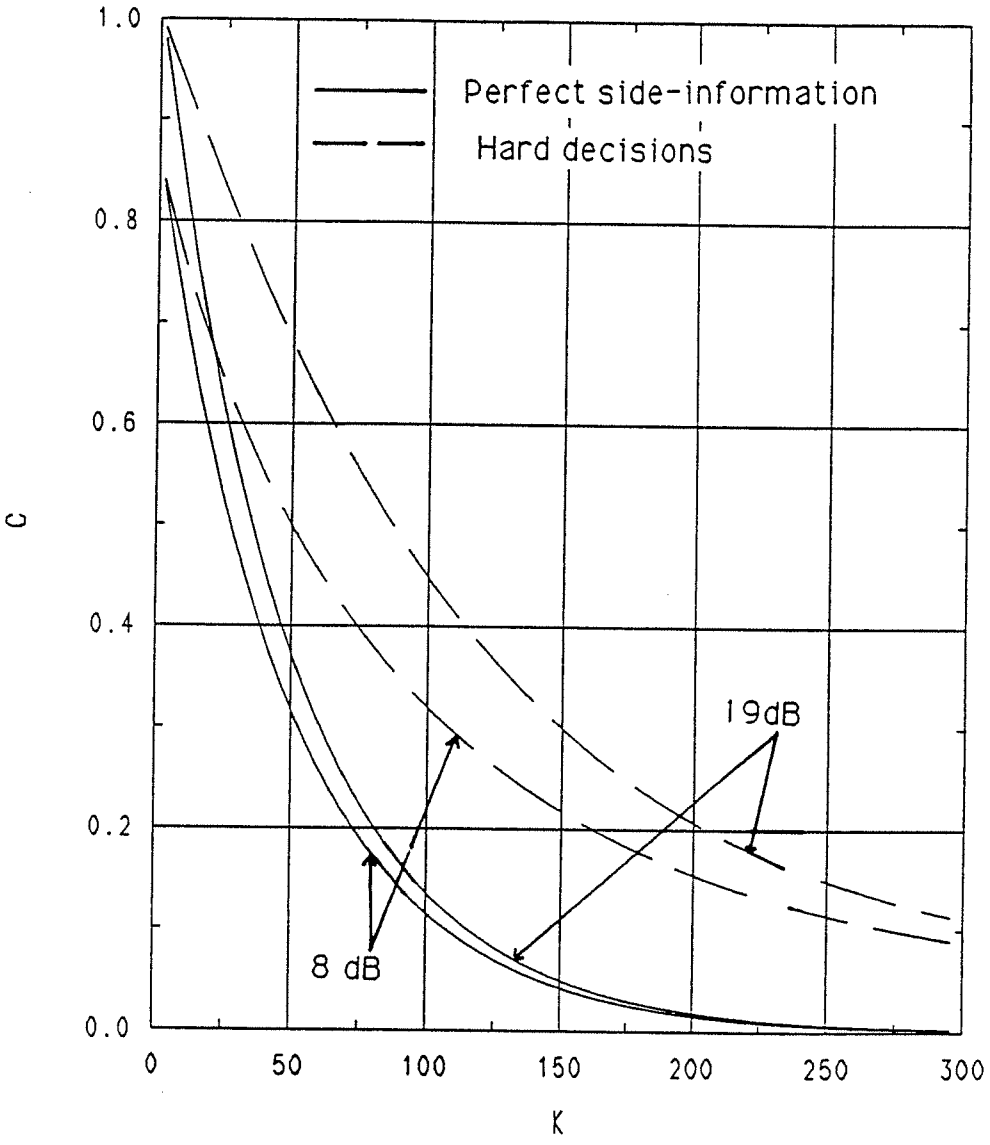

Figure 3.12: Channel capacity for $\frac{E_b}{N_0}$=8,19dB.

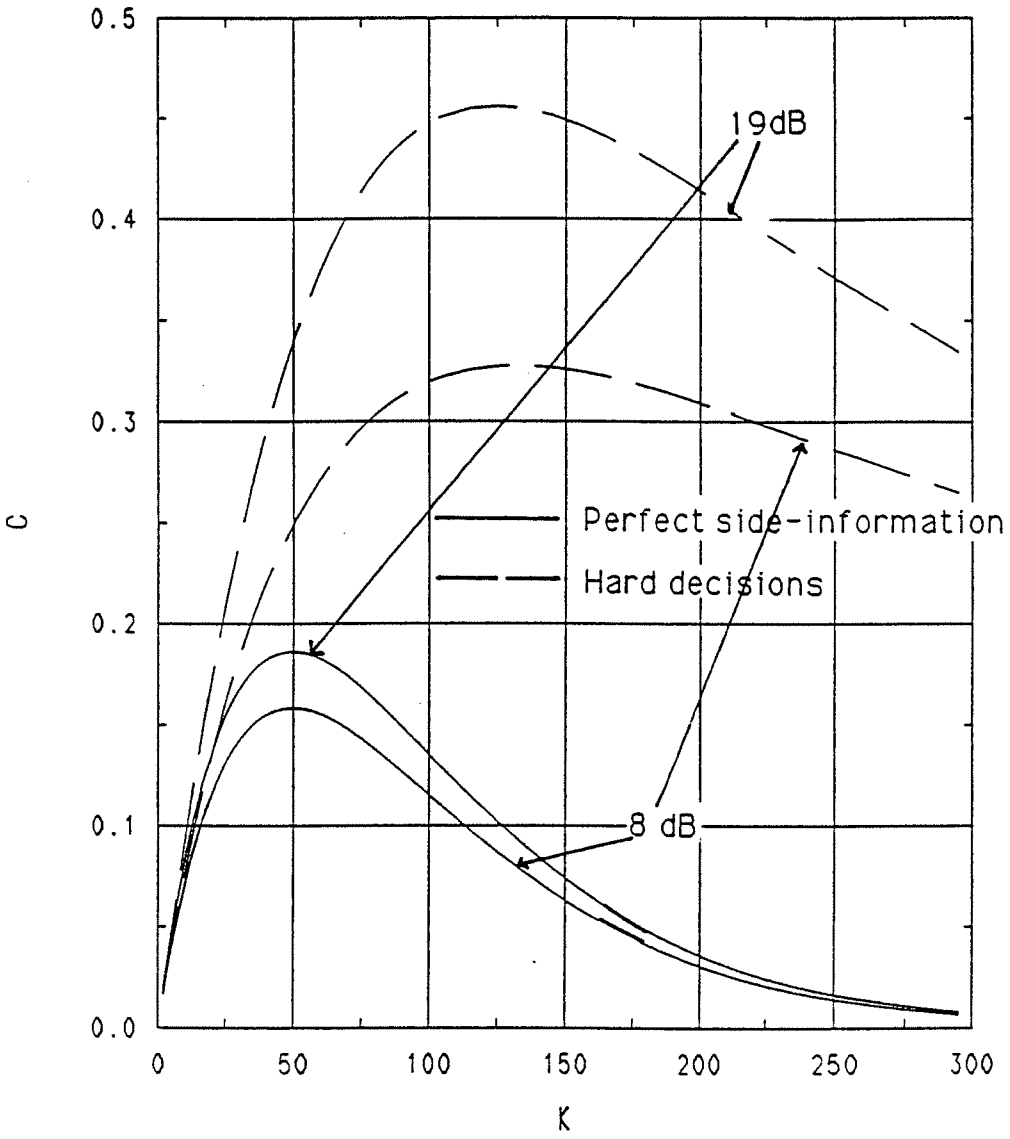

Figure 3.13: Normalized throughput of a coded system that achieves channel capacity.

$\alpha^{(2)}$	K	$(\overline{K}_1, \overline{K}_2)$	P_e (*) (3.30)	*Assuming equal power	*$\frac{1}{2}$ approx.
0.5	11	(5,5)	1.04×10^{-2}	1.79×10^{-2}	9.22×10^{-2}
		(3,7)	7.39×10^{-3}		
		(7,3)	1.34×10^{-2}		
	21	(10,10)	2.03×10^{-2}	3.49×10^{-2}	0.167
		(5,15)	1.27×10^{-3}		
		(15,5)	2.76×10^{-2}		
1.5	11	(5,5)	2.93×10^{-2}	1.79×10^{-2}	9.22×10^{-2}
		(3,7)	3.37×10^{-2}		
		(7,3)	2.47×10^{-2}		
	21	(10,10)	5.57×10^{-2}	3.49×10^{-2}	0.167
		(5,15)	6.58×10^{-2}		
		(15,5)	4.54×10^{-2}		

Table 3.2: Average probability of error for two power level groups. $\frac{E_b}{N_0}$=11dB. q = 100.

In Fig. 3.13, the approximation to the average error probability is shown for $\mu = 1$ and 0.9 (μ was defined in Section 3.2.2.) The trend was that as μ decreases below 0.9, the average error probability tends to increase, above that of $\mu = 1$. Fig. 3.15 shows similar curves when using the $\frac{1}{2}$-approximation. For the bottom curve of Fig. 3.15, μ was optimized for each K for minimum average error probability. This shows again that the conclusions that we obtain from using the $\frac{1}{2}$-approximation could be quite different from what we obtain by using our approximation to the error probability. In this case the difference arises from the fact that the decrease in the hit probability by using $\mu < 1$ does not compensate for the increase in the error probability.

In Fig. 3.16-3.17, the bounds for the error probability when independent hopping patterns are assumed derived in Section 3.2.3 are shown. These results verify that the average probability of error of a system employing Markov hopping patterns is a very good approximation to that of a system employing independent hopping patterns for sufficiently large number of slots. The signal-to-noise ratio for these figures is taken to be 11dB.

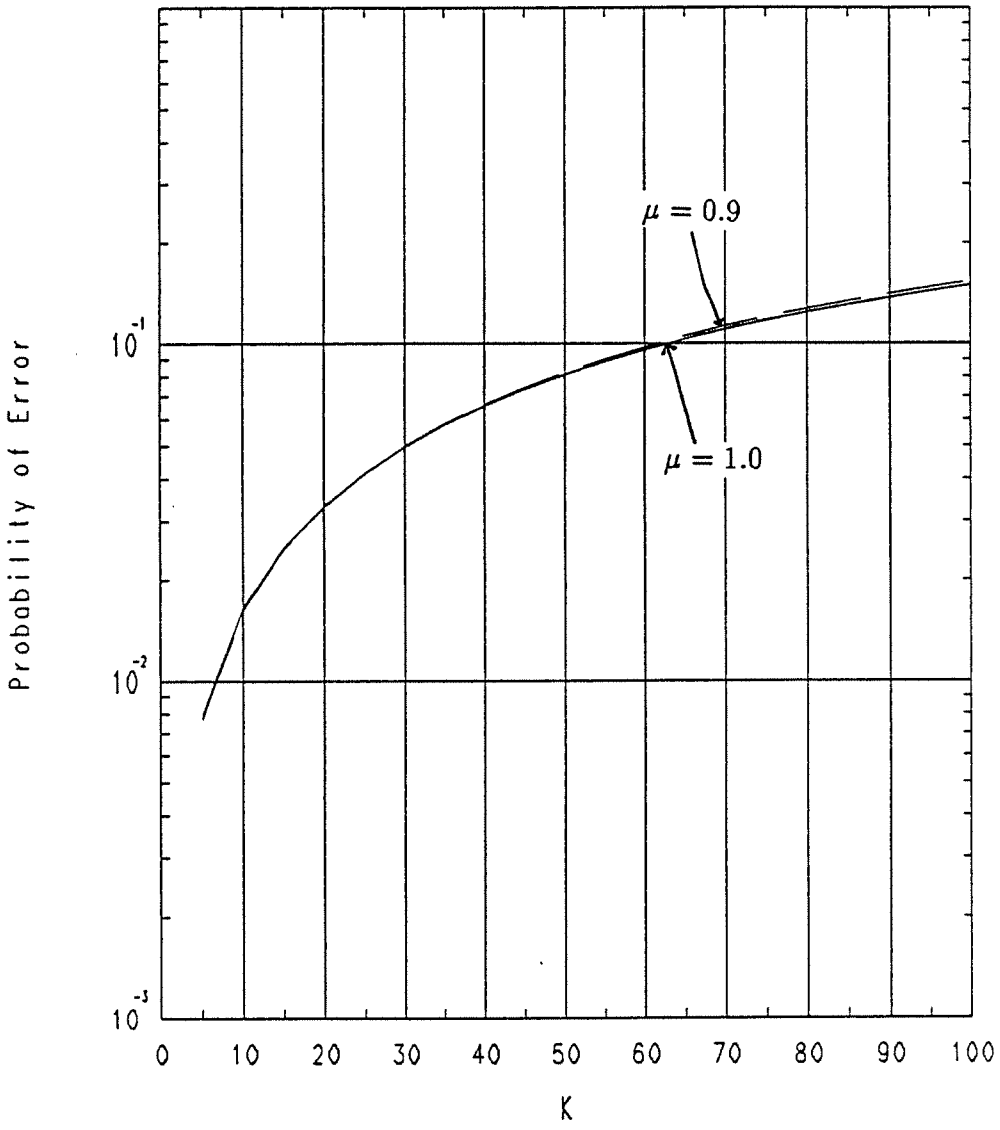

Figure 3.14: Average probability of error using non-orthogonal BFSK. All users have equal power. $\frac{E_b}{N_0}$=11dB. $q = 100$. $\mu = 1, 0.9$.

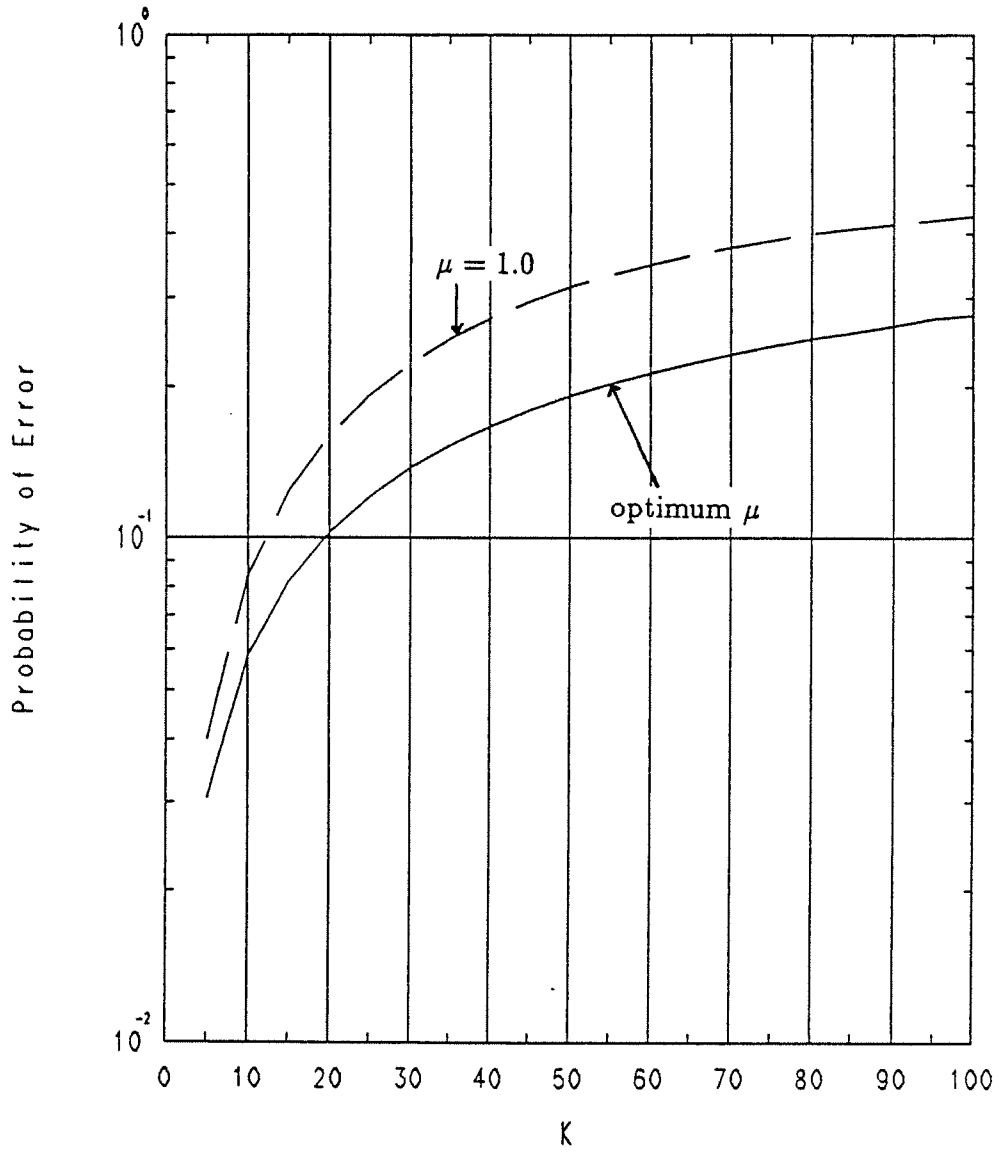

Figure 3.15: Average probability of error using non-orthogonal FSK using the $\frac{1}{2}$-approximation. All users have equal power. $\frac{E_b}{N_0}$=11dB. $q = 100$.

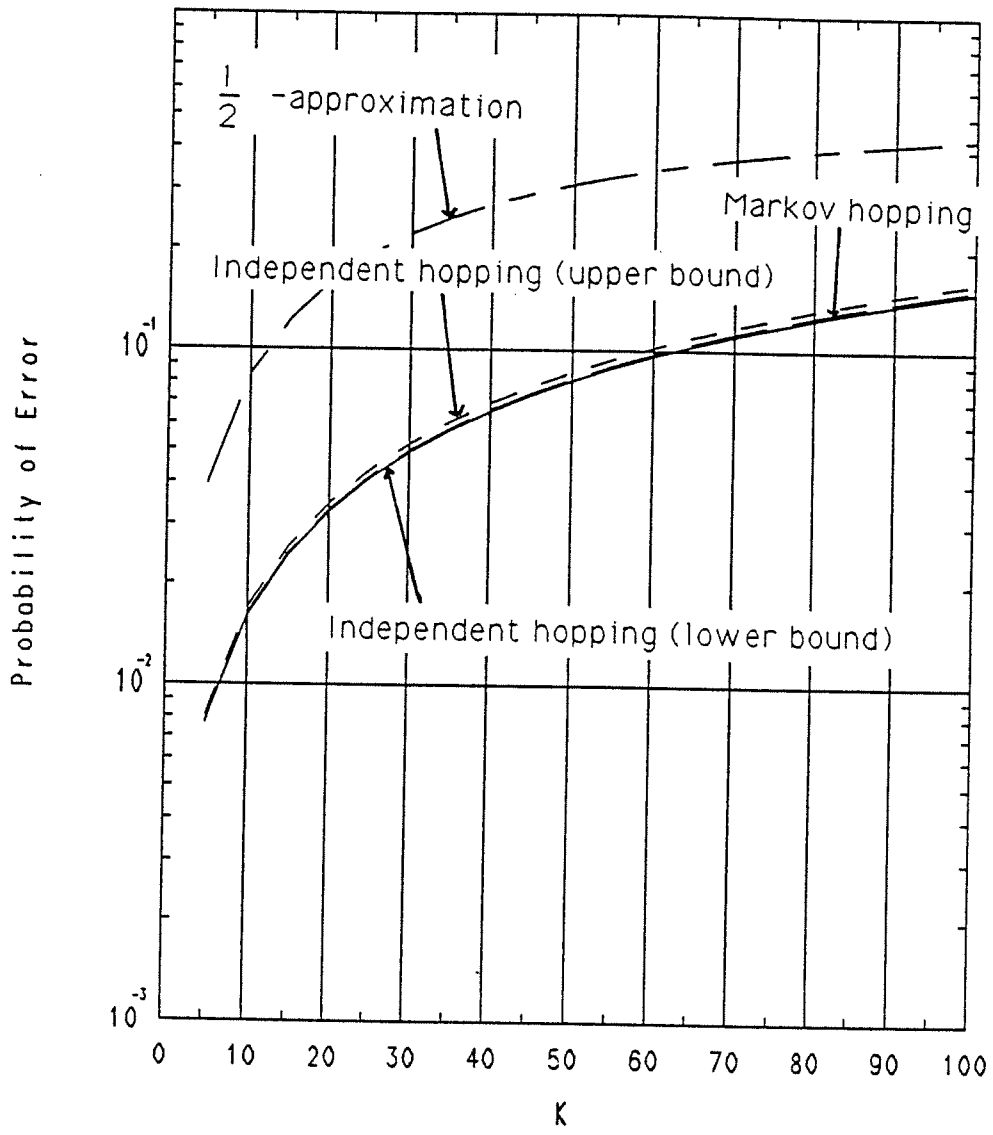

Figure 3.16: Bounds on the average probability of error using independent hopping patterns. All users have same power. Orthogonal signalling. $\frac{E_b}{N_0}$=11dB. $q = 100$. K=10-100.

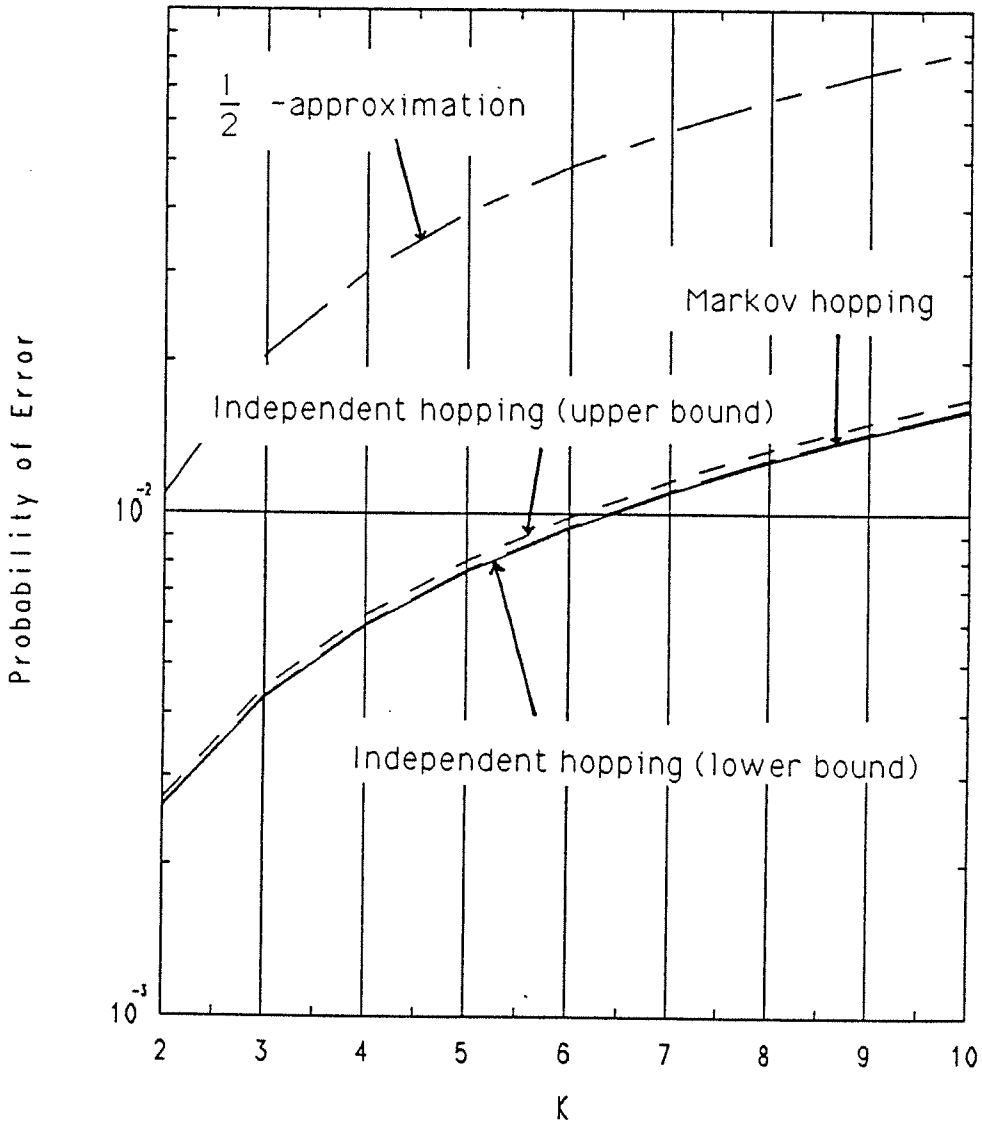

Figure 3.17: Bounds on the average probability of error using independent hopping patterns. All users have same power. Orthogonal signalling. $\frac{E_b}{N_0}$=11dB. $q = 100$. K=2-10.

CHAPTER IV

PERFORMANCE OF VITERBI RATIO THRESHOLDING IN AFHSS-MA NETWORKS

In this chapter we extend the results of Chapter 3 to analyze the performance of Viterbi Ratio Thresholding (VRT) [Vit 85] [Vit 82] in an AFHSS-MA network described in Chapter 2. Using the Viterbi ratio thresholding technique for AFHSS-MA channels to single out unreliable symbols (hops) was first considered in [Kel 88] where Monte-Carlo simulations were performed to estimate the transition probabilities of the resulting DMC when the number of interfering users is small (a precise definition of the VRT scheme is given in the next section). This alternate method of generating information about the quality of the channel (as opposed to side-information) is more interesting at this point since we have shown in Chapter 3 that using perfect side-information to erase all the symbols that were hit actually degrades performance over the simple hard decisions scheme.

Here, we offer analytical expressions for the transition probabilities of the resulting channels when VRT is employed by using basically the same techniques applied in Chapter 3 for the probability of error. Hence these expressions will have all the desirable characteristics of the expressions developed for the probability of error.

Using these expressions, we compute the performance of three and four level

Viterbi ratio thresholding and compare them to various other schemes of interest. The measures of performance used to compare different schemes are the channel capacity, the packet error probability (a packet is simply a unit of data transmitted over the network at a time) and the normalized throughput (when convolutional coding is employed.) Numerical results show that both two and four level Viterbi ratio thresholding gives significant increase in performance for the AFHSS-MA network over simple hard decisions.

4.1 Viterbi Ratio Thresholding

VRT is essentially a quantization scheme that quantizes the output of the channel into an alphabet size greater than that of the channel input based on the observation of the outputs of the matched filters. We consider two types of VRT, three level and four level. For both cases the resulting channel can be accurately modeled as a DMC with binary input.

4.1.1 Three Level VRT

In the three level VRT scheme, a thresholding rule is used to make an error and erasure decision on each hop. In effect, some hops will be declared to be too corrupted to be considered for detection and will be *erased* according to the thresholding rule.

Let $|U_{max}|$ denote the largest of $\{|U_1|, |U_{-1}|\}$ and let $|U_{min}|$ denote the smaller of the two. The rule is to erase the symbol if $1 \leq \frac{|U_{max}|}{|U_{min}|} < \theta$ and decide that the data corresponding to $|U_{max}|$ was sent if $\frac{|U_{max}|}{|U_{min}|} \geq \theta$. Here θ is a number greater than 1 that should be set to an appropriate value. The resulting channel is a BSEEC shown in Fig.2.10.

4.1.2 Four Level VRT

In the four level VRT scheme, the Viterbi ratio thresholding is used to develop a quality bit Q for the demodulated bits. The rule is similar to the three level VRT scheme described above except that when $|U_{max}|/|U_{min}| < \theta$ we decide $|U_{max}|$ was sent and attach a quality bit Q='u' to indicate that it was an *unreliable* decision, and when $|U_{max}|/|U_{min}| \geq \theta$ we attach Q='r' to indicate that it is a *reliable* decision. The output of the channel is written as (z, Q) where $z \in \{+1, -1\}$ is the decision made by the quantizer and $Q \in \{u, r\}$ denotes the estimated reliability of the decision. The resulting channel is a binary input 4-ary output symmetric channel as shown in Fig. 4.1.

The Viterbi ratio thresholding has been shown to be effective against various types of intentional jammers [Vit 82] [Vit 85] [Che 88b]. It will be shown here that it is also effective in discriminating hops that were severely corrupted by multiple-access interference.

4.2 Channel Statistics

In this section we will derive an analytical expression for the transition probabilities of the resulting DMCs as a function of the threshold θ when VRT is employed.

4.2.1 Three Level VRT

In this section we will derive $P_{C|\mathbf{p},\mathbf{b},\mathbf{K}}(\theta)$, $P_{E|\mathbf{p},\mathbf{b},\mathbf{K}}(\theta)$ and $P_{X|\mathbf{p},\mathbf{b},\mathbf{K}}(\theta)$ for a reference user (the first user), that is, the correct, error, and erasure probability of the channel given $\mathbf{p}, \mathbf{b}, \mathbf{K}$ as a function of θ when three level VRT is employed. Since $P_{X|\mathbf{p},\mathbf{b},\mathbf{K}}(\theta) = 1 - P_{C|\mathbf{p},\mathbf{b},\mathbf{K}}(\theta) - P_{E|\mathbf{p},\mathbf{b},\mathbf{K}}(\theta)$, we need only derive the correct and error probabilities. These probabilities can be written as follows given that b_1 ='+1' was

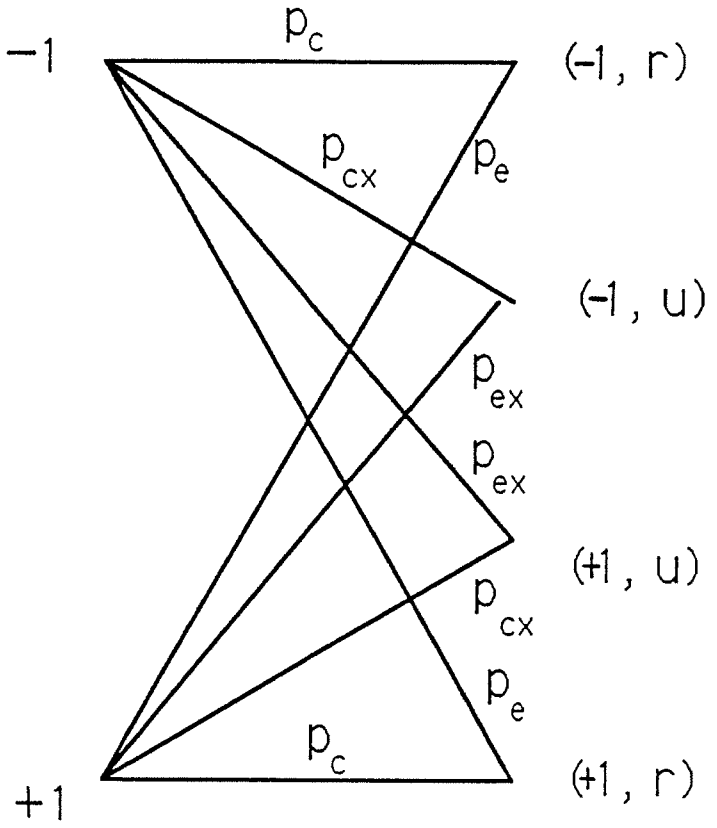

Figure 4.1: Binary input 4-ary output symmetric channel resulting from 4-level VRT.

transmitted.

$$P_{C|\mathbf{p},\mathbf{b},\mathbf{K}}(\theta) = \Pr\{|U_1| > \theta |U_{-1}||b_1 = \text{`+1'}, \mathbf{p}, \mathbf{b}, \mathbf{K}\}.$$

$$P_{E|\mathbf{p},\mathbf{b},\mathbf{K}}(\theta) = \Pr\{|U_{-1}| > \theta |U_1||b_1 = \text{`+1'}, \mathbf{p}, \mathbf{b}, \mathbf{K}\}.$$

First, we derive $P_{C|\mathbf{p},\mathbf{b},\mathbf{K}}(\theta)$.

If we let

$$U_1' = \theta U_1$$

$$U_{-1}' = \theta U_{-1}$$

then

$$\Phi_1'(s) = E\left\{e^{s\theta U_1}\right\} = \Phi_1(s\theta)$$

$$\Phi_{-1}'(s) = E\left\{e^{s\theta U_{-1}}\right\} = \Phi_{-1}(s\theta)$$

where $\Phi_1'(s)$ and $\Phi_{-1}'(s)$ are the characteristic function of U_1' and U_{-1}' and $\Phi_1(s)$ and $\Phi_{-1}(s)$ are the characteristic functions of U_1 and U_{-1} given by (3.19). Now using (3.17), we may express $P_{C|\mathbf{p},\mathbf{b},\mathbf{K}}(\theta)$ in terms of $\Phi_1(s)$ and $\Phi_{-1}(s)$ as follows

$$\begin{aligned} P_{C|\mathbf{p},\mathbf{b},\mathbf{K}}(\theta) &= \Pr\left\{|U_1| > |U_{-1}'||b_1 = \text{`+1'}\right\} \\ &= -\int_0^\infty \Phi_{-1}'(s)\frac{d\Phi_1(s)}{ds}ds \\ &= -\int_0^\infty \Phi_{-1}(s\theta)\frac{d\Phi_1(s)}{ds}ds. \end{aligned} \tag{4.1}$$

Simple calculation shows that

$$\frac{d\Phi_1(s)}{ds} = -e^{-\frac{s^2}{4}}\left[\left(\frac{s}{2}J_0\left(\sqrt{\frac{E_b}{N_0}}s\right) + \sqrt{\frac{E_b}{N_0}}J_1\left(\sqrt{\frac{E_b}{N_0}}s\right)\right)\overline{\Phi}_1(s) - J_0\left(\sqrt{\frac{E_b}{N_0}}s\right)\frac{d\overline{\Phi}_1(s)}{ds}\right]$$

and thus (4.1) can be written as

$$P_{C|\mathbf{p},\mathbf{b},\mathbf{K}}(\theta) = \int_0^\infty e^{-\frac{s^2}{4}(1+\theta^2)}J_0\left(|\rho|\sqrt{\frac{E_b}{N_0}}s\theta\right)\overline{\Phi}_{1,-1}(s,\theta)ds \tag{4.2}$$

where

$$\overline{\Phi}_{1,-1}(s,\theta) = \overline{\Phi}_{-1}(s\theta)\left[\left(\frac{s}{2}J_0\left(\sqrt{\frac{E_b}{N_0}}s\right)+\sqrt{\frac{E_b}{N_0}}J_1\left(\sqrt{\frac{E_b}{N_0}}s\right)\right)\overline{\Phi}_1(s) - J_0\left(\sqrt{\frac{E_b}{N_0}}s\right)\frac{d\overline{\Phi}_1(s)}{ds}\right].$$

Also, since

$$\frac{d\overline{\Phi}_1(s)}{ds} = -\sum_{k=2}^{K'+1} A'_k(1,p_k,b_k)J_1(A'_k(1,p_k,b_k)s)\Pi_{i\neq k}J_0(A'_i(1,p_i,b_i)s)$$

$\overline{\Phi}_{1,-1}(s,\theta)$ can be written as follows

$$\begin{aligned}\overline{\Phi}_{1,-1}(s,\theta) &= \left[\frac{s}{2}J_0\left(\sqrt{\frac{E_b}{N_0}}s\right)+\sqrt{\frac{E_b}{N_0}}J_1\left(\sqrt{\frac{E_b}{N_0}}s\right)\right]\\ &\times \Pi_{k=2}^{K'+1}\left[J_0(A'_k(1,p_k,b_k)s)J_0(A'_k(-1,p_k,b_k)s\theta)\right]\\ &+ J_0\left(\sqrt{\frac{E_b}{N_0}}s\right)\sum_{k=2}^{K'+1}A'_k(1,p_k,b_k)J_1(A'_k(1,p_k,b_k)s)J_0(A'_k(-1,p_k,b_k)s\theta)\\ &\times \Pi_{i\neq k}\left[J_0(A'_i(1,p_i,b_i)s)J_0(A'_i(2,p_i,b_i)s\theta)\right].\end{aligned}$$

This and (4.2) gives the probability of correct detection given $\mathbf{p}, \mathbf{b}$ and $\mathbf{K}$.

We will now average (4.2) over $\mathbf{p}$ and $\mathbf{b}$ to obtain the average probability of correct detection given that the hop is hit by an interference pattern $\mathbf{K}$ and a threshold of θ was employed denoted by $P_C(\theta,\mathbf{K})$. It is easy to see from (4.2) that

$$P_C(\theta,\mathbf{K}) = \int_0^\infty e^{-\frac{s^2}{4}}(1+\theta^2)J_0\left(|\rho|\sqrt{\frac{E_b}{N_0}}s\theta\right)E_{\mathbf{p},\mathbf{b}}\{\overline{\Phi}_{1,-1}(s)\}ds.$$

Under the same assumptions made in Chapter 3 on $\mathbf{p}, \mathbf{b}$, we have

$$\begin{aligned}E_{\mathbf{p},\mathbf{b}}\{\overline{\Phi}_{1,-1}(s)\} &= \left[\frac{s}{2}J_0\left(\sqrt{\frac{E_b}{N_0}}s\right)+\sqrt{\frac{E_b}{N_0}}J_1\left(\sqrt{\frac{E_b}{N_0}}s\right)\right]\Pi_{k=2}^{K'+1}E_1(k,s\theta)\\ &+ J_0\left(\sqrt{\frac{E_b}{N_0}}s\right)\sum_{k=2}^{K'+1}E_2(k,s\theta)\Pi_{i\neq k}E_1(j,s\theta)\end{aligned}$$

where p and b have the generic distribution of p_k's and the b_k's and $E_1(k,s\theta)$, $E_2(k,s\theta)$ are given by

$$\begin{aligned}E_1(k,s\theta) &= E_{p,b}\left\{J_0(A'_k(1,p,b)s)J_0(A'_k(-1,p,b)s\theta)\right\}\\ E_2(k,s\theta) &= E_{p,b}\left\{A'_k(1,p,b)J_1(A'_k(1,p,b)s)J_0(A'_k(-1,p,b)s\theta)\right\}.\end{aligned}$$

Grouping this according to power level groups, we have,

$$\begin{aligned} E_{\mathbf{p},\mathbf{b}}\left\{\overline{\Phi}_{1,-1}(s)\right\} &= \left[\frac{s}{2}J_0\left(\sqrt{\frac{E_b}{N_0}}s\right)+\sqrt{\frac{E_b}{N_0}}J_1\left(\sqrt{\frac{E_b}{N_0}}s\right)\right]\Pi_{n=1}^{N}E_1(n,s\theta)^{\overline{k}_n} \\ &+ J_0\left(\sqrt{\frac{E_b}{N_0}}s\right)\sum_{n=1}^{N}\overline{k}_n E_2(n,s\theta)E_1(n,s\theta)^{\overline{k}_n-1}\Pi_{j\neq n}E_1(j,s\theta)^{\overline{k}_j} \end{aligned}$$

where n denotes the power level group.

We now derive the following conditional error probability

$$P_{E|\mathbf{p},\mathbf{b},\mathbf{K}}(\theta)=\Pr\left\{|U_{-1}|>\theta|U_1||b_1=\text{`}+1',\mathbf{p},\mathbf{b},\mathbf{K}\right\}.$$

Using the notations defined above, this probability can be written as,

$$\begin{aligned} P_{E|\mathbf{p},\mathbf{b},\mathbf{K}}(\theta) &= -\int_0^\infty \Phi_1'(s)\frac{d\Phi_{-1}(s)}{ds}ds \\ &= -\int_0^\infty \Phi_1(s\theta)\frac{d\Phi_{-1}(s)}{ds}ds. \end{aligned} \tag{4.3}$$

Carrying out similar computations as before, we can show that the average error probability $P_E(\theta,\mathbf{K})$, is given by

$$P_E(\theta,\mathbf{K})=\int_0^\infty e^{-\frac{s^2}{4}}(1+\theta^2)J_0\left(\sqrt{\frac{E_b}{N_0}}s\theta\right)E_{\mathbf{p},\mathbf{b}}\{\overline{\Phi}'_{1,-1}(s,\theta)\}ds$$

where

$$\begin{aligned} E_{\mathbf{p},\mathbf{b}}\left\{\overline{\Phi}'_{1,-1}(s,\theta)\right\} &= \left[\frac{s}{2}J_0\left(|\rho|\sqrt{\frac{E_b}{N_0}}s\right)+|\rho|\sqrt{\frac{E_b}{N_0}}J_1\left(|\rho|\sqrt{\frac{E_b}{N_0}}s\right)\right]\Pi_{n=1}^{N}E_1'(n,s\theta)^{\overline{k}_n} \\ &+ J_0\left(|\rho|\sqrt{\frac{E_b}{N_0}}s\right)\sum_{n=1}^{N}\overline{k}_n E_2'(n,s\theta)E_1'(n,s\theta)^{\overline{k}_n-1}\Pi_{j\neq n}E_1'(j,s\theta)^{\overline{k}_j} \end{aligned}$$

and

$$\begin{aligned} E_1'(k,s\theta) &= E_{p,b}\left\{J_0(A_k'(1,p,b)s\theta)J_0(A_k'(-1,p,b)s)\right\} \\ E_2'(k,s\theta) &= E_{p,b}\left\{A_k'(-1,p,b)J_1(A_k'(1,p,b)s)J_0(A_k'(1,p,b)s\theta)\right\}. \end{aligned}$$

4.2.2 Four Level VRT

The average channel statistics $P'_C(\theta, \mathbf{K}), P'_{CX}(\theta, \mathbf{K}), P'_{EX}(\theta, \mathbf{K}), P'_E(\theta, \mathbf{K})$, for the four level Viterbi ratio thresholding channel can be written in terms of that of the three level Viterbi ratio thresholding channel and the hard decisions channel as follow [Vit 85].

$$\begin{aligned} P'_C(\theta, \mathbf{K}) &= P_C(\theta, \mathbf{K}) \\ P'_{CX}(\theta, \mathbf{K}) &= P_C(1, \mathbf{K}) - P_C(\theta, \mathbf{K}) \\ P'_{EX}(\theta, \mathbf{K}) &= P_E(1, \mathbf{K}) - P_E(\theta, \mathbf{K}) \\ P'_E(\theta, \mathbf{K}) &= P_E(\theta, \mathbf{K}). \end{aligned}$$

Note that when $\theta = 1$ the resulting channel is equivalent to hard decisions channel. Hence $P_E(1, \mathbf{K})$ is the probability of error for the hard decisions scheme without VRT derived in Chapter 3. All the expressions for the channel statistics can be further averaged over $\mathbf{K}$ using (3.29). We denote these average probabilities as $P'_E(\theta)$, $P'_C(\theta)$, $P'_{CX}(\theta)$, $P'_{EX}(\theta)$.

This concludes our derivation of the expressions for the transition probabilities of the resulting DMC when VRT is employed. In the next section we look at convolutional codes and bounds on their performance.

4.3 Convolutional Codes and Bounds on Their Performance

In this section we briefly describe binary convolutional codes and the Viterbi algorithm for decoding convolutional codes. We also present an upper bound on the packet error probability when convolutional coding and the Viterbi algorithm [Vit 71] [For 73] is employed. For simplicity of description, we assume that the data bits and the channel symbols are in $\{0, 1\}$ instead of $\{+1, -1\}$.

4.3.1 Binary Convolutional Codes

A binary convolutional encoder is simply a finite state machine (a shift register circuit) shown in Fig. 4.2. The binary input data sequence into the decoder is denoted by $\{i_t\}$ ($i_t \in \{0,1\}$) and $\{\mathbf{z}_t\}$ is the binary output stream where $\mathbf{z}_t = (z_t^1, \cdots z_t^n)$ is the output of the encoder ($z_t^i \in \{0,1\}$, $i = 1,2,\cdots,n$, $t = 1,2,\cdots,$) corresponding to the input data symbol i_t. The rate of the code is then $r = \frac{m}{n}$ [data symbol/code symbol] where m is the number of data bits shifted into the encoder at a time. The number of memory elements m in the decoder is called the memory length of the code and $K = m + 1$ is called the constraint length of the code. An example of a $K = 3$, $r = \frac{1}{2}$ convolutional encoder is shown if Fig. 4.3. The encoder outputs two channel symbols corresponding to switch states 1 and 2 for each input symbol.

It is well known that that a convolutional code can be described by a compact diagram called the *trellis* diagram [Vit 71]. The trellis diagram of the code represented in Fig. 4.3 is given in Fig. 4.4. This trellis has four states a,b,c and d corresponding to the state of the shift register of the encoder $(u_1, u_2) = (0,0)$, $(0,1)$, $(1,0)$, $(1,1)$. In the trellis diagram the encoder initially starts at state a and makes a transition to a new state via one of the two branches emerging from the state for every input symbol and thus follows a path through the trellis according to the input sequence. When the input symbol is a '0', the encoder takes the branch represented by the solid line to the new state and when the input symbol is a '1', it moves to a new state following the dotted branch. The vectors $\mathbf{s}_{ij}$ given above each branch connecting the states i and j are the outputs of the encoder corresponding to the state transitions.

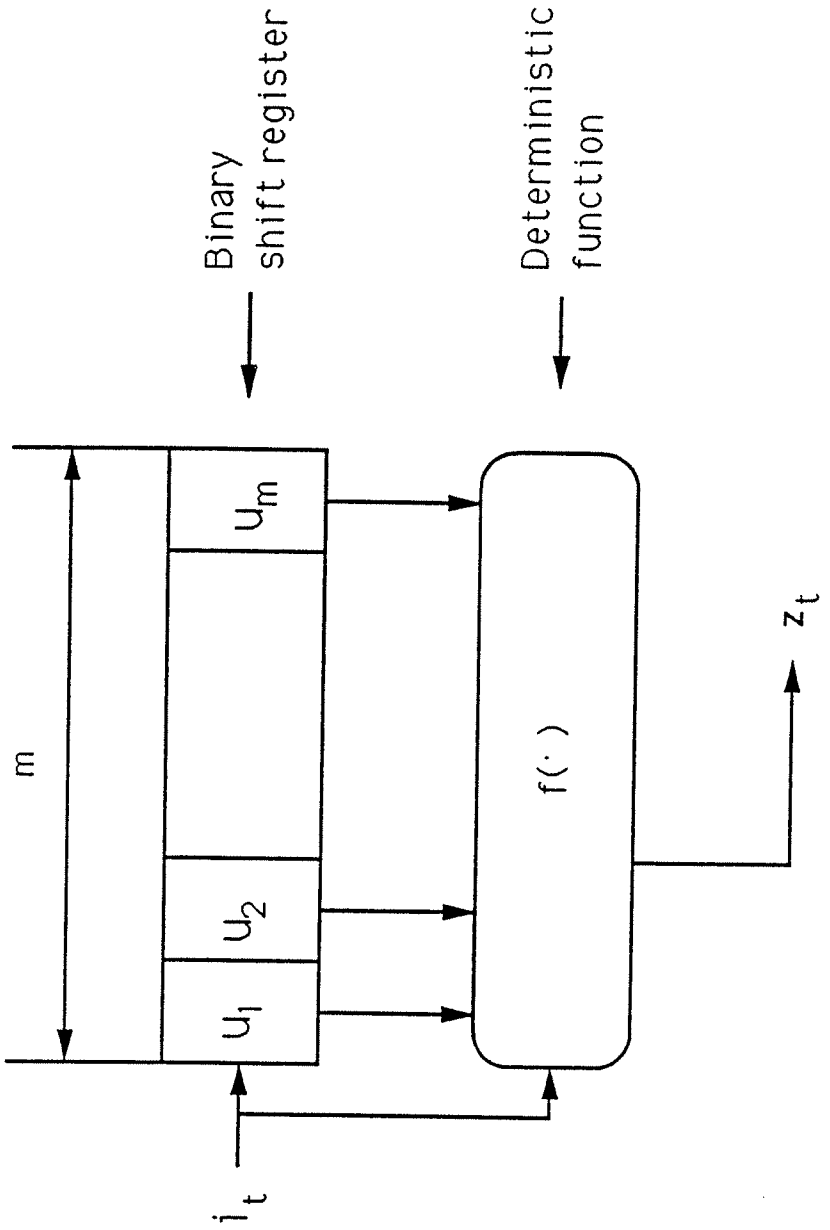

Figure 4.2: Binary convolutional encoder.

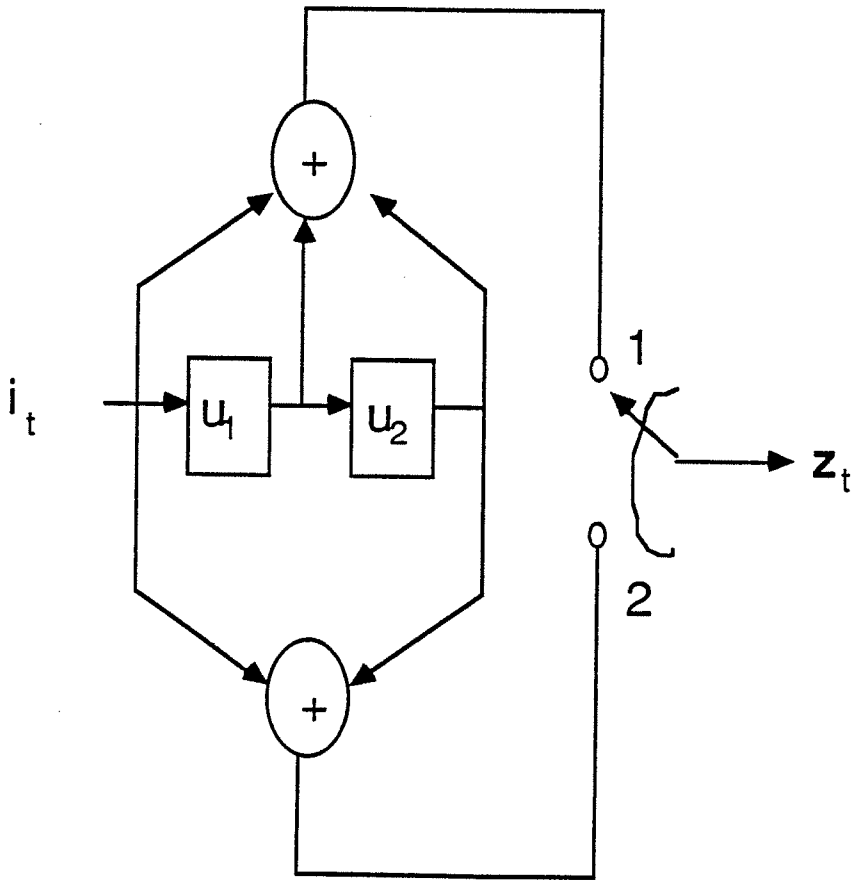

Figure 4.3: Rate $\frac{1}{2}$, $K = 3$ binary convolutional code.

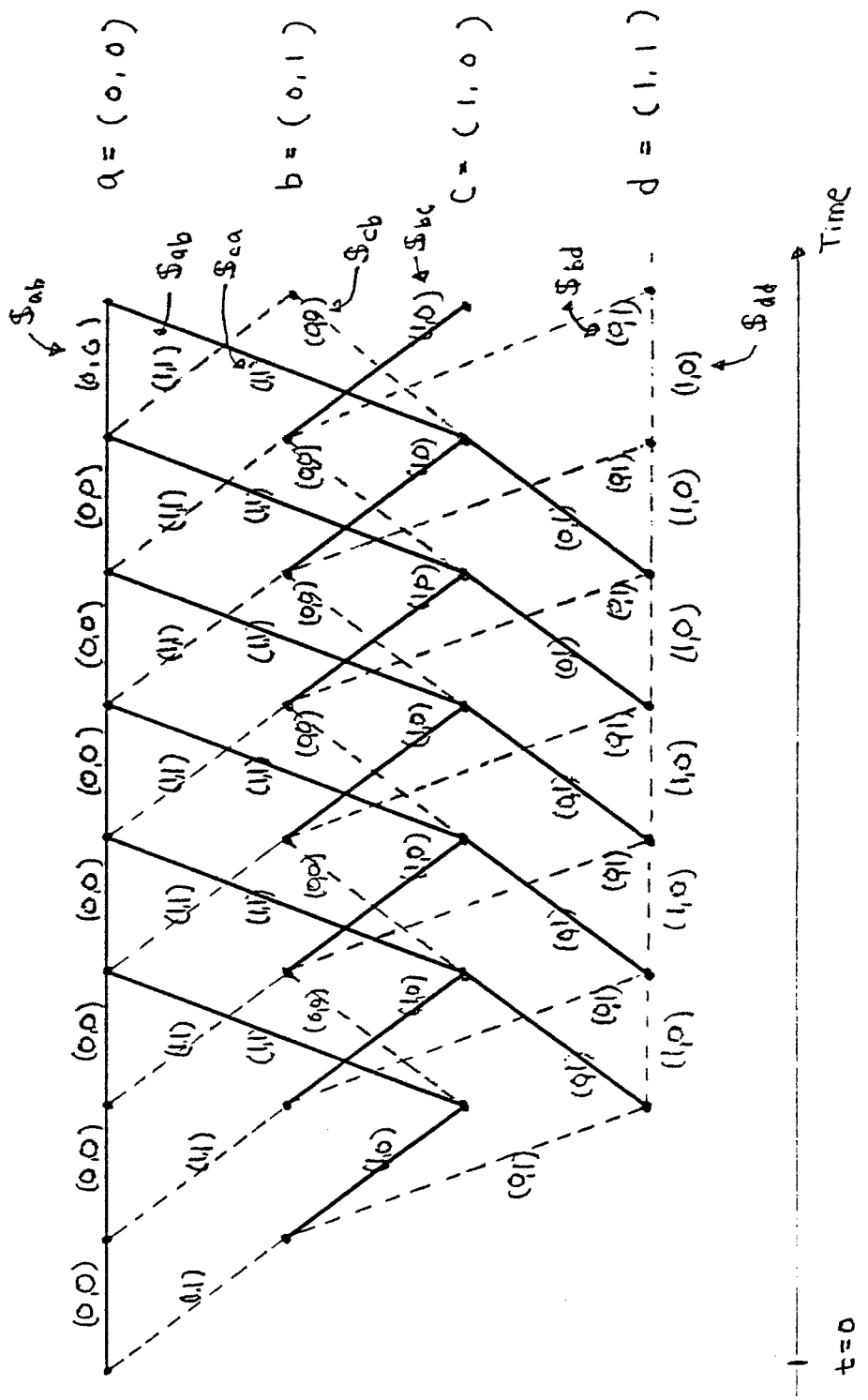

Figure 4.4: Trellis diagram for the code in Fig.4.2.

4.3.2 Decoding of Convolutional Codes

It is well known that the Viterbi algorithm provides a Maximum *a posteriori* probability (MAP) estimate of the path taken by the convolutional encoder through the trellis, i.e., the Viterbi algorithm is a MAP decoding rule [Vit 71] [For 73] [Vit 79a]. We will briefly describe the operation of the Viterbi decoder for the trellis shown in Fig. 4.3 for a BSC with crossover probability less than $\frac{1}{2}$ using the Hamming metric (the Hamming metric will be defined below). It is straightforward to generalize the Viterbi algorithm to general DMCs and metrics [Vit 79a] where a metric is any function between the input and the output sequence of the channel with the property that the total metric between the input and the output sequences is equal to the sum of the metrics of each channel input and output pair of the sequence [Sim 85].

The Hamming distance between two binary vectors is defined to be the number of places in which they differ. Each state of the trellis in the decoder has 'metric memory' devices that stores integer numbers which are initially set to zero. Let the output of the channel (input to the decoder) be denoted by $\mathbf{y}_t$ which is a corrupted version of the encoder output. That is $\mathbf{y}_t = \mathbf{z}_t \oplus \mathbf{n}_t$ where $\mathbf{n}_t$ is a binary n-vector representing noise and $\oplus$ denotes *mod* 2 addition. For the first two branches eminating from state a, the Hamming distance computed between the vector $\mathbf{y}_0$ and the $\mathbf{s}$ vectors for each branch are stored in the memory for state a and b. For the second state transition due to the the second input symbol, the Hamming distance between the vectors $\mathbf{y}_1$ and the $\mathbf{s}$ vectors are computed for each branch and the sum of this value with the value stored in the memories of the originating states are stored in the memories of the new states. After the vector $\mathbf{y}_2$ corresponding to the third input symbol received, a state in the decoder trellis has multiple incoming branches and each incoming branch corresponds to a different path through the trellis that leads

to that state. We attach a number to each incoming path called the path metric. The path metric for a path Π that is t branches long is defined to be the Hamming distance between the sequence $(\mathbf{y}_0, \cdots, \mathbf{y}_t)$ and $(\mathbf{z}_0^{\Pi}, \cdots, \mathbf{z}_t^{\Pi})$ where $\mathbf{z}_{t'}^{\Pi}$ is the output of the encoder for the t'-th branch for path Π.

For each state, the decoder computes the metric corresponding to each of the incoming (competing) branches and chooses the branch with the smallest metric as the *survivor* and sets its metric memory equal to the survivors metric. Note that at each time t there will always be four surviving paths and when the transmitter forces the encoder state to a by transmitting two consecutive zeros, there will only be one survivor left and the input data sequence that would have produced this trellis path is the MAP estimate of the transmitted data sequence. based on the observation of the outputs of the matched filters

4.3.3 Error Performance

In this section, we derive bound on the error performance of convolutional codes. In evaluating the error performance of the Viterbi decoder we need only consider the all zeros input sequence since we only consider linear convolutional codes [Vit 79a]. We refer to the trellis path corresponding to the all zeros input as the *all zeros path.* Also, Hamming weight of a path is defined to be the Hamming weight (the Hamming distance between a vector and the all zeros vector) of the output sequence of the encoder corresponding to the path.

Usually, the data to be transmitted over the network is grouped into *packets* and the transmission is considered successful only if the packet is received error free. Let the length of one packet be L bits long and define the *first event error* as the event that a nonzero path (a path that corresponds to non all zero inputs) eminating from

state a is selected as the survivor over the all zeros path. It is well known [Pro 83] that the probability of first event error denoted by P_f may be upper bounded as follows

$$P_f \leq \sum_{d=d_f}^{\infty} W_d D^d \tag{4.4}$$

where W_d is the number of paths that eminate from state a and remerge to state a with weight d, and d_f is the minimum of weights over all the nonzero paths called the *free distance* of the code. The parameter D is called the Chernoff parameter, and is defined as

$$D = \min_{\lambda \geq 0} E\{\exp(\lambda(\, m(y, \hat{x}; \phi) - m(y, x; \phi)))|x\}|_{x \neq \hat{x}} \tag{4.5}$$

where $m(y, x; z)$ is the metric between the output symbol y and the input symbol x and ϕ is the side-information if any.

It is easy to see that during the transmission of an all zeros vector of length L a packet error will occur if at least one first event error occurs. Hence the packet error probability P_p may be upper bounded as follows

$$P_p \leq L \cdot P_f \tag{4.6}$$

which is a simple union bound.

4.3.4 Metrics

In this section we will look into the metrics used by the Viterbi decoder for different channels. The Chernoff parameter corresponding to these metrics will also be given. We have already mentioned that for a BSC, a Viterbi decoder employing the Hamming metric results in a MAP estimate of the transmitted data symbols. The Chernoff parameter when Hamming metric is used with a BSC with crossover

probability p is given by [Sim 85]

$$D = 2\sqrt{p(1-p)}.$$

Also, for a BSEEC with error and erasure probability p_e and p_x, it can easily be shown that a Viterbi decoder using Hamming distance as the metric and ignoring the erased symbols results is a MAP decoder. In this case the Chernoff parameter can be written as [Sim 85]

$$D = p_x + 2\sqrt{p_e(1-p_e-p_x)}.$$

For a binary input 4-ary output channel resulting from 4-level VRT, we resort to a suboptimal metric called the integer metric [Vit 85] given by

$$\begin{aligned} m((0,r),0) &= N_{met} \\ m((1,r),0) &= -N_{met} \\ m((0,u),0) &= 1 \\ m((1,u),0) &= -1 \end{aligned} \tag{4.7}$$

where N_{met} is an integer that should be chosen appropriately. Straightforward calculation shows that the Chernoff parameter for this case is [Che 88b]

$$\begin{aligned} D(\theta) &= \min_{\lambda \geq 0} \left[P'_C(\theta)e^{-2\lambda N_{met}} + P'_{CX}(\theta)e^{-2\lambda} + P'_{EX}(\theta)e^{2\lambda} \right. \\ &+ \left. P'_E(\theta)e^{2\lambda N_{met}} \right] \end{aligned} \tag{4.8}$$

where the dependence of the Chernoff parameter and the transition probabilities on θ is made explicit.

4.4 Numerical Results

In this section we present numerical results on the performance of VRT in an AFHSS-MA network. For simplicity we will restrict ourselves to the case when

orthogonal BFSK with minimum frequency separation is used and all users have the same power as seen by the first user. The number of slots available is taken to be 100 throughout this section.

4.4.1 Simulation

First, in order to verify that the expressions for the channel statistics developed in this chapter is valid, we plot in Figs. 4.5-4.8, the probability of error and erasure versus the number of interfering users that hit the hop (K') for $\frac{E_b}{N_0}$ =13 and 19dB when three level VRT is employed with $\theta = 1.5$ and 2.5 along with simulation results.

These results show that our expressions for the channel statistics when three level VRT is employed are very close to the simulation results. Also since the channel statistics when four level VRT is employed is a function of the channel statistics when three level VRT is employed with the same θ and the probability of error when hard decisions are made, we may conclude that the results for the channel statistics when four level VRT is employed are also correct.

4.4.2 Channel Capacity and Associated Throughput

In this section we use the formulas developed in Section 5 of Chapter 2 to compute the channel capacity and the associated throughput under the following conditioned.

1. Hard decisions.
2. Perfect side-information: Erase the symbols that are hit.
3. Perfect side-information.
4. Knowledge of the exact number of interfering users in each hop.
5. Three level VRT.

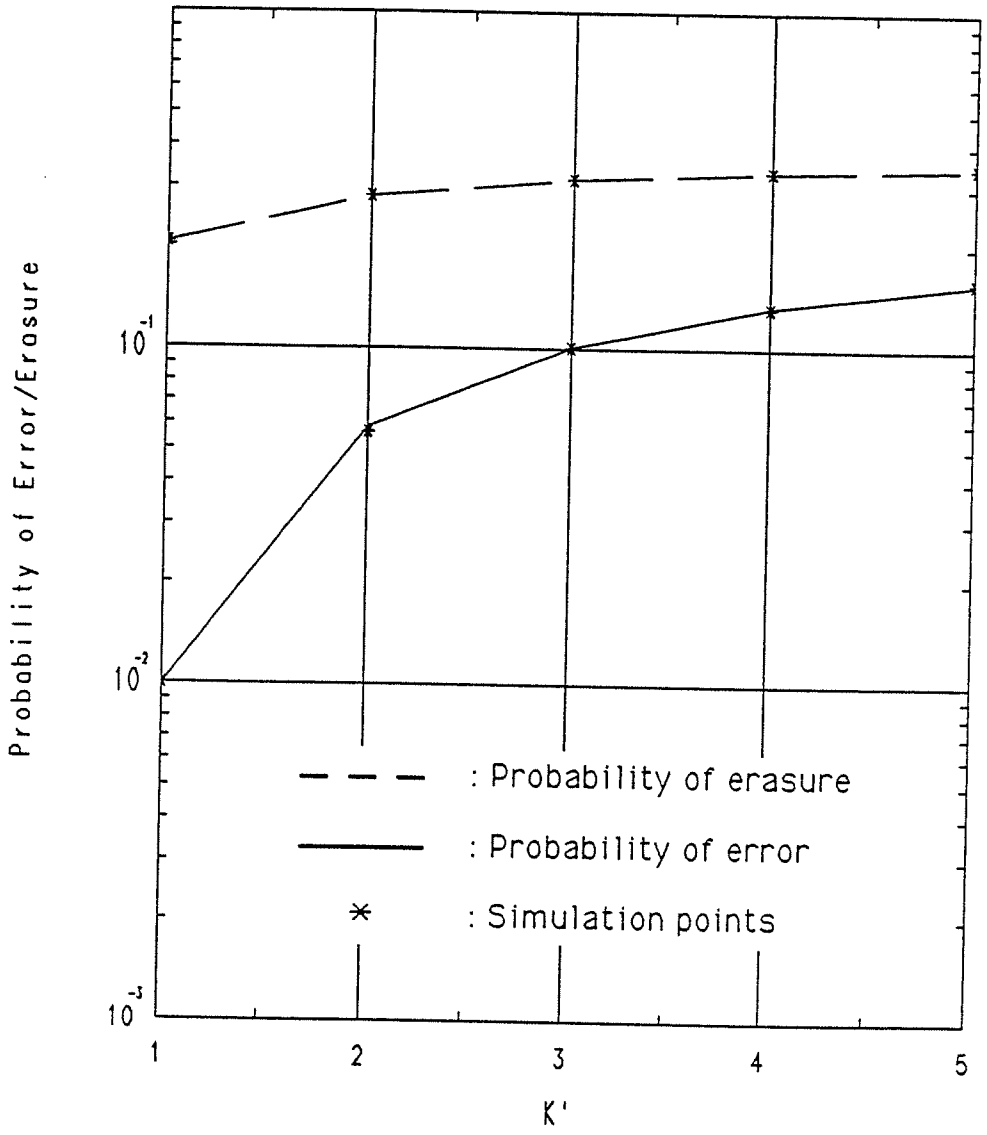

Figure 4.5: Probability of error and erasure versus K' for three level VRT with $\theta =$ 1.5. $\frac{E_b}{N_0}$ =13d.

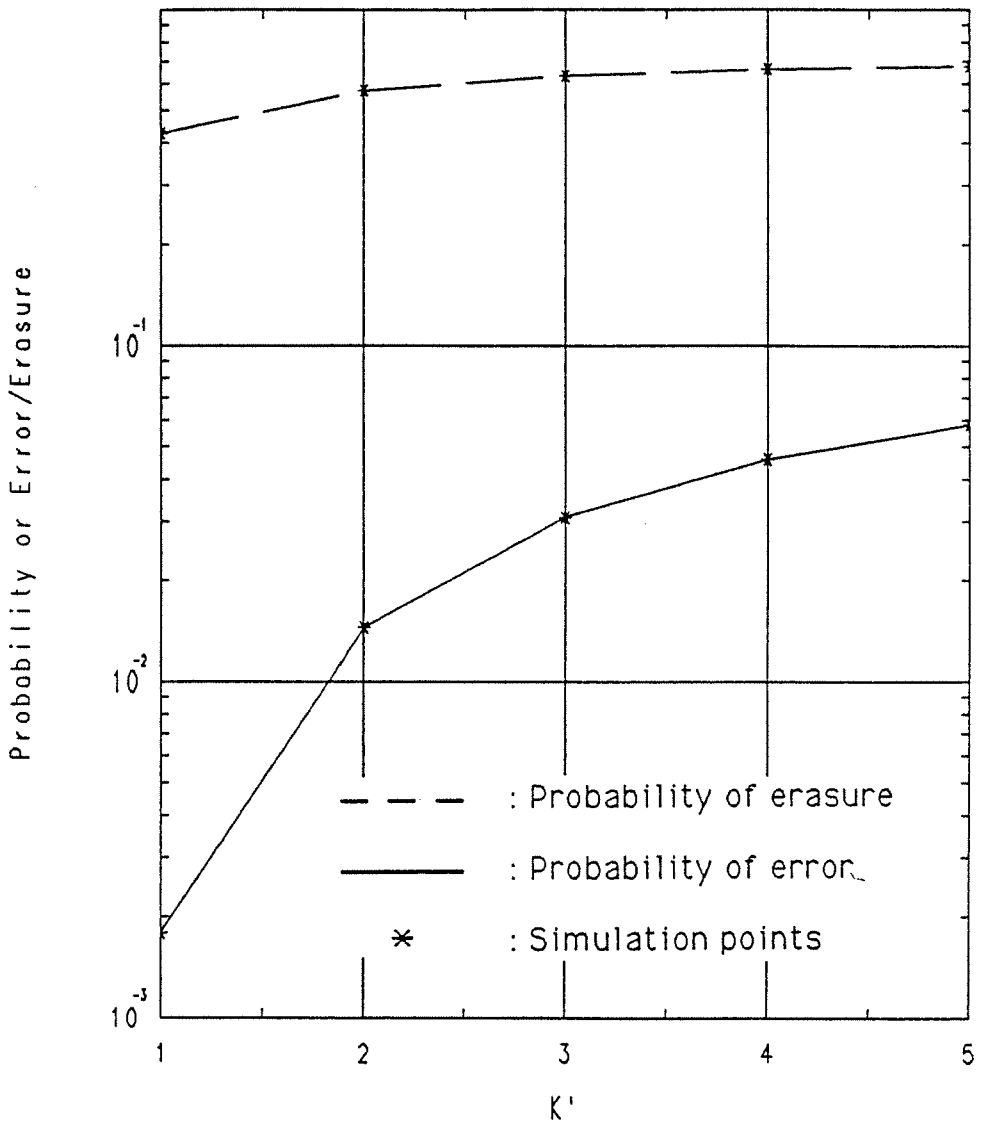

Figure 4.6: Probability of error and erasure versus K' for three level VRT with $\theta =$ 2.5. $\frac{E_b}{N_0}$ =13dB.

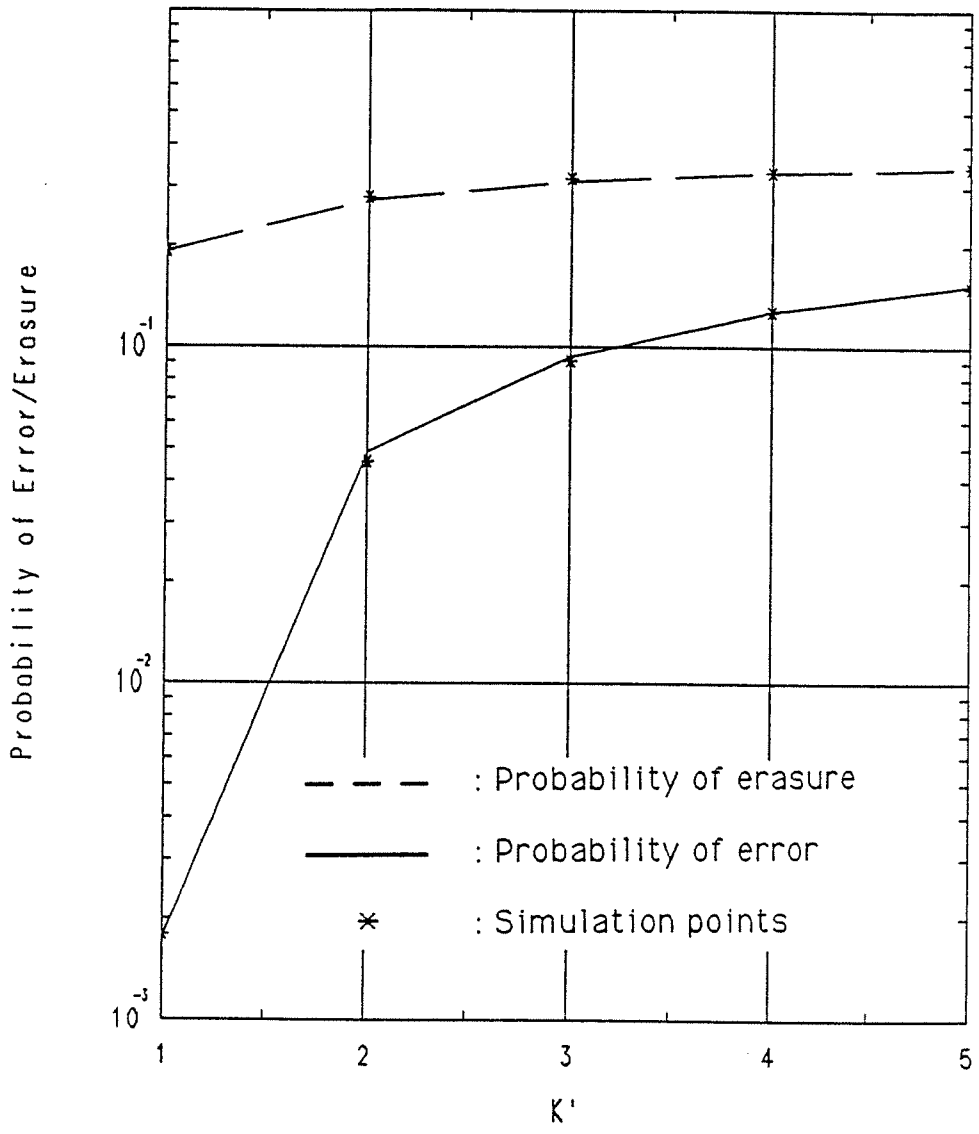

Figure 4.7: Probability of error and erasure versus K' for three level VRT with $\theta =$ 1.5. $\frac{E_b}{N_0}$ =19dB.

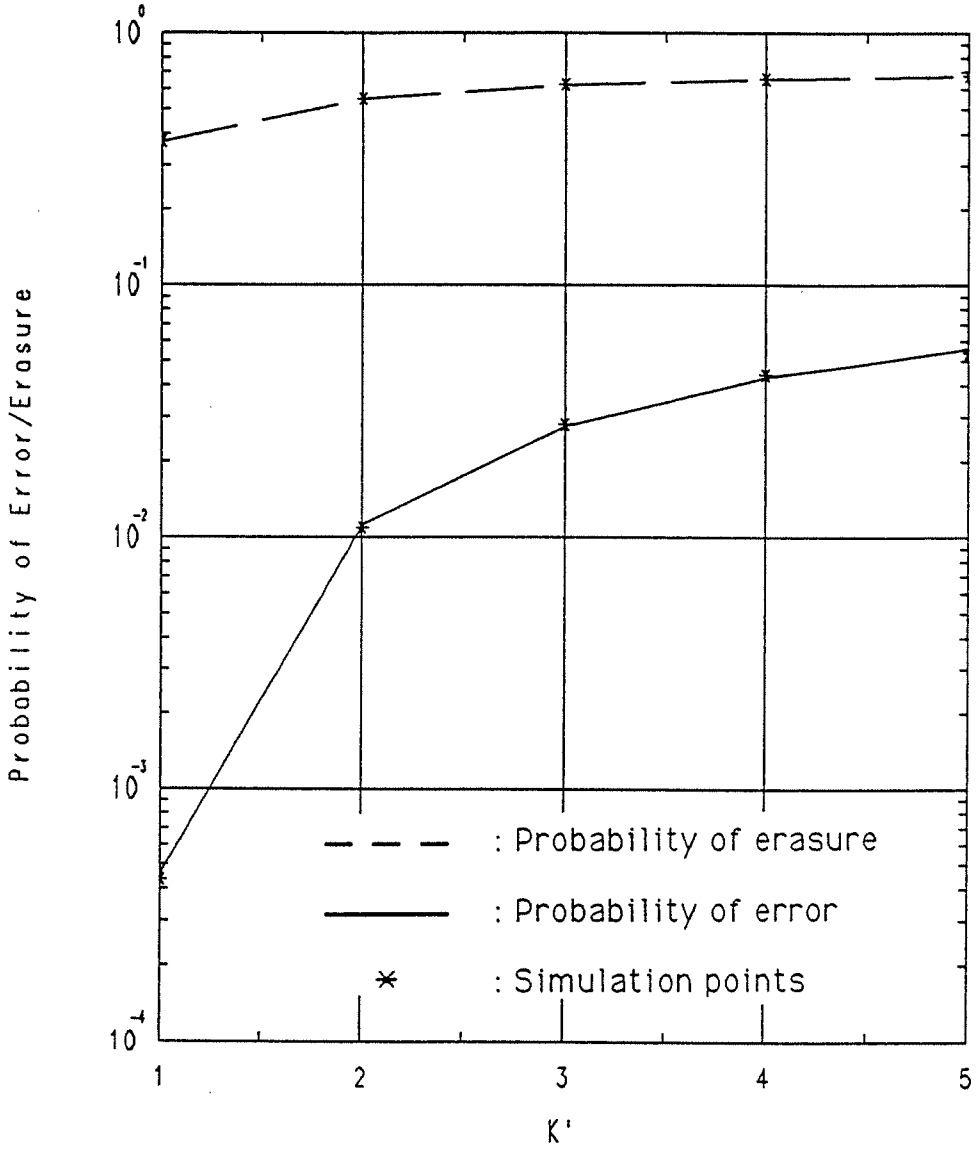

Figure 4.8: Probability of error and erasure versus K' for three level VRT with $\theta = 2.5$. $\frac{E_b}{N_0}$ =19dB.

6. Four level VRT.

The difference between system (2) and (3) is that system (2) first erases all the symbols that are hit and then makes maximum likelihood decisions on the codewords and system (3) does maximum likelihood decoding on the codewords without first erasing the symbols that were hit. Figs. 4.9-4.11 are the plots of the channel capacity corresponding to these systems for $\frac{E_b}{N_0}$ =13dB and θ = 1.5, 2.0, 2.5, and Figs. 4.12-4.14 are the associated throughput for the the same parameters. We note from these figures that with an appropriate choice of θ, we gain up to 15% in maximum throughput over system (1) with system (5) and almost 25% with system (6). Also note that using perfect side-information and ML decoding (3) only gives a mediocre gain over system (1) (hard decisions) and both systems (5) and (6) perform better than system (4). This indicates that side-information as to the exact number of interfering users is less informative than information about the relative magnitudes of the matched filters at the demodulator. This can be intuitively explained by looking at Fig. 3.1 and noting that the probability of error (when the hop is hit by one interfering user) is strongly dependent on the relative delay and the data bit of the interfering user. Hence the fact that a hop is hit does not guarantee that the hit rendered the hop useless. This observation has far reaching consequences since systems (5) and (6) are quite easily implementable whereas systems (2) (3) and (4) are not. In order to study the dependence of the performance on the threshold value θ, we plot the throughput versus K for systems (5) and (6) with θ as a parameter in Figs. 4.15-4.16. We note that the optimum value of θ that maximizes throughput for these systems is very robust against variations in the number of users in the network and globally (with respect to K) optimum values of θ exists. Also, for system (6) the performance of the network is relatively insensitive of small

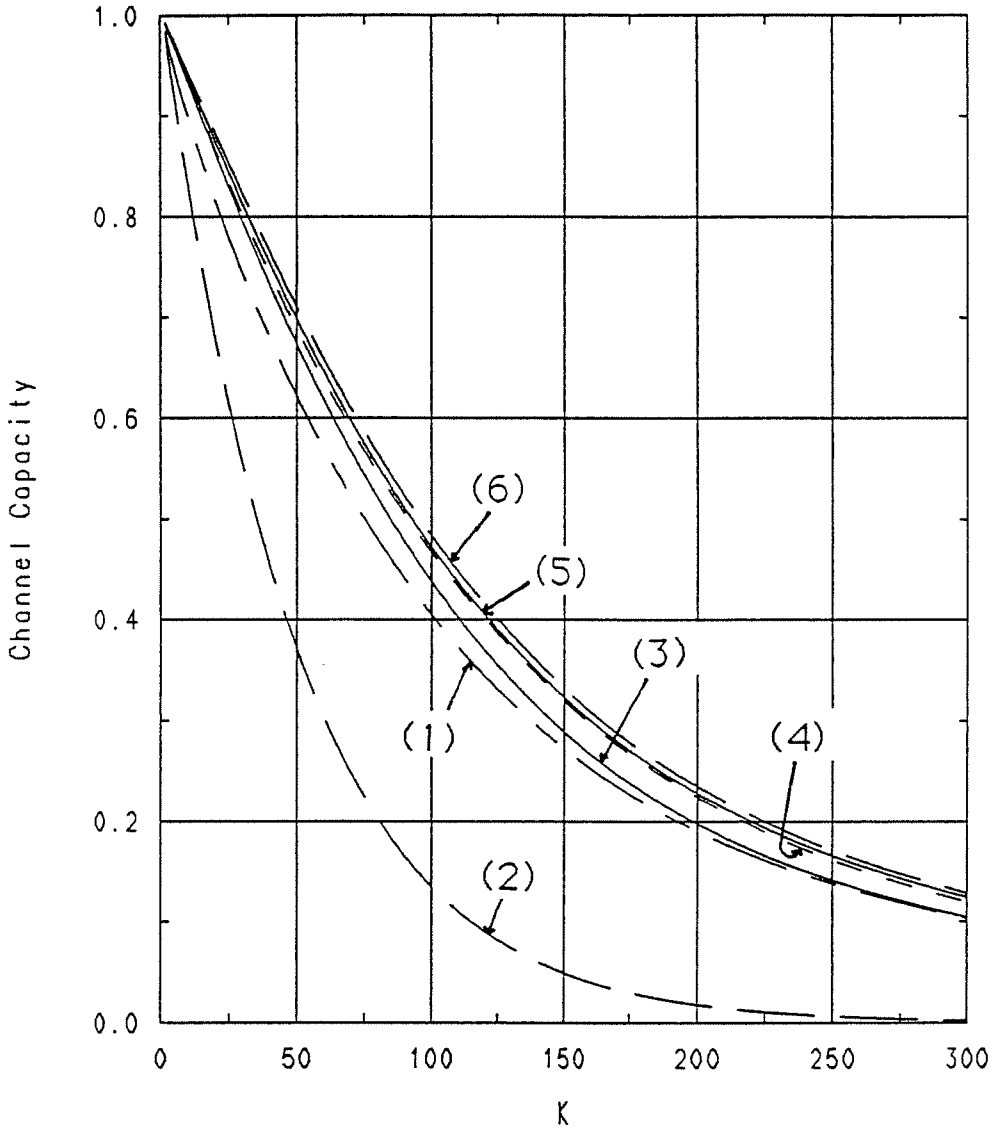

Figure 4.9: Channel capacity versus the number of users in the network of various systems for $\frac{E_b}{N_0}$ =13dB and $\theta = 1.5$.

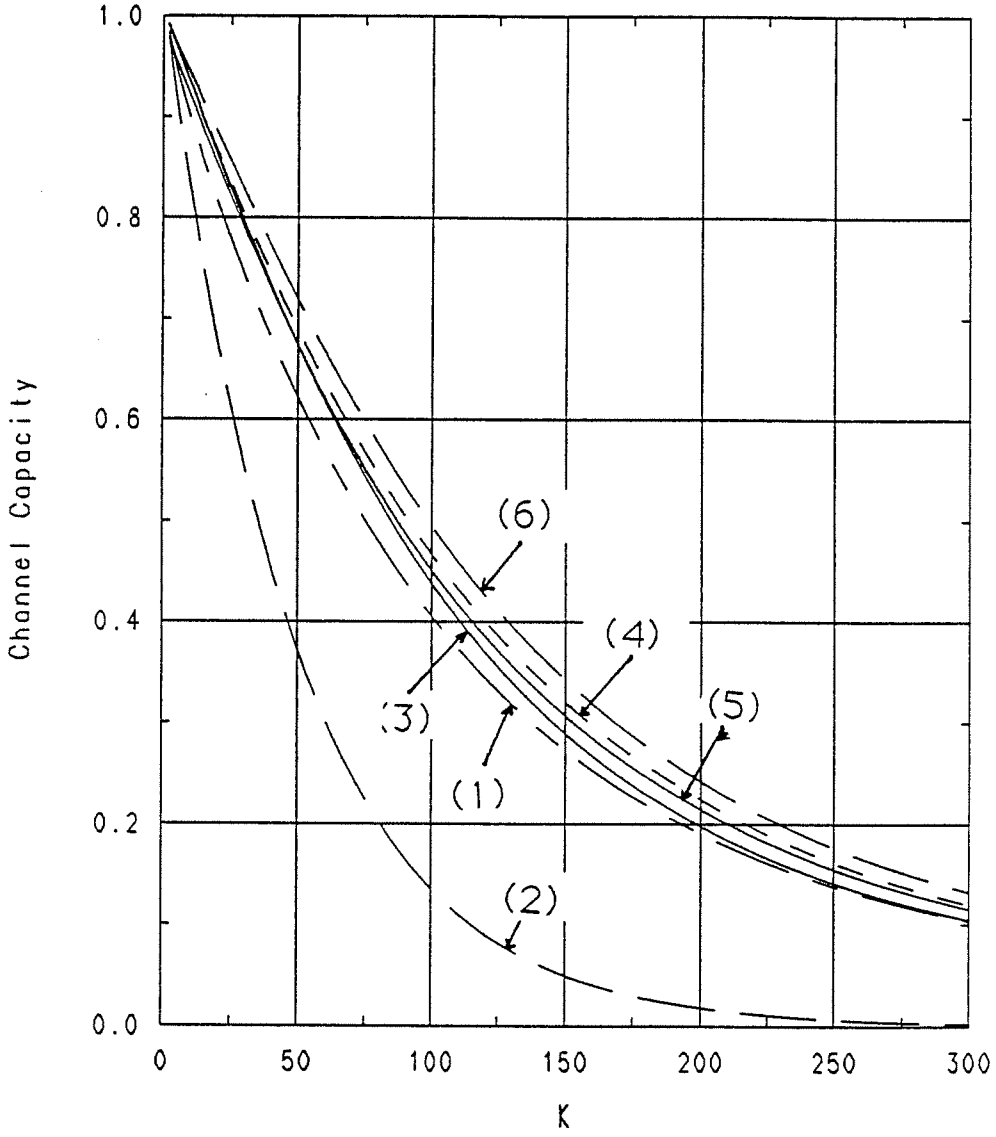

Figure 4.10: Channel capacity versus the number of users in the network of various systems for $\frac{E_b}{N_0}$ =13dB and $\theta = 2.0$.

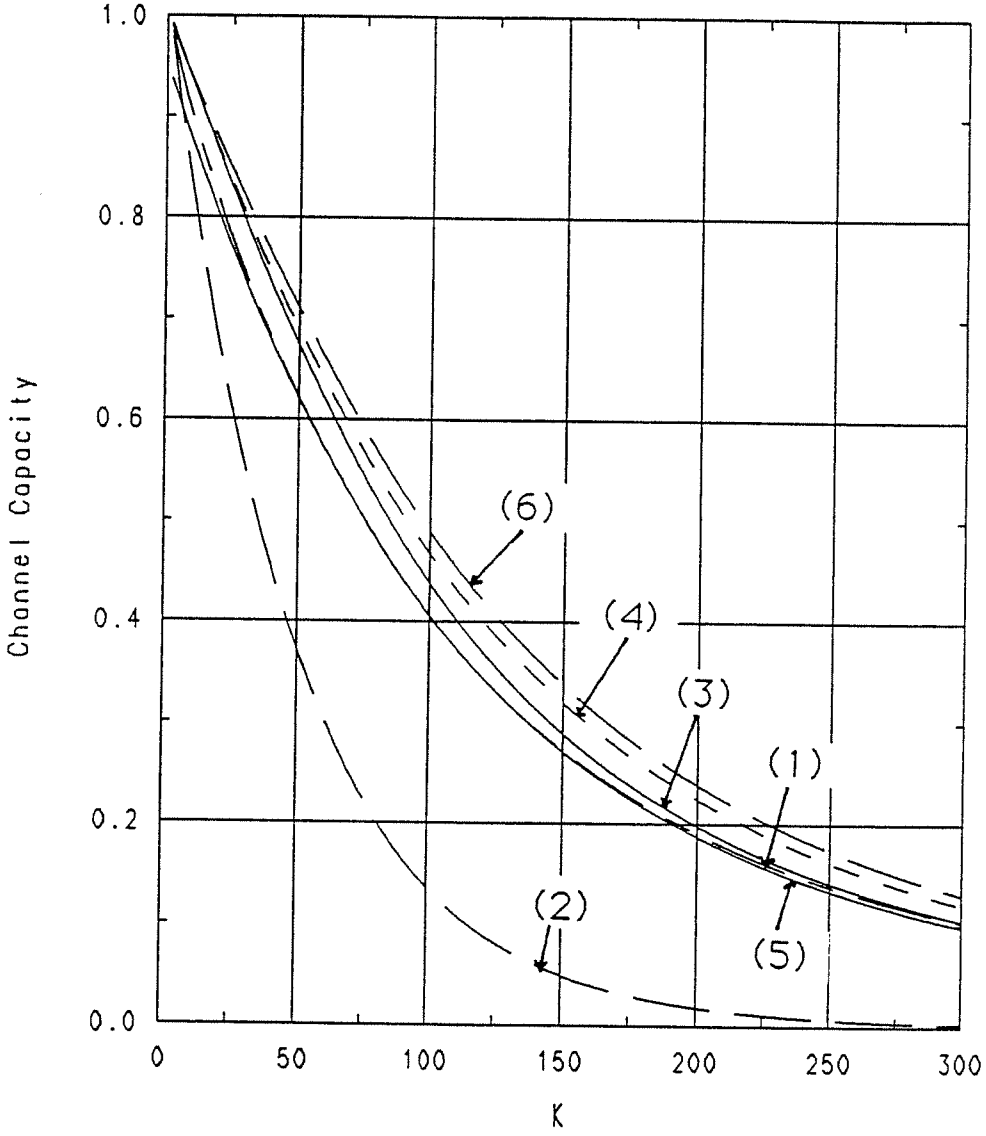

Figure 4.11: Channel capacity versus the number of user in the network of various systems for $\frac{E_b}{N_0}$ =13dB and $\theta = 2.5$.

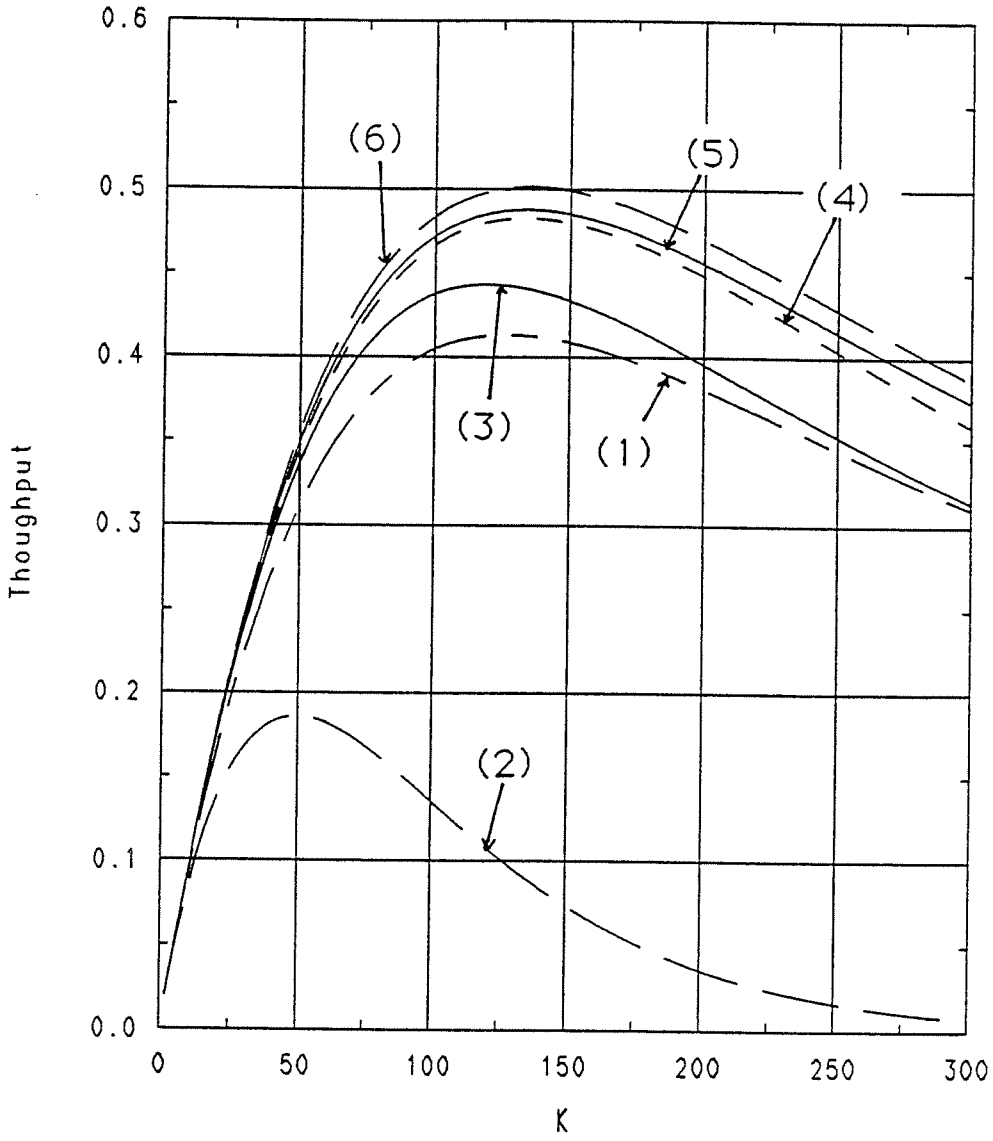

Figure 4.12: Throughput associated with channel capacity versus the number of users in the network of various systems for $\frac{E_b}{N_0}$ =13dB and $\theta = 1.5$.

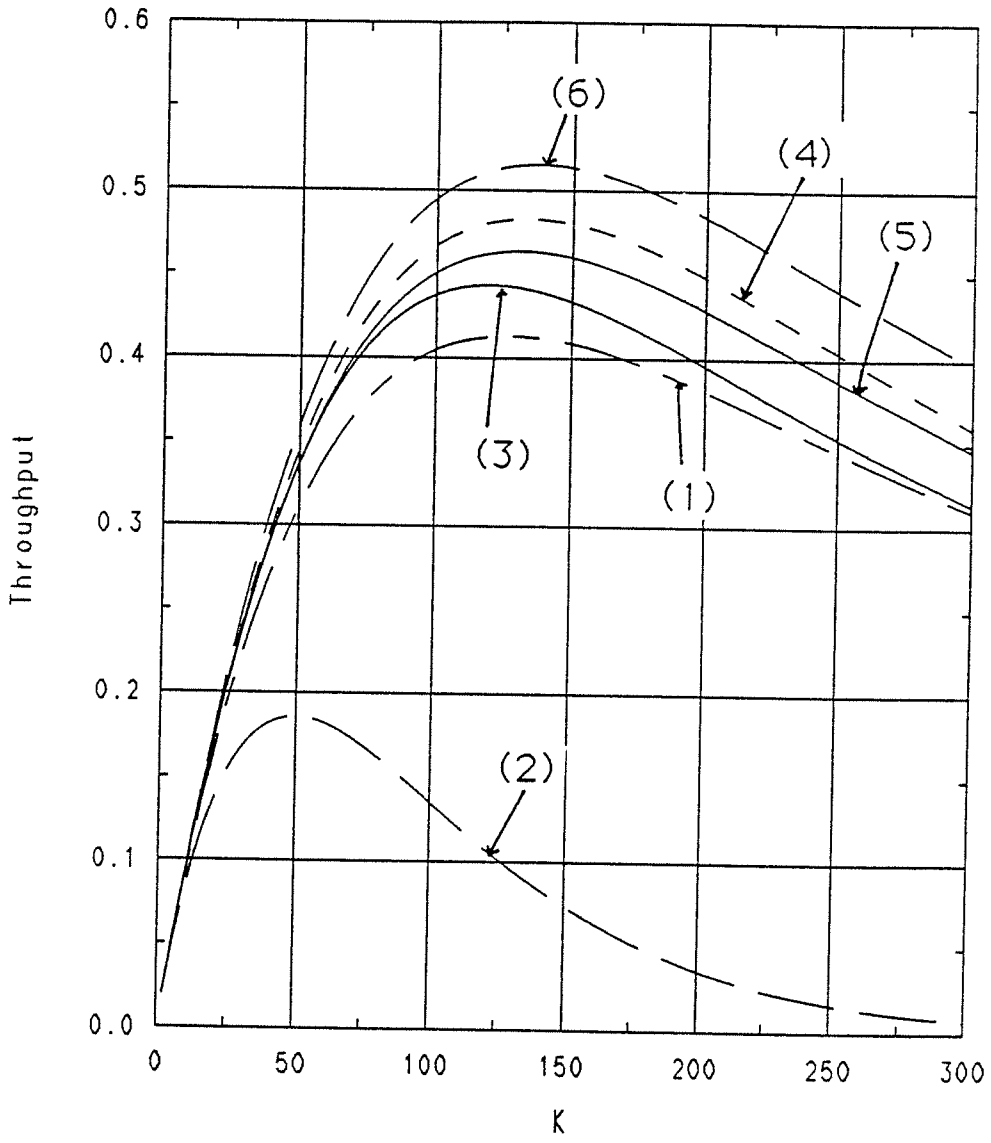

Figure 4.13: Throughput associated with channel capacity versus the number of users in the network of various systems for $\frac{E_b}{N_0}$ =13dB and $\theta = 2.0$.

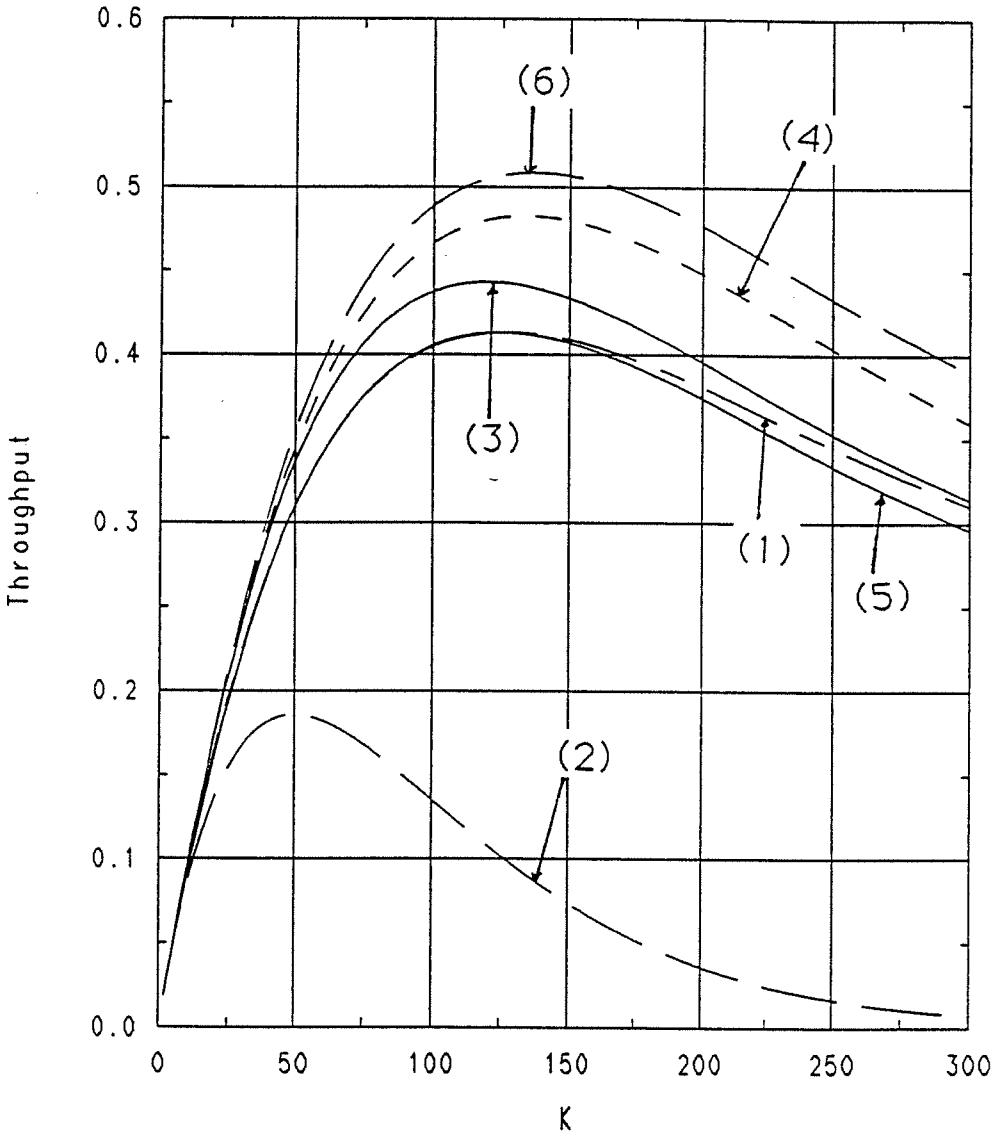

Figure 4.14: Throughput associated with channel capacity versus the number of users in the network of various systems for $\frac{E_b}{N_0}$ =13dB and $\theta = 2.5$.

perterbations of θ about its optimal value.

4.4.3 Convolutional Coding

In this section we consider the performance of some of the practical systems considered in the previous section when a rate $\frac{1}{2}$, $K = 7$ convolutional code is employed. Here we also present for reference, the results for the case when hard decisions are made and the $\frac{1}{2}$-approximation is used in the analysis. We refer to to this case as system (0).

The length of one packet is taken to be 70 bits long ($L = 70$). In Figs. 4.17-4.19, we plot the lower bounds on the normalized throughput for systems (0), (1), (2), (5) and (6) for $\theta = 1.5$, 2.0, 2.5 and $N_{met} = 5$ using (4.4) and (4.6) for $\frac{E_b}{N_0}$ =13dB. We note that we obtain close to a two fold gain in performance over simple hard decisions by using VRT. Again, in order to study the dependence of the throughput on θ for systems (5) and (6) we plot the throughputs of systems (5) and (6) with θ as a parameter in Figs. 4.20-4.21. These figures indicate that the optimal values of θ are close to that predicted by a system achieving channel capacity. Also, there is the problem of choosing N_{met}. Numerical results indicate that N_{met} =3,4,5 gives comparable performance and that $N_{met} \geq 7$ is too high.

We wish to emphasize that the results presented in Figs. 4.17-4.21 are derived from bounds (4.4) and (4.6) which are, respectively, the union-Chernoff bound on the first event error probability and the union bound on the packet error probability. These bounds on the error probabilities can be quite tight when the associated probabilities are small, say $< 10^{-4}$. Unfortunately, the regions of interest here (regions of high throughput) are where the probability of error is relatively high in this case, these bounds are quite loose. Also, the sharp drop in the normalized throughput

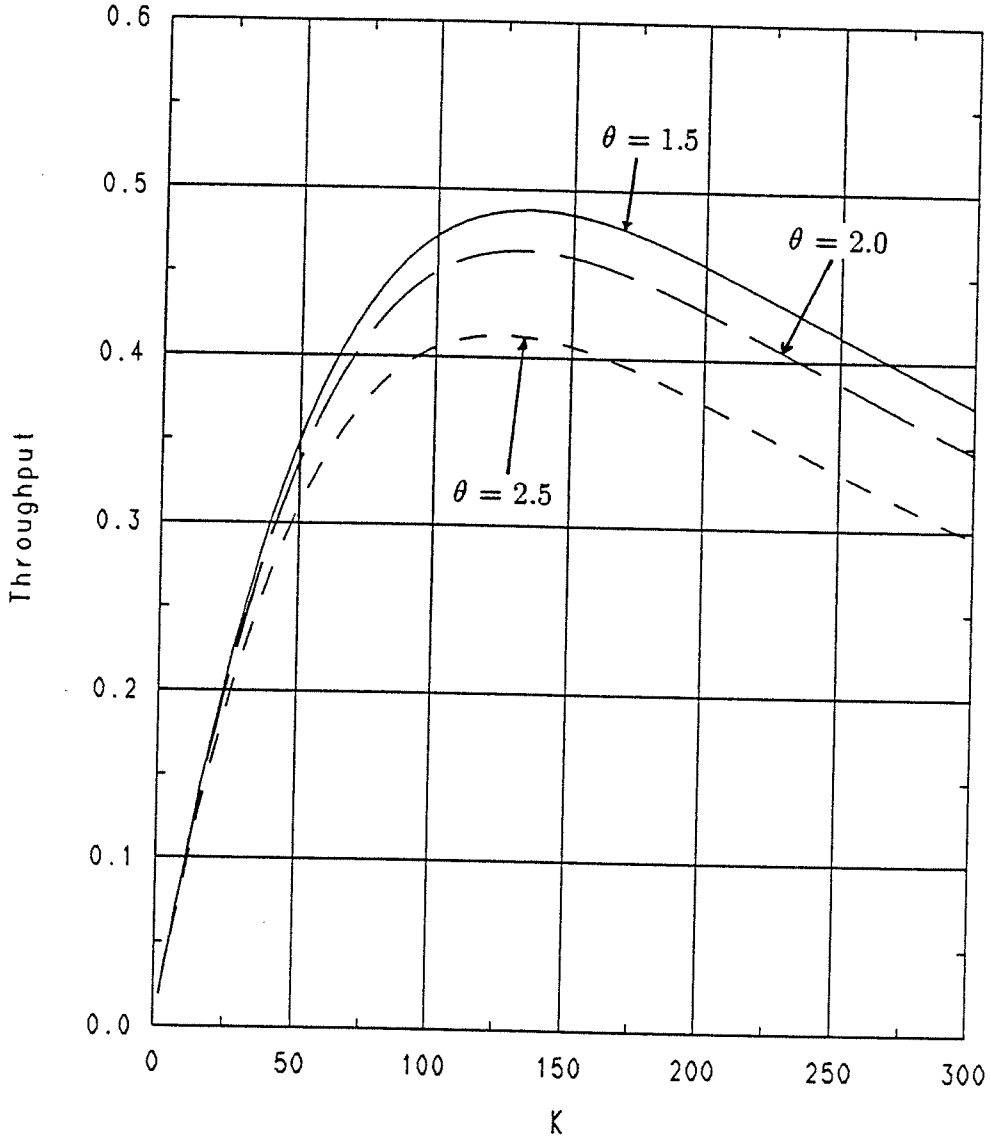

Figure 4.15: Throughput associated with channel capacity versus the number of users in the network of system (5) for $\frac{E_b}{N_0}$ =13dB with θ as a parameter.

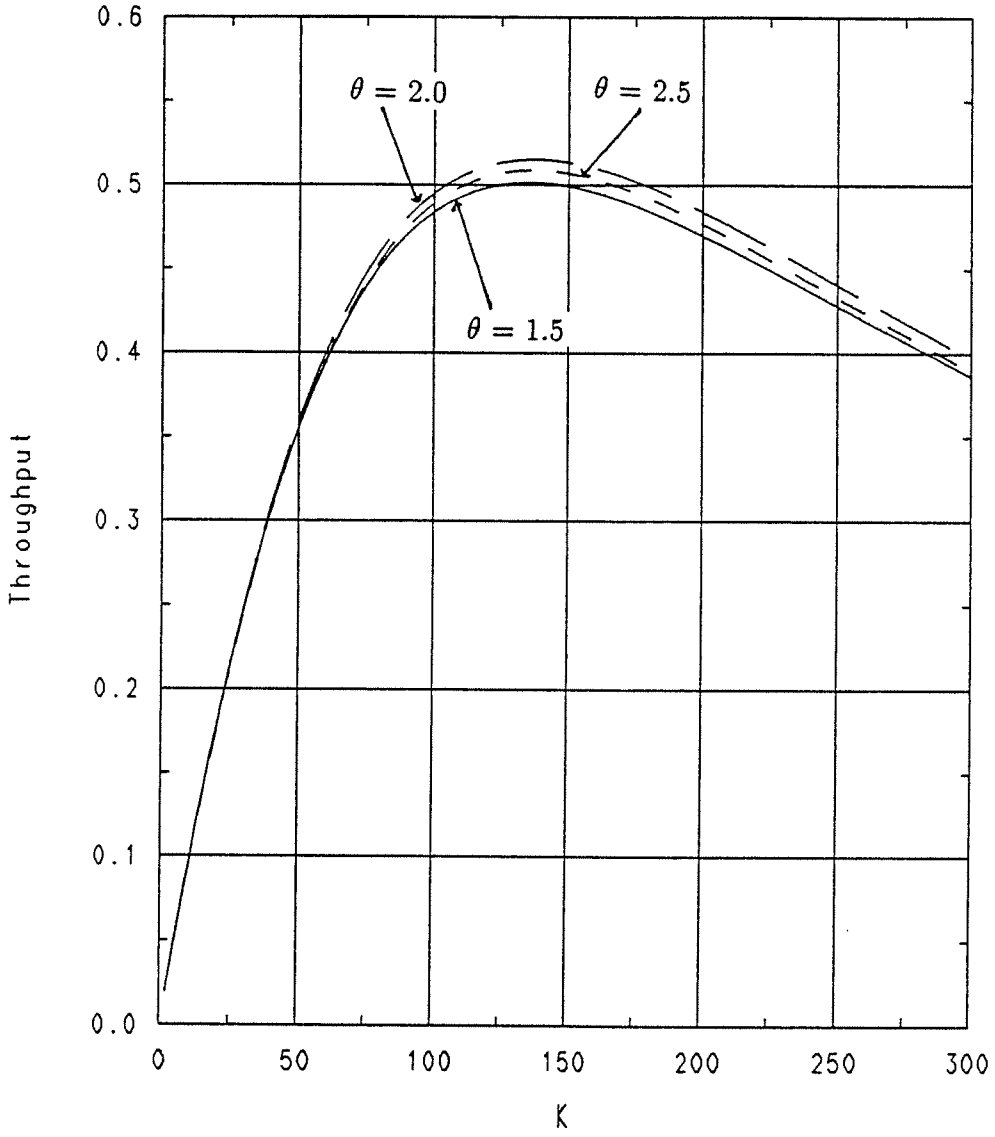

Figure 4.16: Throughput associated with channel capacity versus the number of users in the network of system (6) for $\frac{E_b}{N_0}$ =13dB with θ as a parameter.

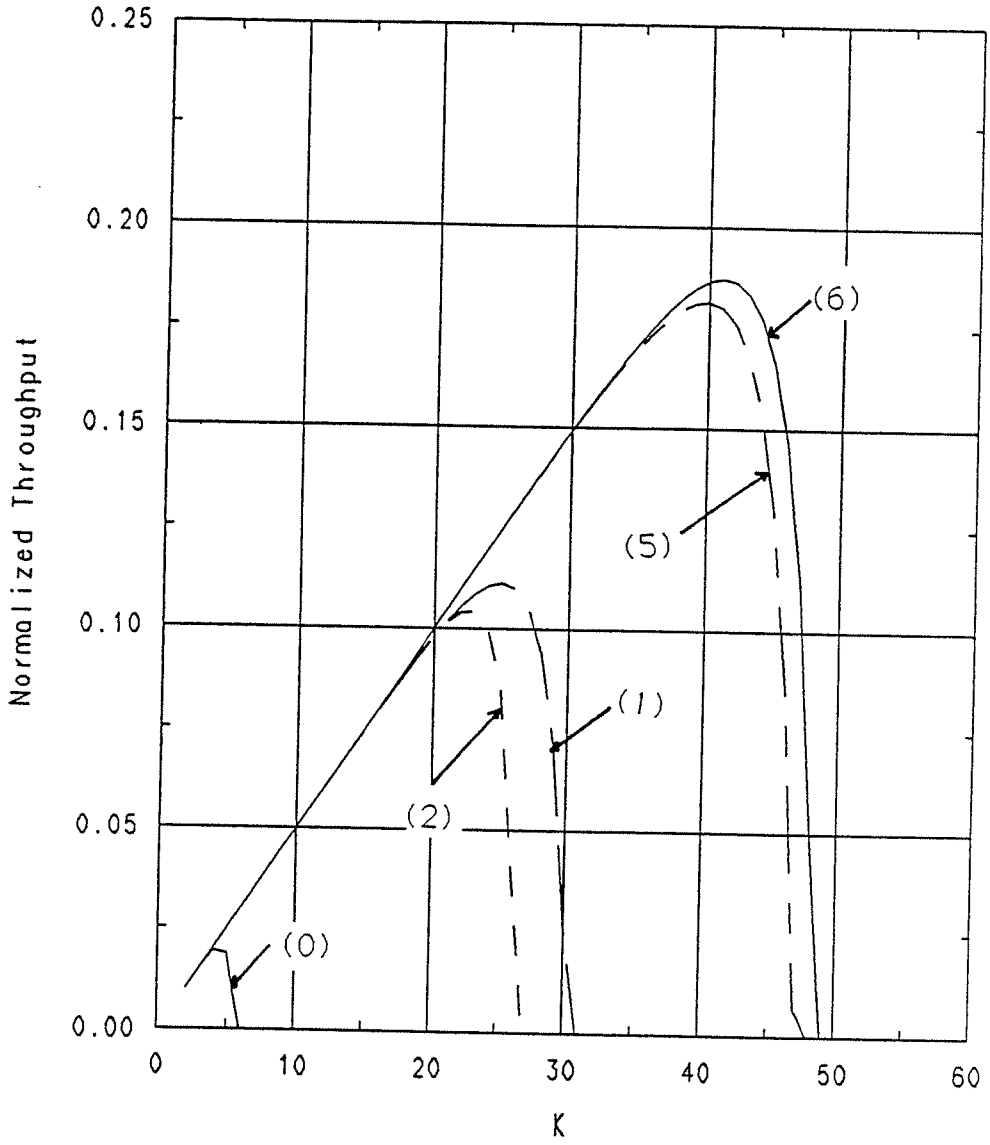

Figure 4.17: Lower bound on the normalized throughput when rate $\frac{1}{2}$, $k = 7$ convolutional codes are employed versus the number of users in the network. $\frac{E_b}{N_0}$ =13dB, θ =1.5, N_{met} =5, L =70.

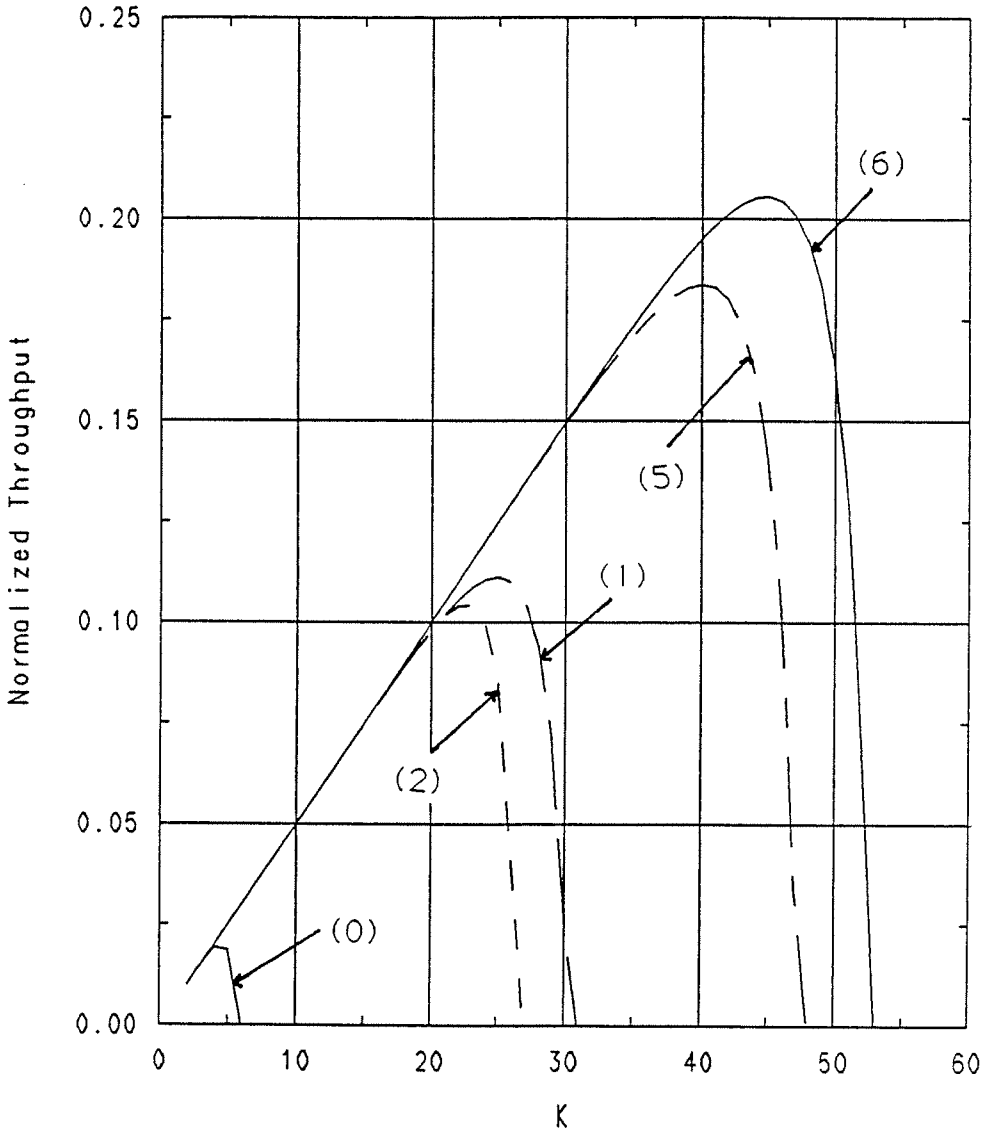

Figure 4.18: Lower bound on the normalized throughput when rate $\frac{1}{2}$, $k = 7$ convolutional codes are employed versus the number of users in the network. $\frac{E_b}{N_0}$ =13dB, θ =2.0, N_{met} =5, L =70.

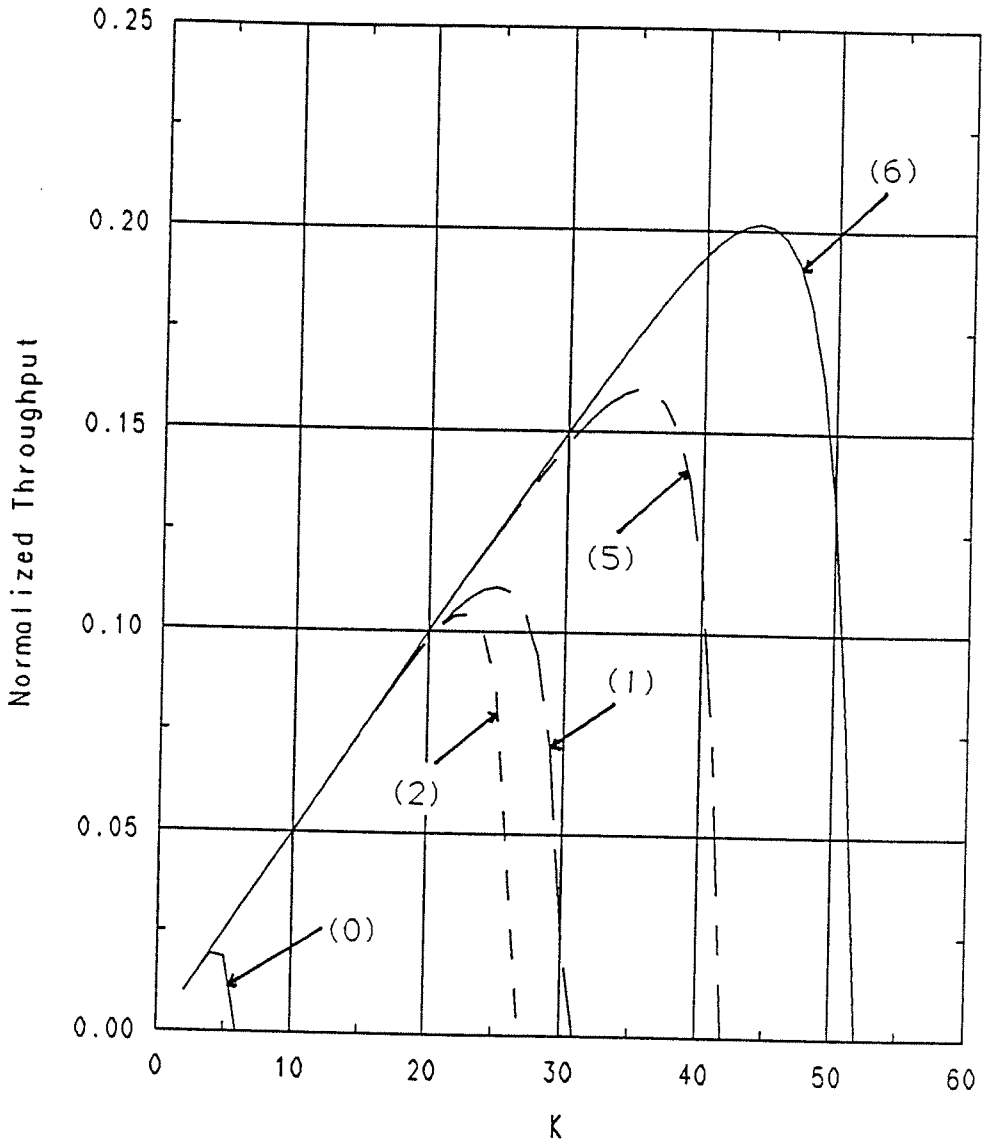

Figure 4.19: Lower bound on the normalized throughput when rate $\frac{1}{2}$, $k = 7$ convolutional codes are employed versus the number of users in the network. $\frac{E_b}{N_0}$ =13dB, θ =2.5, N_{met} =5, L =70.

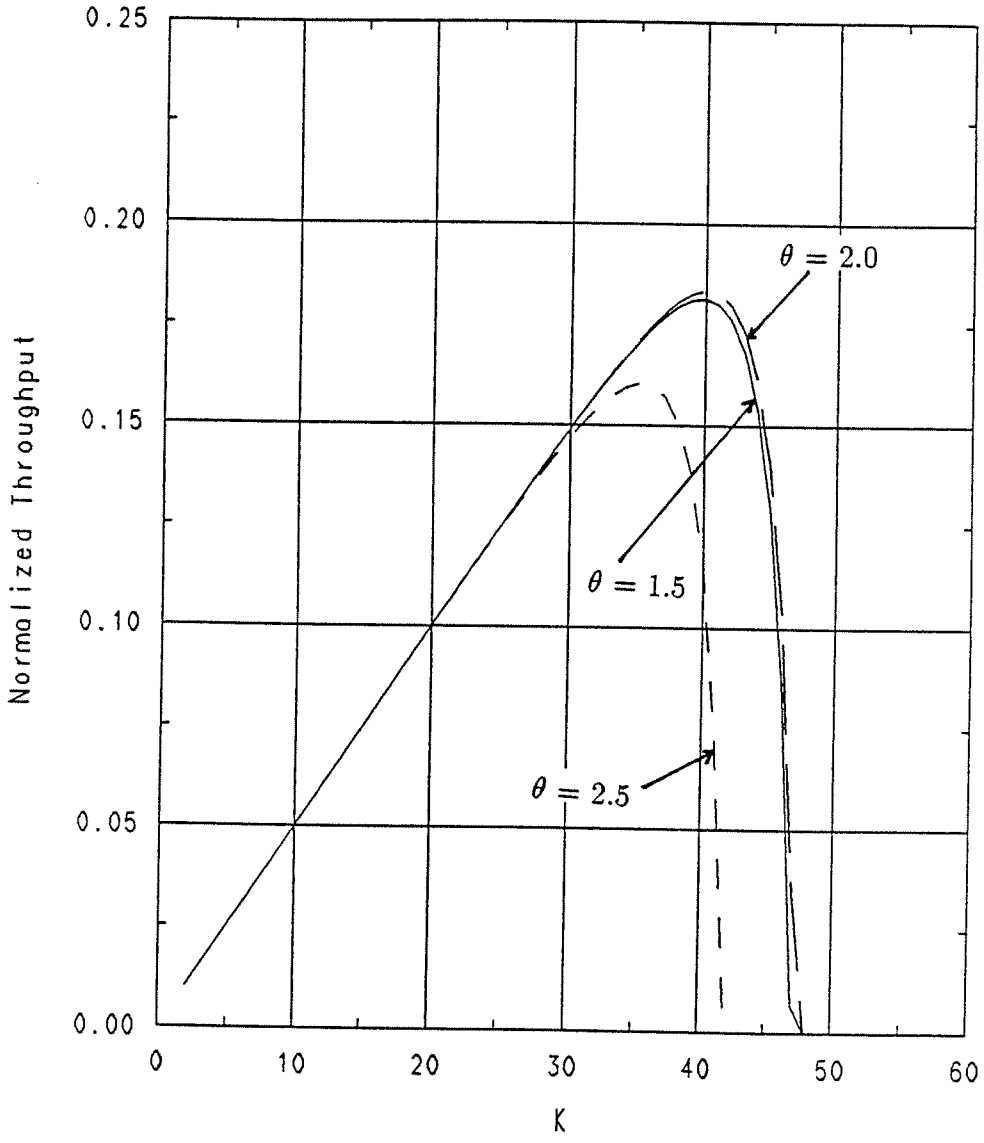

Figure 4.20: Lower bound on the normalized throughput of system (5) when rate $\frac{1}{2}$, $k = 7$ convolutional codes are employed versus the number of users in the network with θ as a parameter. $\frac{E_b}{N_0}$ =13dB, N_{met} =5, L =70.

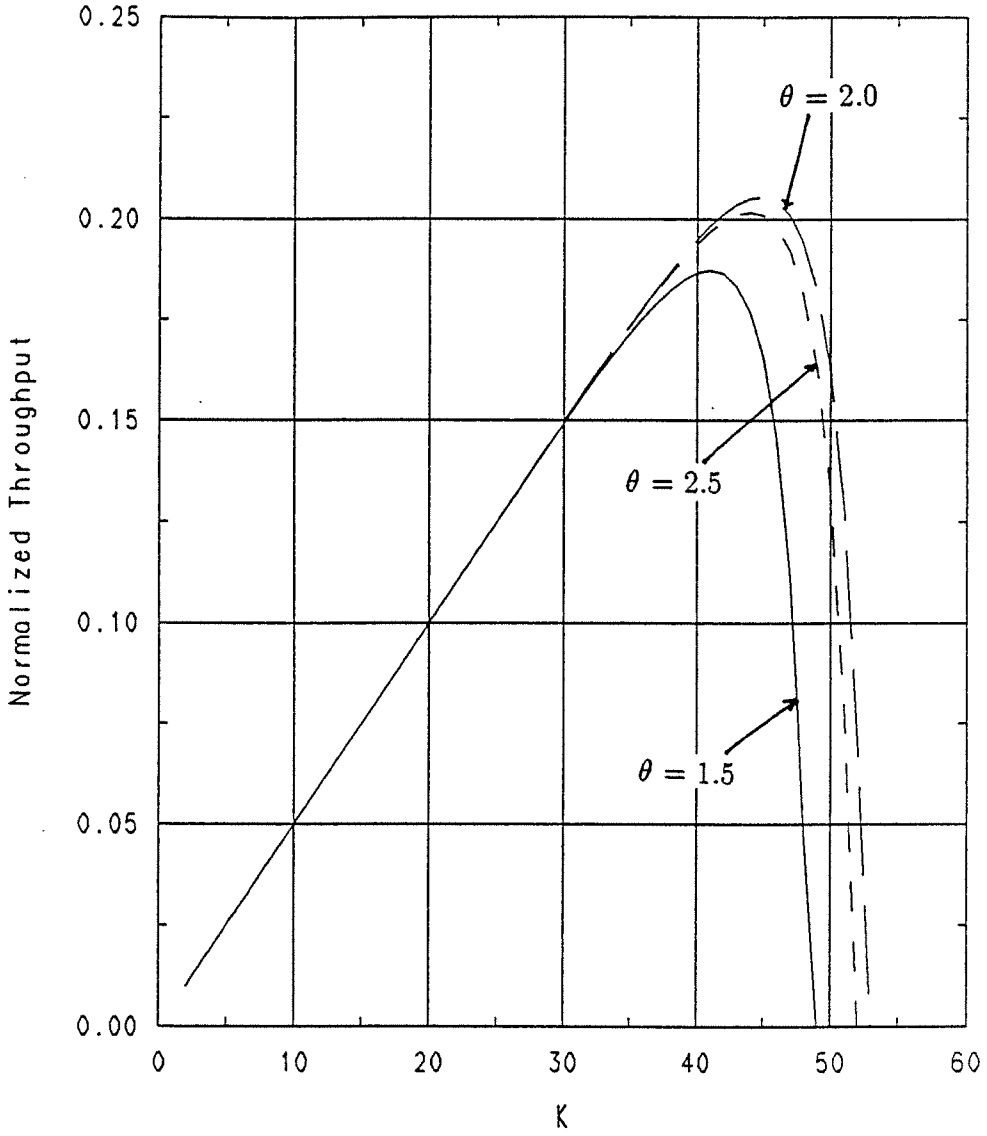

Figure 4.21: Lower bound on the normalized throughput of system (6) when rate $\frac{1}{2}$, $k = 7$ convolutional codes are employed versus the number of users in the network with θ as a parameter. $\frac{E_b}{N_0}$ =13dB, N_{met} =5, L =70.

after the number of users in the network increases beyond a certain point reinforces the suggestion that the bounds are loose beyond this point. Therefore we carry out simulations to determine exactly how loose these bound are.

Simulations

In order to evaluate the system performance more exactly, we simulate the Viterbi decoder using the channel statistics derived above. In Fig. 4.22 we plot the normalized throughput of systems (1), (2), (5) and (6) using the simulated values for the packet error probability with the parameters $\frac{E_b}{N_0}$ =13dB, θ =2.0, N_{met} =5, L =70. We note that the combined bound of (4.4) and (4.6) are indeed very loose and give very pessimistic results. For example, the optimum (in the sense of maximizing the normalized throughput) number of users in the network predicted by the bound (Fig. 4.18) for system (6) is around 45 where that predicted by the simulation results is approximately 75. This means that the bound is pessimistic by as much as 67%. In order to study the the bounds more closely, we consider the following two cases. First, we simulate the first event error probability of the Viterbi decoder and use the union bound (4.6) to compute the packet error probability. Next we use the simulated values for the channel statistic and use (4.4) to obtain an upper bound on the first event error probability and then further upper bound the packet error probability using (4.6). This is just what we used to plot Fig. 4.18. Fig. 4.23 shows the normalized throughput computed for the above two cases along with the simulated values. We note that most of the error is due to the union-Chernoff bound on the first event error probability. Since the region where the difference is most severe is where the packet error probability, hence the first event error probability, is quite high, simulating the first event error probability for this region can be done quite fast. In conclusion, we have seen that unless we simulate the Viterbi decoder to obtain

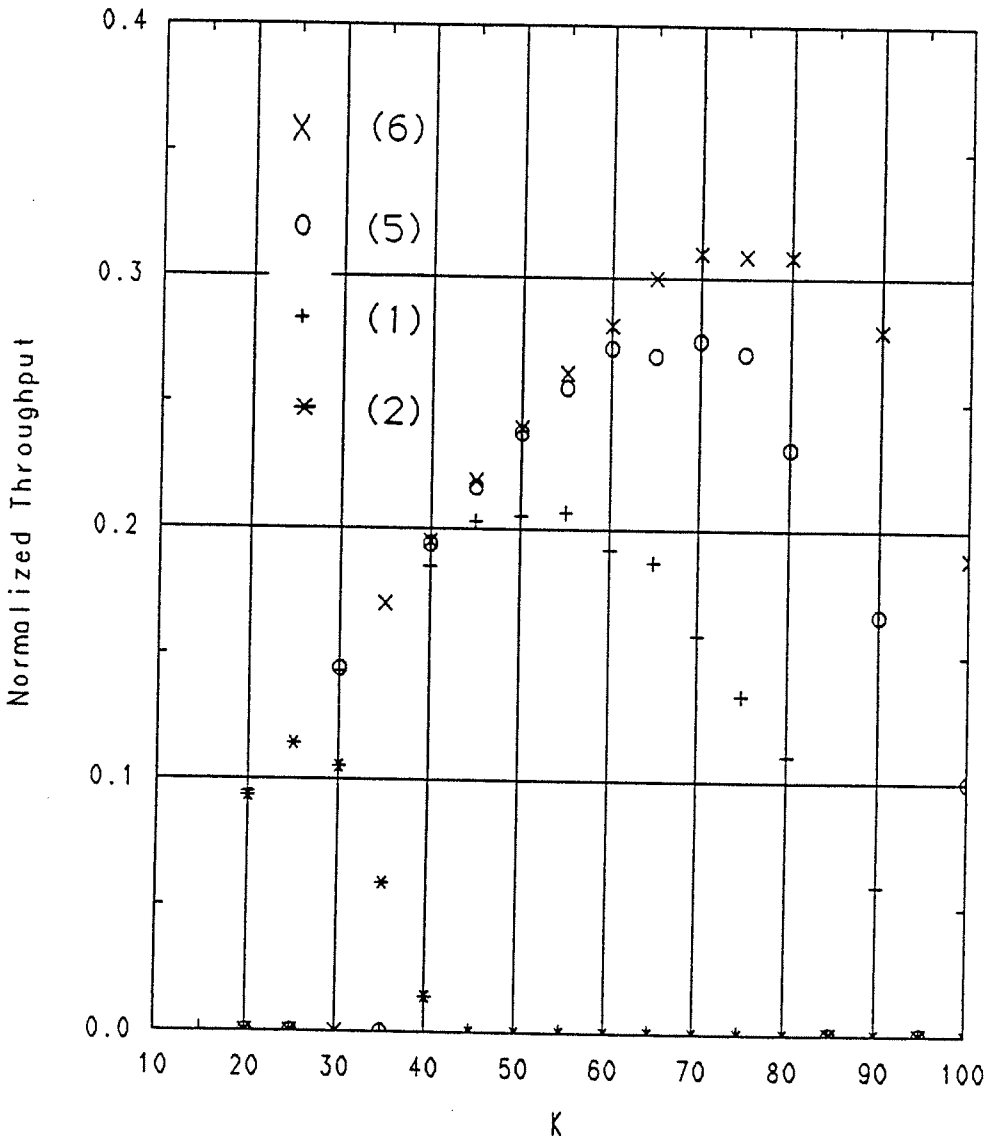

Figure 4.22: Simulated normalized throughput when rate $\frac{1}{2}$, k = ? convolutional codes are employed versus the number of users in the network. $\frac{E_b}{N_0}$ =13dB, N_{met} =5, L =70.

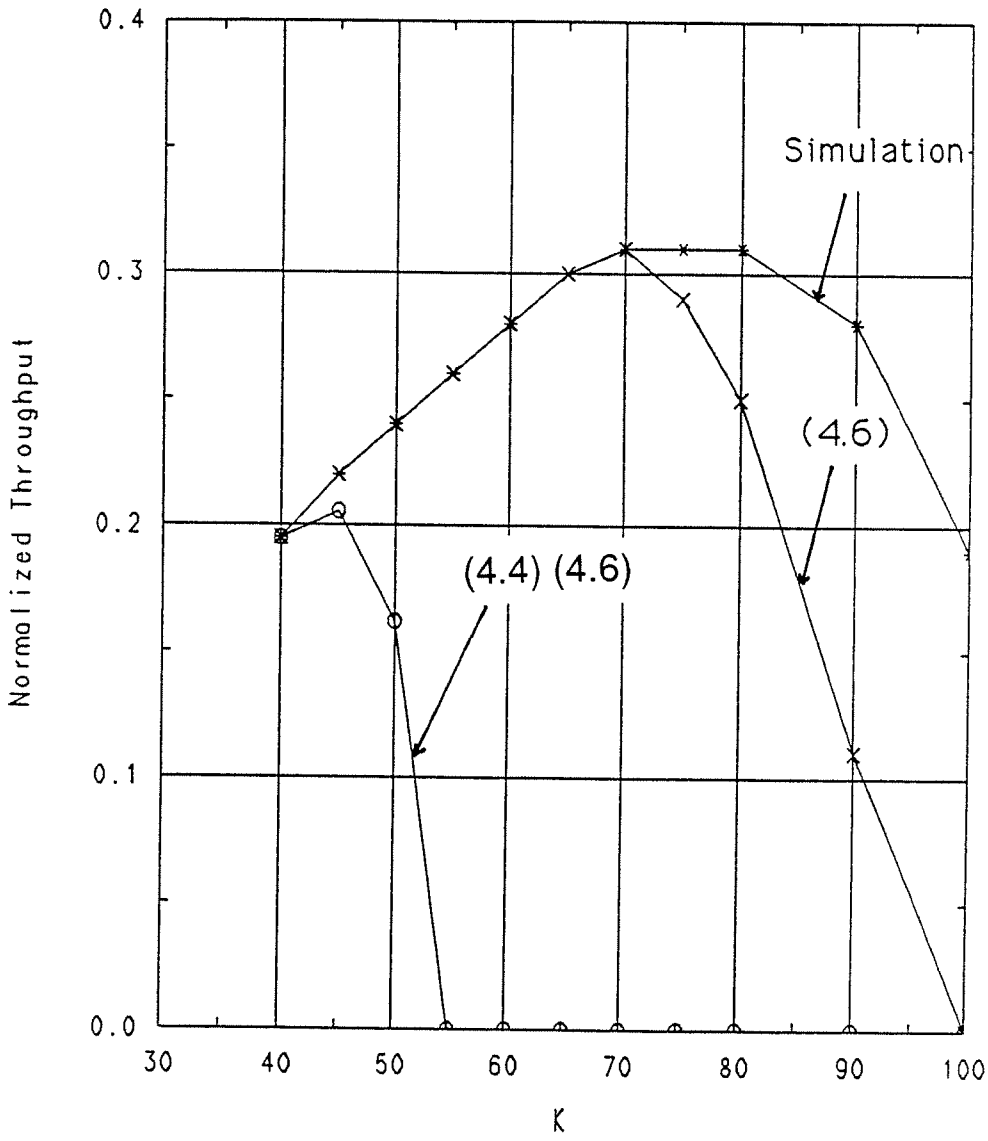

Figure 4.23: Effects of bounding techniques on the evaluation of normalized throughput when rate $\frac{1}{2}$, $k = 7$ convolutional codes are employed with four level VRT. $\frac{E_b}{N_0}$ =13dB, N_{met} =5, L =70.

an accurate value for the packet error probability given the channel statistics, the results one gets by using the usual bounding techniques give excessively pessimistic results.

CHAPTER V

PERFORMANCE OF ERROR CORRECTING CODES IN GENERATING SIDE-INFORMATION FOR SLOW AFHSS-MA NETWORKS

In this chapter we consider using an (n_I, k_I) binary error correcting code to encode the k_I information bits to be transmitted in a hop in a slow frequency-hop system described in Section 2.3. In the following section, we will give a brief introduction to the problem and describe a related work by Pursley [Pur 87a]. Then, we will derive the probability that l out of the n_I binary code symbols transmitted in a hop will actually be hit given that the hop is hit. This is a very general result and may be applied to various types of error models. Then using the usual model that when a binary symbol is hit, the error probability is $\frac{1}{2}$, and the errors within the hop are independent, we will derive the average probability that j symbols out of the n_I symbols will be in error. We will later give a heuristic justification that the $\frac{1}{2}$ approximation should be more accurate in a slow AFHSS-MA network compared to tne 'fast' AFHSS-MA network. We use this result to evaluate the performance of the (concatenated) coding scheme we propose. We also consider the case when Rayleigh fading is present in addition to additive white Gaussian noise.

5.1 Introduction

In this section we will give a brief introduction to the problems considered in this chapter. We describe the system model and the coding technique employed. Consider an AFHSS-MA network with one packet consisting of L, (N_o, K_o) Reed-Solomon (RS) codewords [Bla 83]. An (N_o, K_o) RS code is a code with symbols in GF(M), i.e., the Galois field of size M [Bla 83] where M is a power of a prime and $N_o = M-1$, M, or $M+1$. When $N_o = M+1$, the code is called the extended Reed-Solomon code. We will adopt this code in this chapter. Hence each code symbol can be represented by $m = \lceil \log_2 M \rceil$ binary symbols. This code takes in K_o M-ary information symbols and produces codewords of length N_o and has minimum distance $d_{min} = N_o - K_o + 1$ which is the minimum Hamming distance among all the codewords in the code and hence can correct up to t errors and e erasures as long as $2t + e \leq N_o - K_o$ [Bla 83].

One packet is composed of L of these RS codewords and hence there are $m \cdot L \cdot K_o$ binary data bits in a packet. Each packet is transmitted in N_o hops where in the j-th hop, $j = 1, \cdots, N_o$, the j-th symbols of the L, RS codewords in the packet are transmitted as $k_I = m \cdot L$ bits. In addition to transmitting the k_I bits, we further encode them using an (n_I, k_I) binary code. This is illustrated in Fig. 5.1. We will refer to this binary code as the *inner code* and the Reed-Solomon code as the *outer code* since what we have described is in fact a concatenated coding scheme [For 77]. The decoders for the inner and the outer code are assumed to be bounded distance decoders [Bla 83] where we set up a decoding region about each of the codewords and the decoder attempts to decode only if the received vector falls within one of these regions. For example, for the inner code, we can set the decoder so that it outputs

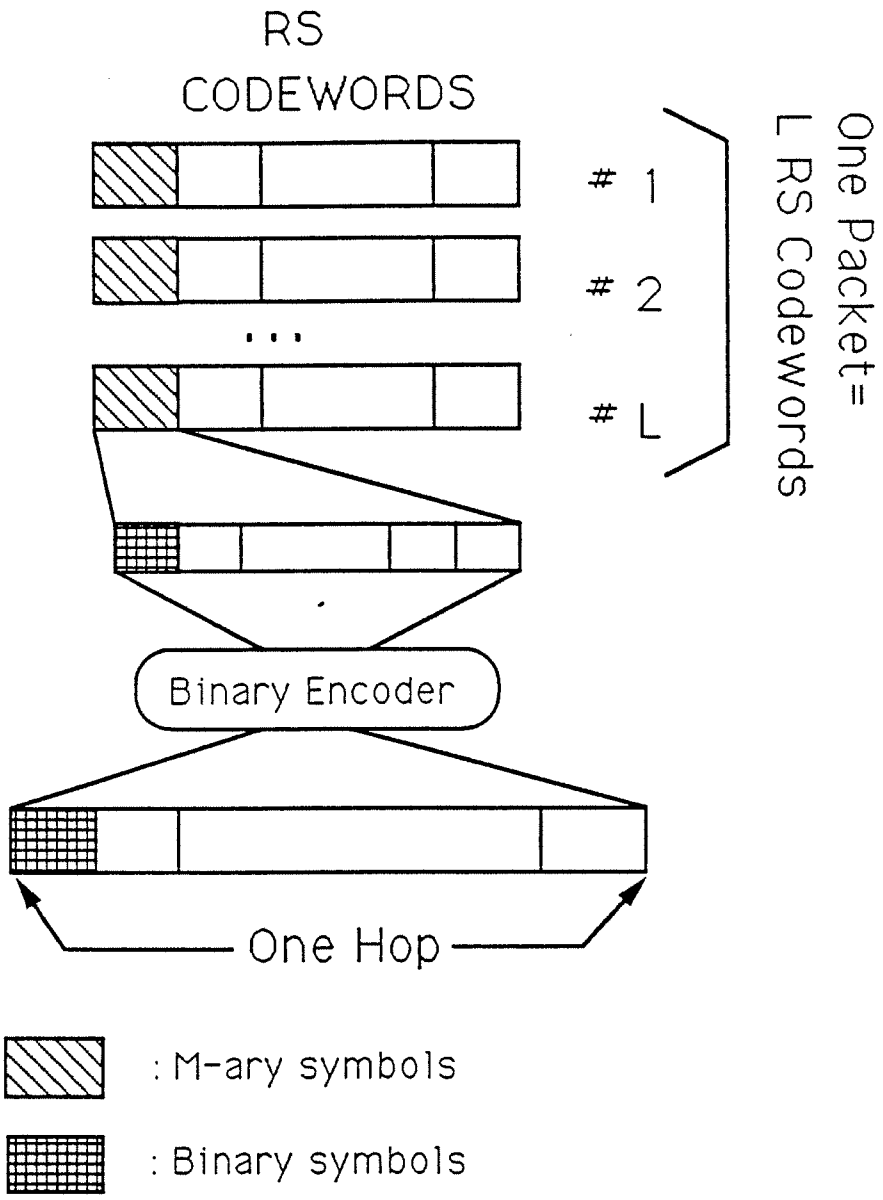

Figure 5.1: Construction of a packet and the coding scheme.

a decoded codeword (correct or not) only if it differs from a codeword in at most $t < \lfloor \frac{d^I_{min}-1}{2} \rfloor$ places and otherwise abort decoding where d^I_{min} denotes the minimum distance of the inner binary code. The RS decoder would then use this information and erase the RS code symbols corresponding to the hop thus taking advantage of the larger erasure correcting capability of the RS decoder. The idea behind this is that we are trying to single out the hops that were severely corrupted while trying to correct the few errors caused by additive white Gaussian noise or a hit resulting from a small (one or two) number of interfering users. The parameter t should be optimized to maximize performance (e.g. throughput). The tradeoff resulting from varying t is that as we increase t, the inner decoder will be able to correct more errors but if the number of errors exceed t, then the probability of decoding to a wrong codeword will also increase. On the other hand as t is decreased, the number of correctable errors is decreased but a large portion of the uncorrectable errors will be detected. Hence the inner decoder generates (imperfect) side-information that tells the outer decoder how severe a hit was.

A related work in generating imperfect side-information in AFHSS-MA networks is [Pur 87a] where known test patterns are attached at the beginning and at the end of each hop to detect whether a hop was hit or not (Fig. 5.2). Here the rule is that if more than Υ out of the n_{test} test bits at either of the test patterns are received in error the hop is declared hit and the RS symbols corresponding to the hop are erased. We will show in the numerical results section that the coding scheme proposed in this chapter gives a significant improvement in performance over the test pattern scheme of [Pur 87a] and a system having perfect side-information.

In order to analyze this concatenated coding system, we first compute the probability that l out of the n_I binary symbols transmitted in a hop are actually hit given

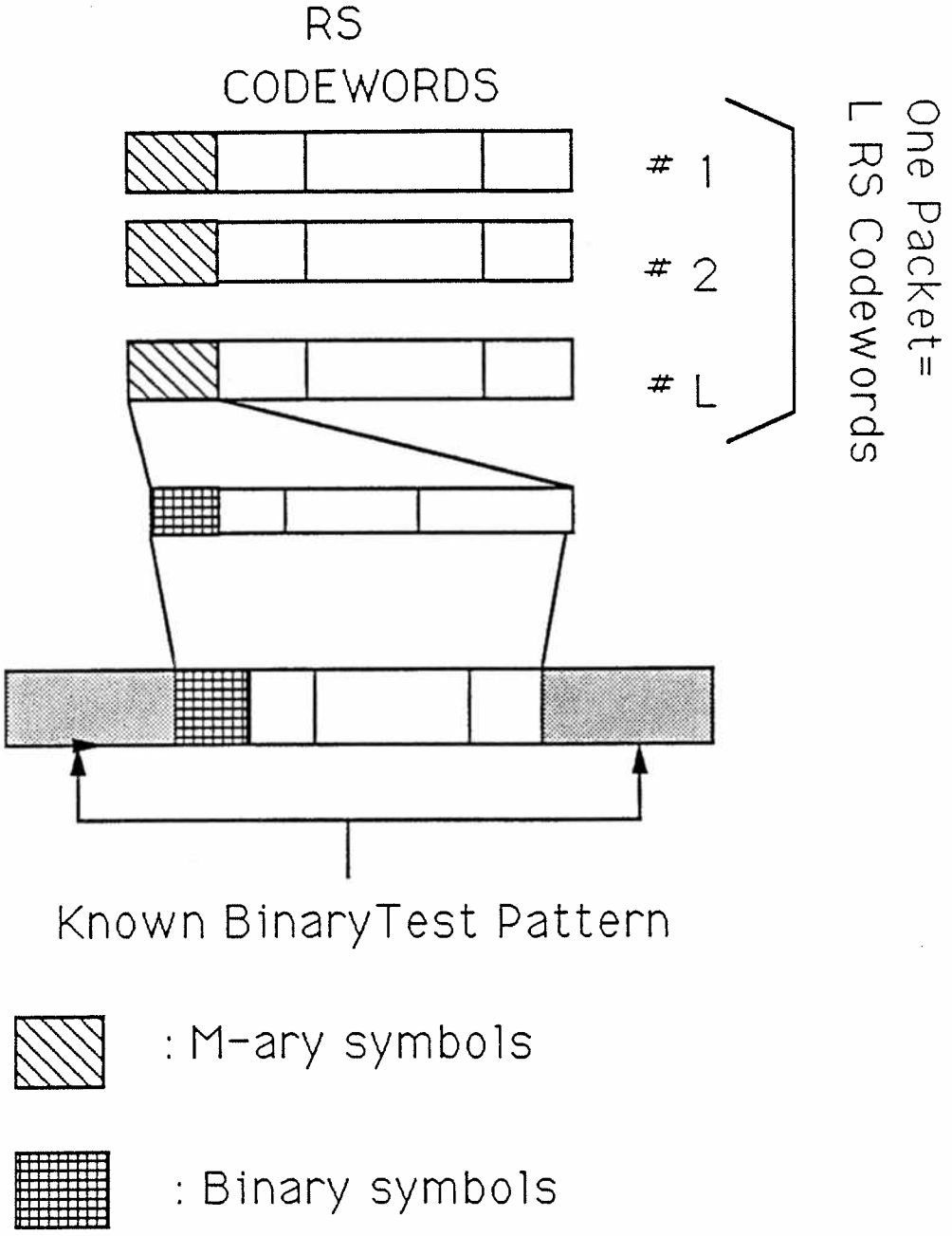

Figure 5.2: Test pattern scheme.

that the hop is hit by k interfering users. This is a very general result and may be applied in the analysis of various forms of slow AFHSS-MA networks. To analyze the error performance of the inner code, we need to know the error statistics within a hop, that is, the probability that j bits will actually be in error given the hit pattern. It is very difficult to generalize the results of Chapter 3 to the slow AFHSS-MA case. Hence we fall back on the usual assumption that whenever a symbol within a hop is hit, that symbol will be in error with probability $\frac{1}{2}$ and that the symbol errors within a hop are independent. This approximation is probably more accurate here than the case when one symbol is transmitted per hop since for slow AFHSS-MA networks most of the symbol hits will be full hits (i.e., an interfering signal will overlap the symbols for the entire symbol duration) and it was shown in Chapter 3 that the probability of error is close to $\frac{1}{2}$ when this is the case (see Fig. 3.1).

Other than the fact that more than $n_I > 1$ binary symbols are transmitted per hop, the system model is same as the ones assumed in previous chapters. Again Markov hopping patterns are assumed to facilitate the analysis. But as shown in Chapter 3, for practical values of q, this will provide a good approximation to the independent hopping pattern case.

Lastly, we mention that this sort of concatenated coding scheme was considered in [Kim 87] for random inner codes using approximations for the probability that l out of the n_I binary symbols transmitted in a hop is actually hit given that the hop is hit by k interfering users. In the next section we proceed with the analysis of the system described above.

5.2 Analysis

In this section we analyze the coding scheme described in the previous section and offer an upper bound on the packet error probability. First, let us define the following variables and events.

- S_h : Number of binary symbols that are hit out of the n_I binary symbols that were transmitted in a hop.
- S_e : Number of symbols that are in error out of the n_I symbols that were transmitted in a hop.
- $H(k)$: The event that a hop is hit by k interfering users.

We break up the analysis into four parts as follows. First we compute the probability of l bits out of the n_I bits being hit given that a hop is hit by k interfering users denoted by $\Pr(S_h = l|H(k))$. Next we compute the average probability of j bits being in error, $\Pr(S_e = j)$. From these it is easy to derive the probability of correct decoding P_{cd}, the probability of undetected error P_{ud}, and the probability of detected error P_d for the binary inner code given the weight distribution of the code and assuming that whenever a symbol within a hop is hit, that symbol will be in error with probability $\frac{1}{2}$ and that the errors within a hop are independent. Finally using these results, we are able to derive an upper bound on the packet error probability P^u_{packet}. We assume without loss of generality, that the hop is initiated at time 0 and normalize the hop duration to 1. This simplifies the notation in the analysis.

5.2.1 Derivation of $\Pr(S_h = l|H(k))$

In this section we derive the probability that l symbols will actually be hit given that the hop is hit by k interfering users. This is the crucial part of the analysis. To

facilitate the derivation, we further break down the analysis into three parts.

(1) $l = 1$

Obviously for this case

$$\Pr(S_h = 1|H(k)) = 2\left(\frac{1}{2n_I}\right)^k$$

(2) $l \neq 1$, $l \neq n_I$

For this case there are three possible hit patterns α, β, γ defined as follows.

- α : The event that the first l symbols are hit and the last $(n_I - l)$ symbols are not hit.
- β : The event that the last l symbols are hit and the first $(n_I - l)$ symbols are not hit.
- γ : The event that the first $n_1 < l$ symbols and the last $(l - n_1)$ symbols are hit and the symbols in between are not hit.

These events are depicted in Fig. 5.3. Let t_{begin} and t_{end} denote the beginning and the end of transmission time for an interfering user. Now since hit pattern α can only occur if the end of transmission time t_{end} for at least one of the k interfering users is in the interval $\left[\frac{l-1}{n}, \frac{l}{n}\right]$ and other $(k-1)$ interfering users have $t_{end} \in \left[0, \frac{l}{n}\right]$, the probability of hit pattern α given that the hop is hit by k users $\Pr(\alpha|H(k))$ is given by

$$\begin{aligned}
\Pr(\alpha|H(k)) &= \sum_{i=1}^{k} \binom{k}{i} \left(\frac{1}{2n_I}\right)^i \left(\frac{l-1}{2n_I}\right)^{k-i} \\
&= \left(\frac{l}{2n_I}\right)^k - \left(\frac{l-1}{2n_I}\right)^k \\
&= \frac{l^k - (l-1)^k}{(2n_I)^k}.
\end{aligned}$$

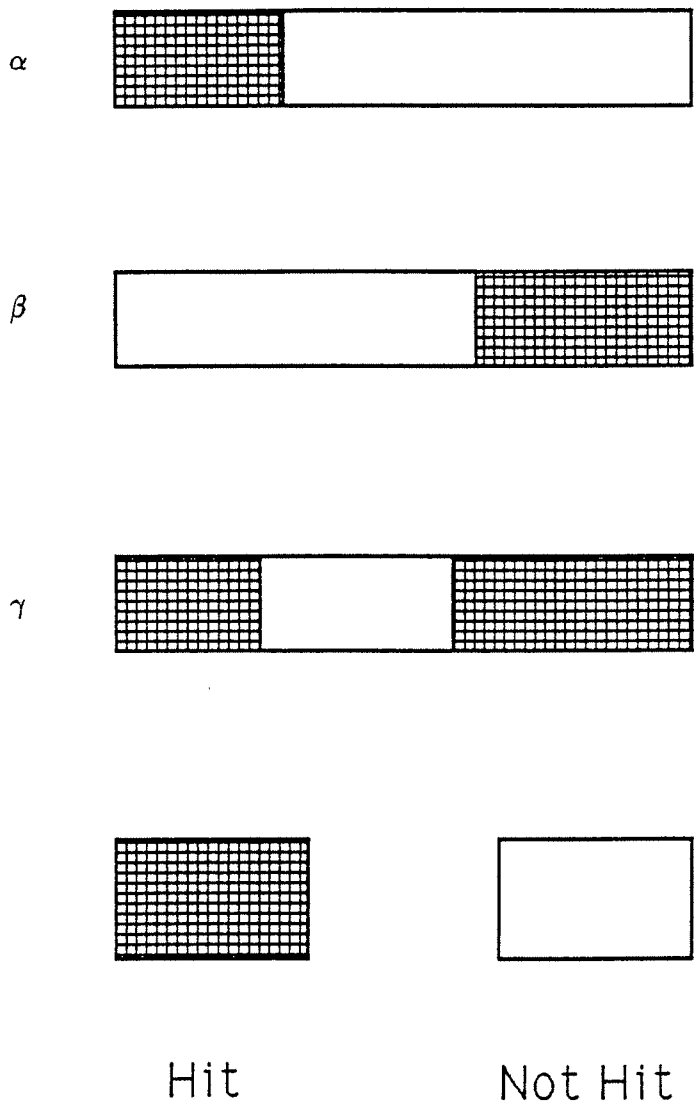

Figure 5.3: Hit patterns α, β and γ.

By symmetry $\Pr(\beta|H(k))$ is equal to $\Pr(\alpha|H(k))$. To compute the probability of hit pattern γ given that the hop is hit by k users, let us define the following events.

- $E_{1,k'}(n)$: The event that k' interfering users have $t_{end} \in \left[0, \frac{n}{n_I}\right]$.
- $E_{2,k'}(n)$: The event that k' interfering users have $t_{begin} \in \left[\frac{n}{n_I}, 1\right]$.
- $E_{3,k'}(n)$: The event that at least one out of k' users of event $E_{1,k'}(n)$ has $t_{end} \in \left[\frac{n-1}{n_I}, \frac{n}{n_I}\right]$.
- $E_{4,k'}(n)$: The event that at least one out of k' users of event $E_{2,k'}(n)$ has $t_{begin} \in \left[\frac{n}{n_I}, \frac{n+1}{n_I}\right]$.

where $n \in \{1, 2, \cdots, n_I - 2\}$. Using these definitions, the probability of hit pattern γ given that a hop is hit by k users can be written as follows

$$\Pr(\gamma|H(k)) = \sum_{i=1}^{k-1} \binom{k}{i} \Pr\left(E_{1,i}(n_1), E_{2,(k-i)}(l-n_1), E_{3,i}(n_1), E_{4,(k-i)}(l-n_1)\right).$$

Since the events $(E_{1,i}(n_1), E_{3,i}(n_1))$ and $(E_{2,(k-i)}(l-n_1), E_{4,(k-i)}(l-n_1))$ are independent, we have

$$\Pr\left(E_{1,i}(n_1), E_{2,(k-i)}(l-n_1), E_{3,i}(n_1), E_{4,(k-ki)}(l-n_1)\right) =$$
$$\Pr\left(E_{1,i}(n_1), E_{3,i}(n_1)\right) \Pr\left(E_{2,(k-i)}(l-n_1), E_{4,(k-i)}(l-n_1)\right).$$

Since

$$\Pr(E_{1,i}(n_1), E_{3,i}(n_1)) = \Pr(E_{3,i}(n_1)|E_{1,i}(n_1)) \Pr(E_{1,i}(n_1))$$

and

$$\Pr(E_{3,i}(n_1)|E_{1,i}(n_1)) = 1 - \Pr(E_{1,i}(n_1 - 1)|E_{1,i}(n_1)),$$

it follows that

$$\Pr(E_{1,i}(n_1), E_{3,i}(n_1)) = \Pr(E_{1,i}(n_1)) - P(E_{1,i}(n_1 - 1)).$$

Similarly,

$$\Pr(E_{2,(k-i)}(l-n_1), E_{4,(k-i)}(l-n_1)) = \Pr(E_{2,(k-i)}(l-n_1)) - \Pr(E_{2,(k-i)}(l-n_1+1)).$$

Thus

$$\begin{aligned}
\Pr(\gamma|H(k)) &= \sum_{i=1}^{k-1} \binom{k}{i} [\Pr(E_{1,i}(n_1)) - P(E_{1,i}(n_1-1))] \\
&\times [\Pr(E_{2,(k-i)}(l-n_1)) - \Pr(E_{2,(k-i)}(l-n_1+1))] \\
&= \sum_{i=1}^{k-1} \binom{k}{i} \left[\left(\frac{n_1}{2n_I}\right)^i - \left(\frac{n_1-1}{2n_I}\right)^i\right] \left[\left(\frac{l-n_1}{2n_I}\right)^{k-i} - \left(\frac{l-n_1+1}{2n_I}\right)^{k-i}\right] \\
&= \frac{l^k + (l-2)^k - 2(l-1)^k}{(2n_I)^k}.
\end{aligned}$$

Note that $\Pr(\gamma|H(1)) = 0$ since the hit pattern γ cannot occur when the hop is hit by only one other user. Since the hit patterns α, β, γ are the only hit patterns possible when $l \neq 1$ nor $l \neq n_I$ and since the hit patterns are disjoint, the probability of l symbols being hit when the hop is hit by k interfering users is the sum of the probabilities of event α, β and γ. Thus

$$\Pr(S_h|H(k)) = \frac{3l^k - 4(l-1)^k + (l-2)^k}{(2n_I)^k}$$

when $l \neq 1$, $l \neq n_I$.

(3) $l = n_I$

The probability of all n_I symbols being hit when the hop is hit is just 1 minus the sum of the probabilities that $l = 1, 2, \ldots, n_I - 1$ symbols are hit. Hence

$$P(S_h = n_I|H(k)) = 1 - \sum_{l=1}^{n_I-1} P(S_h = l|H(k)).$$

In summary, the probability of l symbols being hit when the hop is hit by k

interfering users is given by

$$\Pr(S_h = l|H(k)) = \begin{cases} 2\left(\frac{1}{2n_I}\right)^k, & l = 1 \\ \frac{3l^k - 4(l-1)^k + (l-2)^k}{(2n_I)^k}, & 2 \le l \le n_I - 1 \\ 1 - \frac{2 - \sum_{j=2}^{n_I-1}(3j^k - 4(j-1)^k + (j-2)^k)}{(2n_I)^k}, & l = n_I. \end{cases}$$

This result is very general and applies to all slow frequency-hop asynchronous multiple-access channels that satisfy the general assumptions made in this thesis whether the modulation is binary or M-ary.

5.2.2 Derivation of $\Pr(S_e = j)$

In this section we derive the average probability of j bits out of n_I bits that were transmitted in a hop being in error denoted by $\Pr(S_e = j)$ under the assumption that the probability of error is $\frac{1}{2}$ whenever a symbol is hit and that the errors within a hop are independent. The probability $\Pr(S_e = j)$ can be decomposed into two parts according to whether the hop is hit or not as follows.

$$\Pr(S_e = j) = \Pr(S_e = j|H)P_{hit} + \Pr(S_e = j|\overline{H})(1 - P_{hit})$$

where H denotes the event that the hop is hit, $\overline{H}$ denotes the compliment of H and P_{hit} is the probability that the hop is hit given by (2.4). It is easy to see that the probability $\Pr(S_e = j|H)P_{hit}$ is given by the following summation.

$$P(S_e = j|H)P_{hit} = \sum_{k=1}^{K-1} \binom{K-1}{k} \Pr(S_e = j|H(k))p_h^k(1 - p_h)^{K-1-k}$$

where p_h is given by (2.2). By further conditioning on the number of bits that are actually hit given the hop is hit by k users, the probability $\Pr(S_e = j|H(k))$ can be written as follows, which is a sum of the terms that can easily be computed in terms

of results given in the previous section.

$$\Pr(S_e = j|H(k)) = \sum_{l=1}^{n_I} \Pr(S_e = j|S_h = l)P(S_h = l|H(k)).$$

Straightforward computation yields

$$\Pr(S_e = j|S_h = l) = \left(\frac{1}{2}\right)^l \sum_{h=0}^{j} \binom{l}{h} \binom{n_I - l}{j-h} P_0^{j-h}(1-P_0)^{n_I-l-j+h}.$$

The probability $\Pr(S_e = j|\overline{H})(1 - P_{hit})$ is easily computed to be

$$\Pr(S_e = j|\overline{H})(1 - P_{hit}) = \binom{n_I}{j} P_0^j(1-P_0)^{n_I-j}(1-P_{hit})$$

where P_0 denotes the binary symbol error probability due only to AWGN. This concludes the derivation of $\Pr(S_e = j)$.

Again, though the derivation given in this section is for the binary case, it can easily be extended to the M-ary channel symbol case. The above two sections were concerned with the channel statistics for the inner code. The following section deals with the performance of the binary inner code using these results.

5.3 Analysis of the Inner Code

In this section the probability of correct decoding P_{cd}, the probability of undetected error P_{ud}, and the probability of detected error P_d are derived for the (n_I, k_I) binary inner code. With a bounded distance decoder that corrects up to $t \leq \left\lfloor \frac{d^I_{min}-1}{2} \right\rfloor$ errors, the probability of correct decoding is simply the probability of there being no more than t errors in the received vector. Thus

$$P_{cd} = \sum_{j=0}^{t} \Pr(S_e = j).$$

To compute the probability of undetected error we define $N(w, j; t')$ to be the number of vectors of Hamming weight j with Hamming distance t' away from a particular codeword of weight w. This is known to be [Bla 83]

$$N(w, j; t') = \begin{pmatrix} n-w \\ \frac{t'+w-j}{2} + j - w \end{pmatrix} \begin{pmatrix} w \\ \frac{t'+w-j}{2} \end{pmatrix}$$

if $\frac{t'+w-j}{2}$ is even and 0 otherwise. To go any further with the standard analysis, we need to assume *random shuffling* of the n_I bits of the codeword before transmission and *deshuffling* after reception at this point, in order to ensure that different error patterns of same weight are equi-probable. That is, every time a codeword is transmitted in a hop, the ordering of the code symbols within the hop are randomized. Without this assumption, the analysis is not tractable since the error probability is not simply a function of the weight distribution of the code and different error patterns of same weight have different probabilities of occurring. We also mention that instead of making this assumption, one could try to design a code specific to this *nonsymmetric* channel. This will not be further pursued in this thesis. Hence, assuming shuffling and deshuffling, P_{ud} can be written as follows [Bla 83].

$$\begin{aligned} P_{ud} &= \sum_{j=t+1}^{n_I} \Pr(E_{ud} | S_e = j) \Pr(S_e = j) \\ &= \sum_{j=t+1}^{n_I} \begin{pmatrix} n_I \\ j \end{pmatrix}^{-1} \sum_{w=d_{min}^I}^{n_I} \sum_{t'=0}^{t} A_w N(w, j; t') \Pr(S_e = j) \end{aligned}$$

where $\{A_w\}$ is the weight distribution (i.e., the number of codewords with Hamming weight w) of the code and E_{ud} denotes the event that an error pattern is not detected. The probability of detected error is simply given by

$$P_d = 1 - P_{cd} - P_{ud}.$$

5.4 Packet error probability

As with most of the asynchronous slow-frequency-hop multiple-access networks with more than one codeword per packet, it is extremely difficult to compute the exact packet error probability (P^{ex}_{packet}) of the system due to the dependence of errors between the codewords in a packet. Instead of trying to compute the exact packet error probability, we make a simplifying assumption and obtain an upper bound P^{u}_{packet} on the packet error probability. First we note that an erasure in a symbol of a RS codeword implies that all the corresponding $(L-1)$ RS codeword symbols (i.e., symbols that were transmitted in the same hop) are erased, since once it is decided that a hop is severely corrupted by the inner code, all the data bits corresponding to the codeword are erased. Let us further assume that an error in a RS symbol also implies that all the corresponding RS symbols are in error. Under this assumption, the packet error probability is equal to the RS codeword error probability and this results in an upper bound on the exact packet error probability. This is given by the following well known formula [Cla 81]

$$P_{packet} \leq P^{u}_{packet} = 1 - \sum_{e=o}^{N_o-K_o} \sum_{t=0}^{\lfloor \frac{N_o-K_o-e}{2} \rfloor} \begin{pmatrix} N_o \\ e \ , \ t \end{pmatrix} P_d^e \cdot P_{ud}^t \cdot P_{cd}^{N_o-e-t}$$

where $\lfloor x \rfloor$ denotes the largest integer not exceeding x.

5.5 Performance Comparison

In this section we will describe two systems whose performance will be used to evaluate the performance of the concatenated coding scheme proposed here. One is a system having perfect side-information that erases the symbols corresponding to the hop whenever the hop is hit. The second is the test pattern scheme analyzed in [Pur 87a].

5.5.1 System with perfect side-information

In this system the receiver is provided with the information as to whether a particular hop was hit or not. If a hop is known to be hit by multiple-access interference, then all the RS code symbols transmitted in the hop are erased. For this case, the exact packet error probability can easily be computed as follows. First we condition on the number of hops (i.e., erasures) that are hit. Then the distribution for all other symbols are statistically independent and identically distributed since they are corrupted only by thermal noise. Thus the packet error probability can be written as

$$P_{packet} = 1 - \sum_{e=0}^{N_o-K_o} \binom{N_o}{e} P_{hit}^{e}(1-P_{hit})^{N_o-e} \left[\sum_{t=0}^{\lfloor \frac{N_o-K_o-t}{2} \rfloor} \binom{N_o-e}{t} P_{s,0}^{t}(1-P_{s,0})^{N_o-e-t} \right]^{L}$$

where $P_{s,0}$ is the quiescent RS code symbol error probability given by $P_{s,0} = 1-(1-P_0)^m$.

5.5.2 System employing test patterns

In this system, we attach known test patterns of length n_{test} at the beginning and at the end of each hop. A hop is declared hit and the corresponding symbols erased if at least one of the test patterns contain more than Υ errors, where Υ is a threshold chosen to optimize system performance. An upper bound on the packet error probability for this system was derived by Pursley in [Pur 87a].

5.6 Rayleigh Fading Channels

In this section we assume that the multiple-access channel is further corrupted by Rayleigh fading. We carry over the assumption that the binary symbol error probability is $\frac{1}{2}$ when hit by multiple-access interference. With this assumption, we only need to alter the expression for the probabilities of those events that involve errors caused by AWGN in the results given in Section 5.2. These are $\Pr(S_e = j|S_h = l)$ and $\Pr(S_e = j|\overline{H})$. To compute these probabilities let us define $\alpha(L', U)$ to be the average probability of a specific error pattern of weight U in a block of L' binary symbols subject to same amount of fading. This is known to be [Has 88]

$$\begin{aligned}
\alpha(L', U) &= E_B[P_b(B)^U(1 - P_b(B))^{L'-U}] \\
&= \left(\frac{1}{2}\right)^U \int_0^\infty e^{-\frac{U\frac{E_s}{N_0}\beta^2}{2}} \left(1 - \frac{1}{2}e^{-\frac{U\frac{E_s}{N_0}\beta^2}{2}}\right)^{L'-U} \left(2\beta e^{-\beta^2}\right) d\beta \\
&= \sum_{i=0}^{L'-U} \binom{L'-U}{i} \frac{\left(\frac{1}{2}\right)^{U+i}(-1)^i}{(U+i)\frac{E_s}{2N_0} + 1}
\end{aligned}$$

where $P_b(\beta) = \frac{1}{2}e^{-\frac{E_s}{2N_0}\beta^2}$ and $\frac{E_s}{N_0}$ is the binary symbol signal-to-noise ratio. Using this, $\Pr(S_e = j|S_h = l)$ and $\Pr(S_e = j|\overline{H})$ can be written as follows.

$$\Pr(S_E = j|S_h = l) = \left(\frac{1}{2}\right)^l \sum_{m=0}^{j} \binom{l}{m} \binom{n_I - l}{j - m} \alpha(n_I - l, j - m)$$

$$\Pr(S_e = j|\overline{H}) = \binom{n_I}{j} \alpha(n_I, j).$$

For the system having perfect side-information, we cannot easily compute the exact packet error probability as before since the errors are not independent conditioned on the number of symbols erased. This forces us to resort to the Union bound where we upper bound the packet error probability by L times the RS codeword

error probability. Let $P_{s,r}$ be the RS symbol error probability given that it is not erased. Then $P_{s,r}$ can be written as

$$P_{s,r} = 1 - \alpha(m, 0).$$

Thus the codeword error probability is given by

$$\begin{aligned} P_{cdwd} &= 1 - \sum_{e=0}^{N_o - K_o} \binom{N_o}{e} P_{hit}^{e} (1 - P_{hit})^{N_o - e} \\ &\times \sum_{t=0}^{\lfloor \frac{N_o - K_o - t}{2} \rfloor} \binom{N_o - e}{t} P_{s,r}^{t} (1 - P_{s,r})^{N_o - e - t}. \end{aligned}$$

5.7 Numerical Results

In this section we give numerical results for a slow frequency-hop multiple-access system utilizing the concatenated coding technique presented in this paper. We use a (63,45) BCH code as our inner code and (32,14) extended RS code as our outer code. There are nine RS codewords per packet (L=9). The (63,45) BCH code has a minimum distance of 8 and hence, any error pattern with less than or equal to e errors may be corrected and any error pattern with less than or equal to f errors can be detected as long as $e + f < 8$ ($f \geq e$). Also the weight distribution of this code is completely known [Cla 81]. For the same overall rate, the test pattern scheme is allowed to use 18 test bits. Following [Pur 87a], we place 9 of these at the beginning of the hop and 9 at the end. The number of frequency slots q was chosen to be 100.

The Figs. 5.4-5.8 are the plots of the bounds on the packet error probability versus the number of users in the network of the three schemes considered for different quiescent error probabilities. They demonstrate that the packet error probability of the system with perfect side-information is a tight lower bound on the packet error

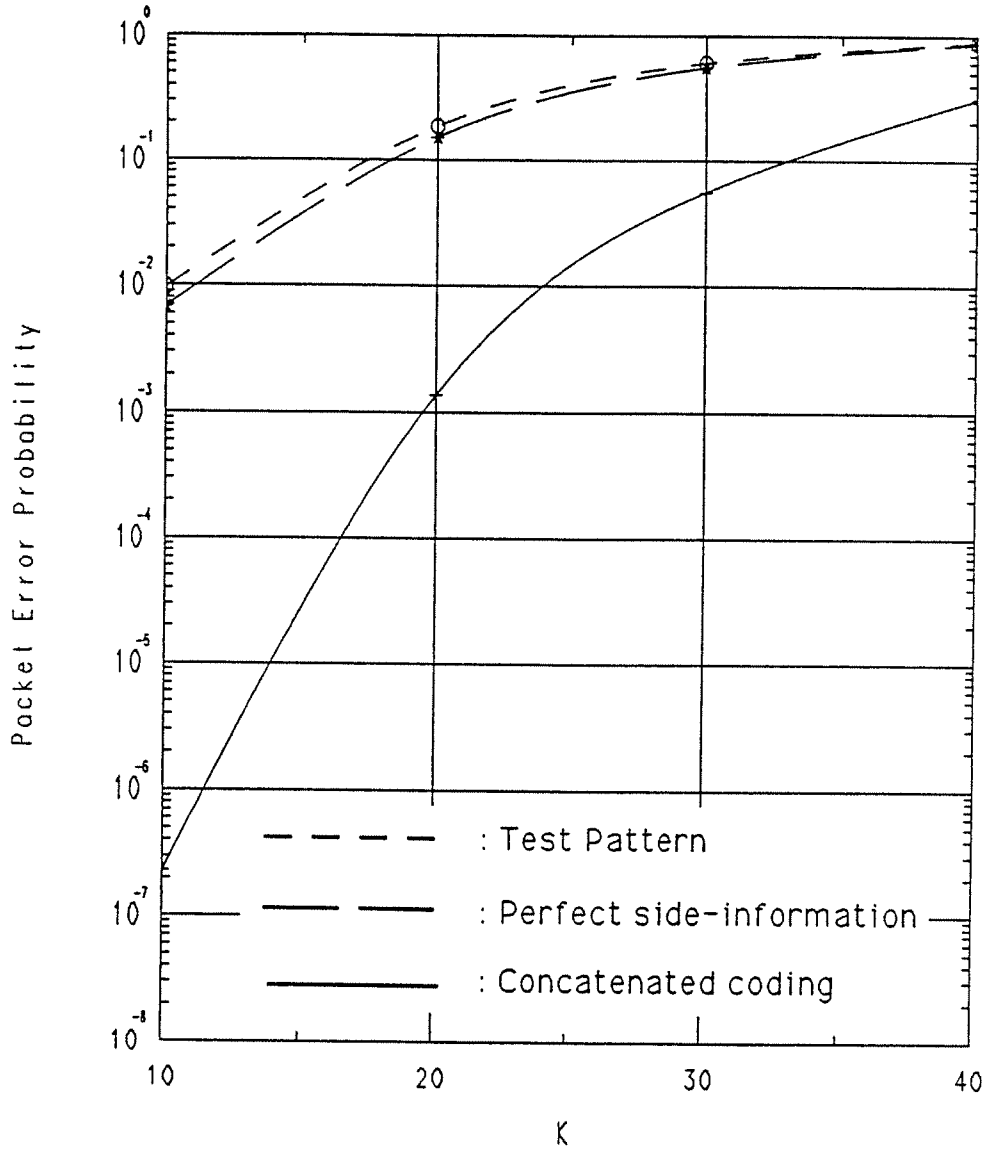

Figure 5.4: Packet error probability versus the number of users in the network. $P_0 = 10^{-2}$.

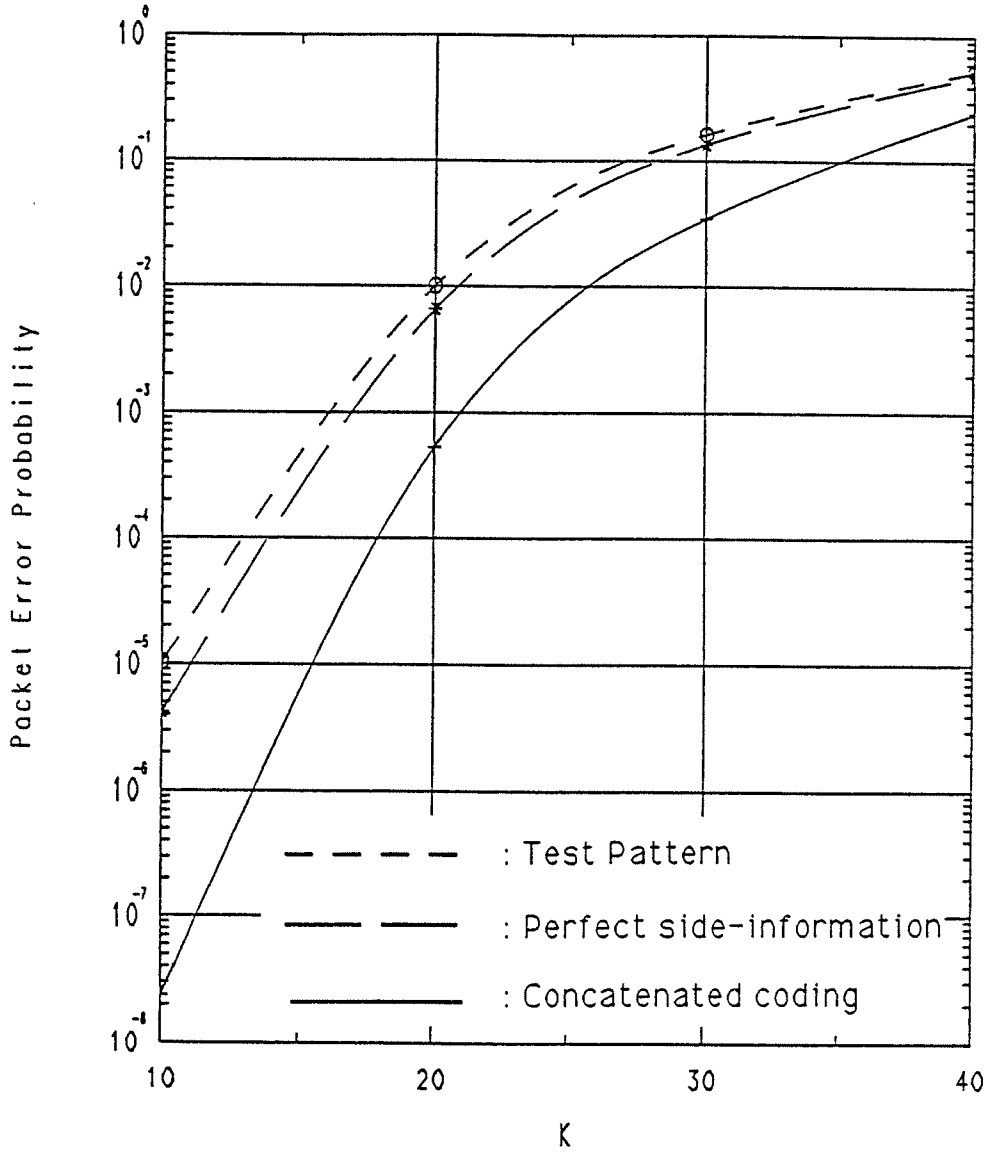

Figure 5.5: Packet error probability versus the number of users in the network. $P_0 = 10^{-3}$.

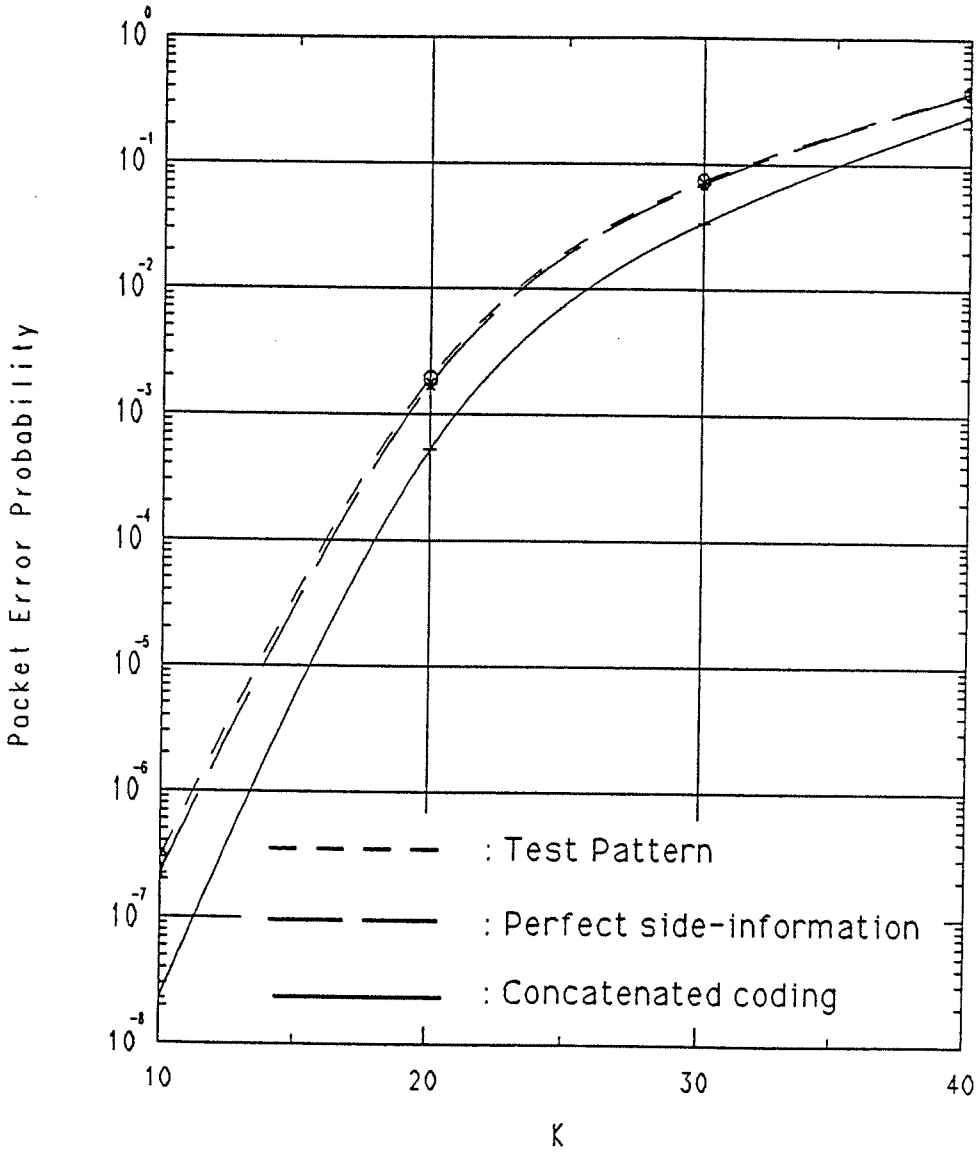

Figure 5.6: Packet error probability versus the number of users in the network. $P_0 = 10^{-4}$.

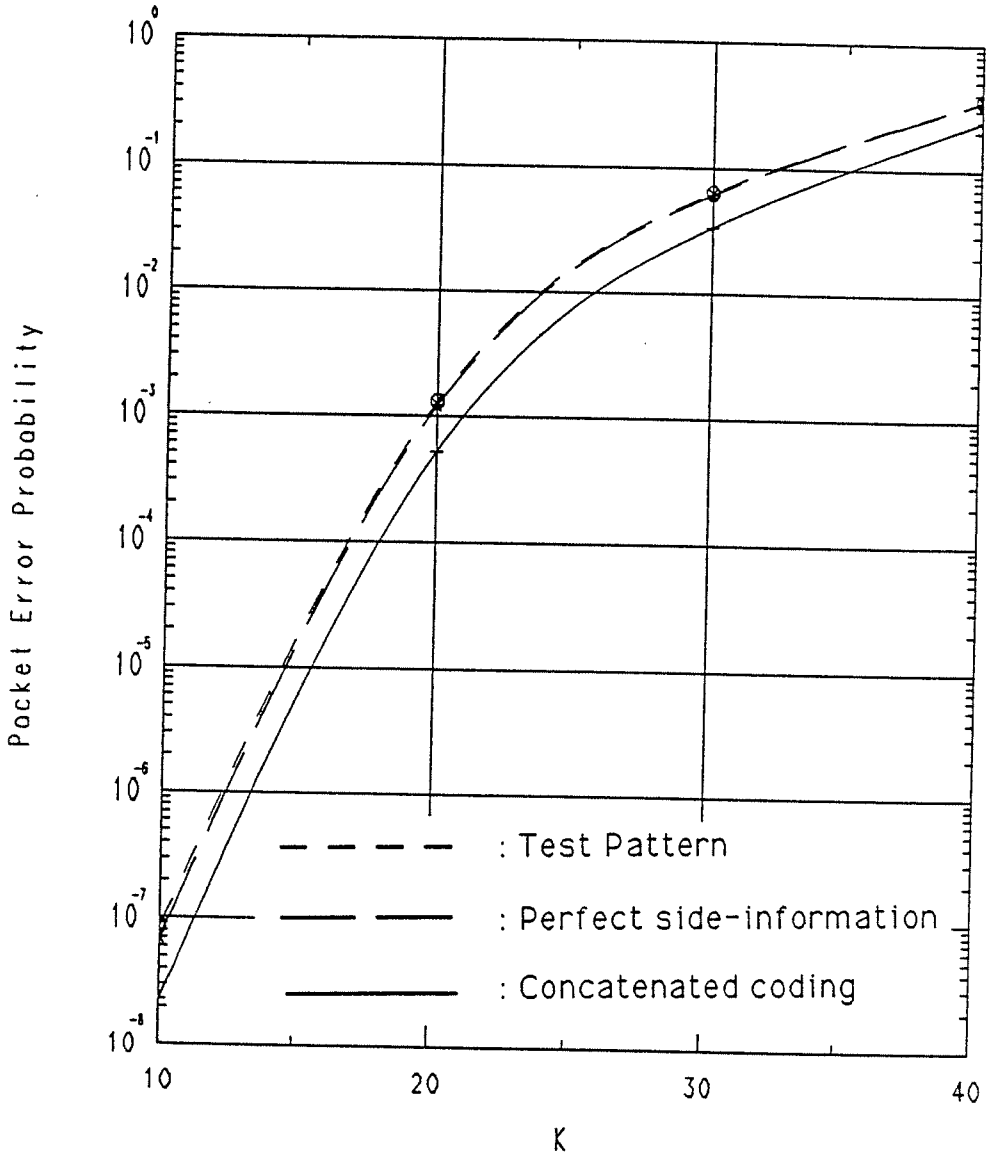

Figure 5.7: Packet error probability versus the number of users in the network. $P_0 = 10^{-5}$.

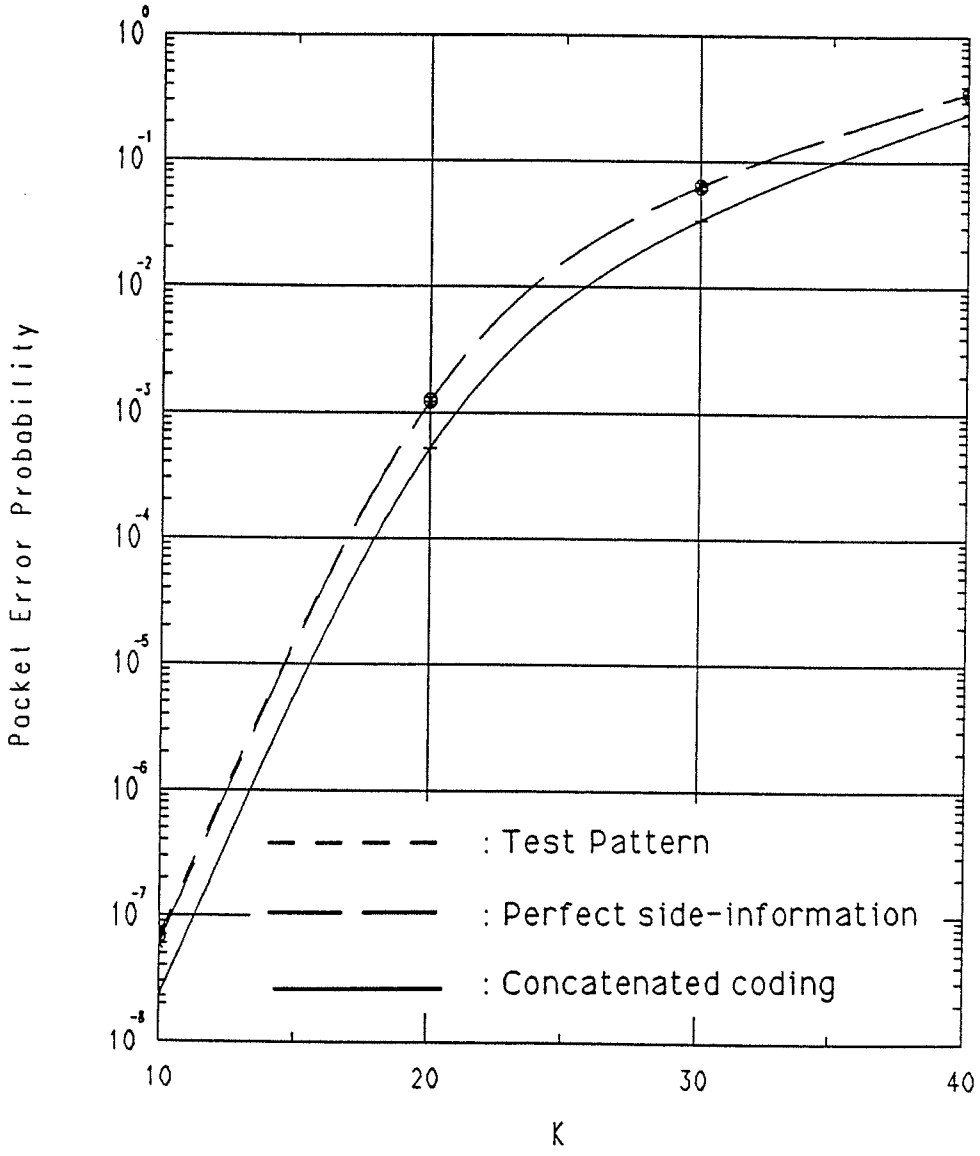

Figure 5.8: Packet error probability versus the number of users in the network. $P_0 = 10^{-6}$.

probability of the system employing the test pattern scheme. This shows that for the chosen parameters, the test pattern is performing up to its expectations, providing reliable side-information to the RS decoder. Figs. 5.4-5.5 show the improvement we get over other schemes by using an error correcting/detecting inner code. For $P_0 = 10^{-2}$ which corresponds to the overall signal-to-noise ratio of 13.99 dB with BFSK and noncoherent demodulation, the gain is over four orders of magnitude for $K = 10$ and one order of magnitude for $K = 30$. For $P_0 = 10^{-3}$ (overall signal-to-noise ratio=16.00 dB) the gains are reduced to approximately two orders of magnitude for $K = 10$ and 3.5 for $K = 30$ respectively which is still a considerable improvement. The gain we see at this range is mostly due to the inner code's ability to correct the errors caused by AWGN. For $P_0 \leq 10^{-5}$, the packet error probability is dominated by multiple-access interference and the error probabilities have stabilized with respect to P_0. The gain at these values of P_0 is the gain due to the inner code's ability to correct the errors caused mainly by multiple-access interference. This in a sense reduces the probability of hit since a multiple-access hit which results in less than t errors will be received error free (ignoring the background noise). Figs. 5.9-5.11 are the same plots with the different schemes as the parameter. These set of figures allows us to compare the immunity of the schemes against thermal noise. Fig. 5.9 shows that this concatenated coding scheme is quite impervious to the background noise. The plots have converged for $P_0 \leq 10^{-3}$. In contrast, Figs. 5.10-5.11 show that the performance of other schemes are quiet dependent on the background noise unless it is almost negligible ($P_0 \leq 10^{-5}$). The optimal value of t, the number of errors corrected by the inner code was fixed at 2 for all the cases considered. The optimal erasure threshold for the test pattern scheme varied as a function of the background noise and the number of users in the network for

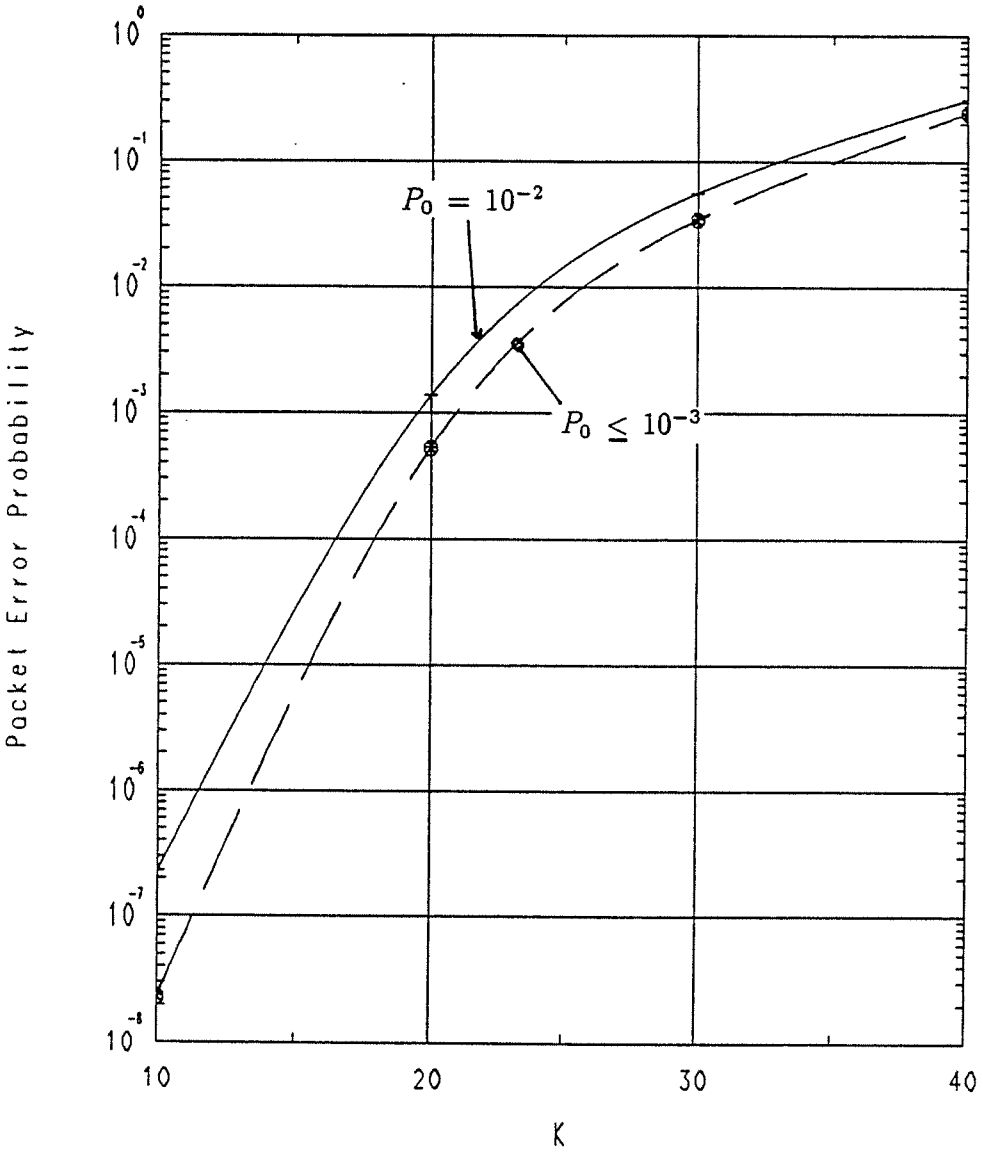

Figure 5.9: Packet error probability *vs* the number of users in the network. Concatenated coding scheme.

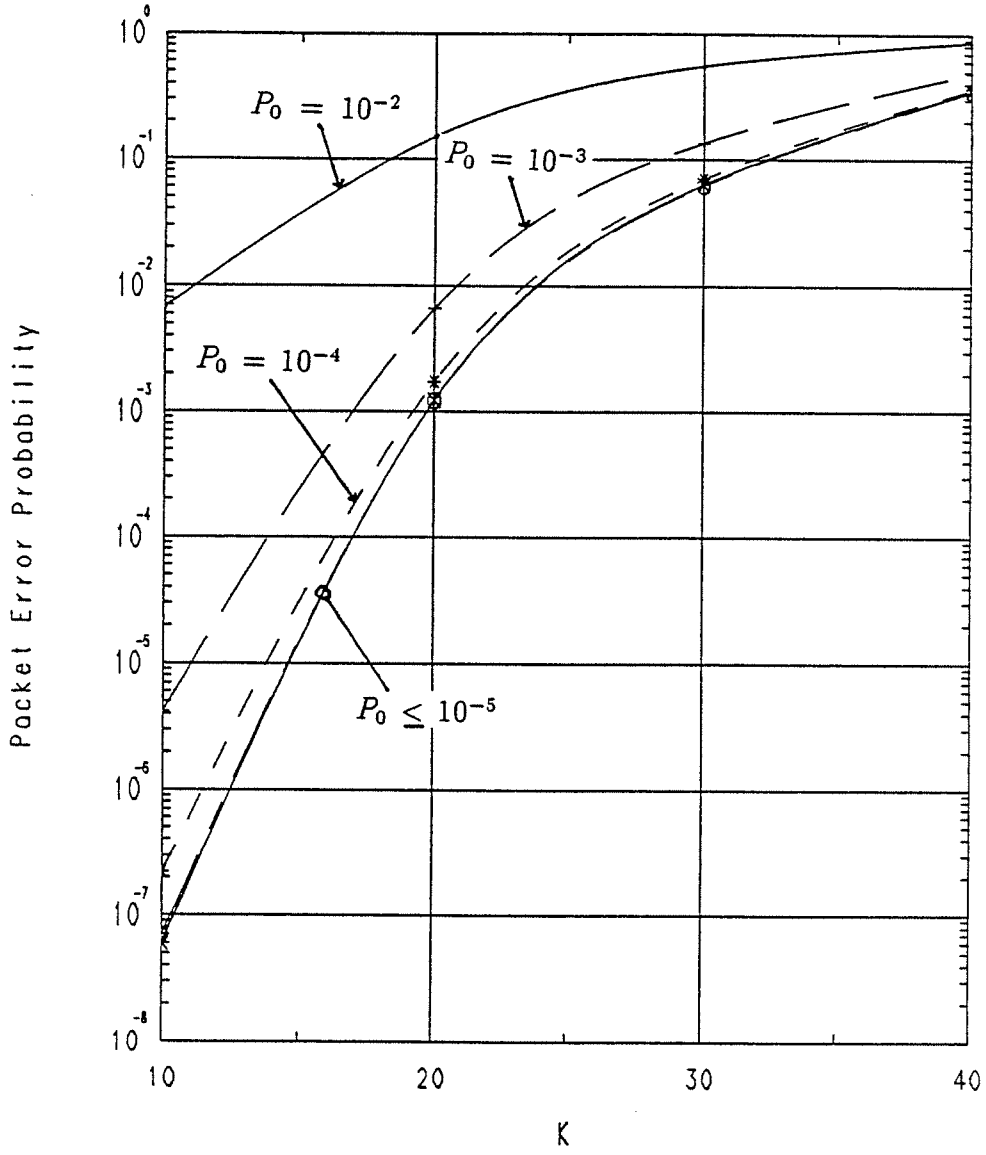

Figure 5.10: Packet error probability *vs* the number of users in the network. Perfect side-information.

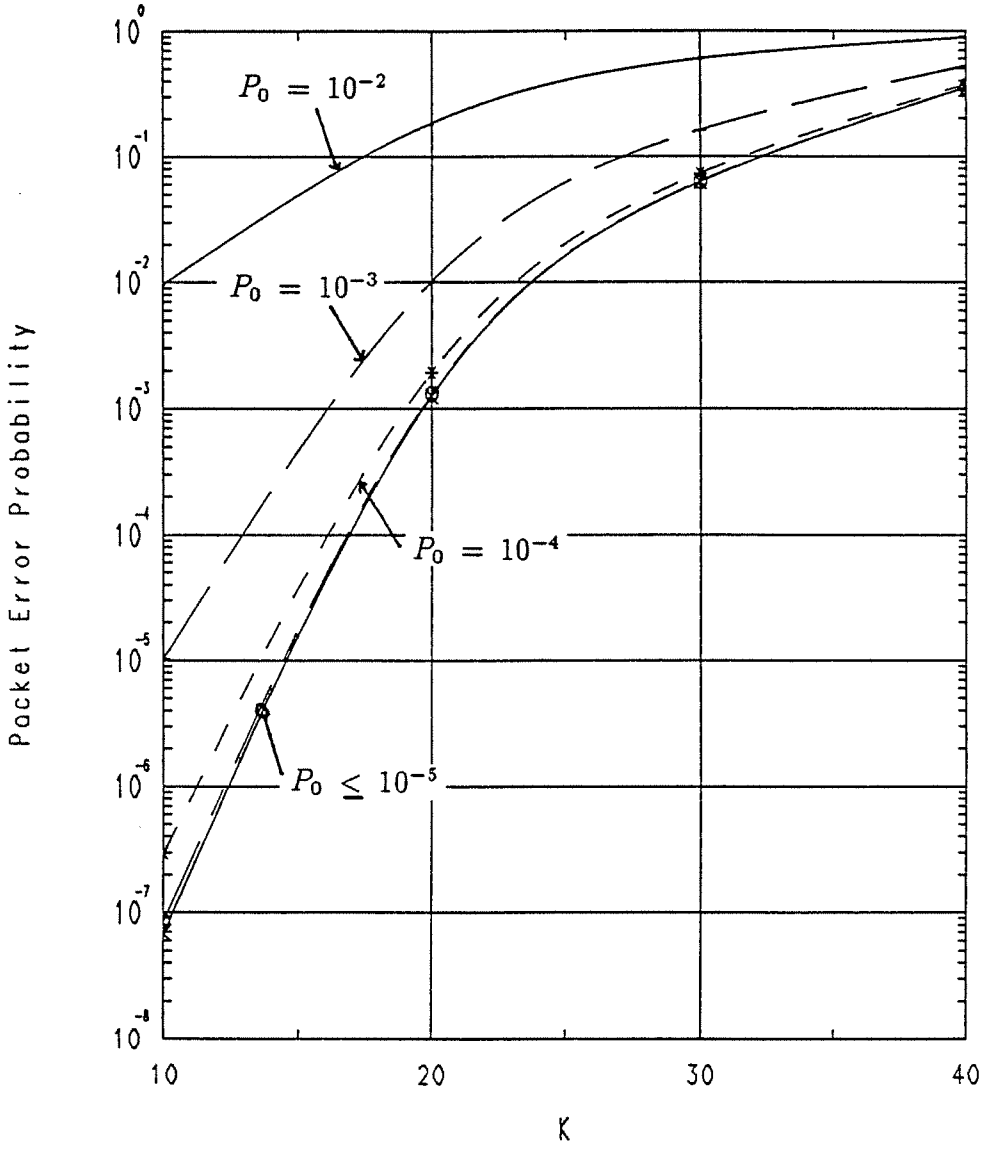

Figure 5.11: Packet error probability *vs* the number of users in the network. Test pattern scheme.

$P_0 \geq 10^{-3}$. For $P_0 \leq 10^{-4}$ the optimal threshold was fixed at zero. Figs. 5.12-5.16 are the plots of the unnormalized throughput W defined by $W = P_c \cdot K$ for different background noise levels. Here P_c is the probability that a packet is received correctly and K is the total number of users in the network. Observations similar to the packet error probabilities can be made for these figures. For $P_0 = 10^{-2}$ there is approximately a 65% increase in the maximum throughput. This reduces to approximately a 18% increase as P_0 decreases. Finally, Figs. 5.17-5.18 show the upper bounds on the packet error probability of the concatenated coding scheme and the perfect side-information case when the channel is corrupted by Rayleigh fading. The figures are for signal-to-noise ratios corresponding to quiescent error probabilities of 10^{-5} and 10^{-6} when there is no fading. These values correspond to error probabilities of 4.23×10^{-2} and 3.54×10^{-2} respectively with fading. These figures show that the concatenated coding scheme performs quiet well in channels with Rayleigh fading.

5.8 Conclusions

In this chapter we presented a new method for obtaining reliable side-information for slow AFHSS-MA networks. With an appropriate choice of parameters, this method not only provides reliable side-information to the outer decoder but also corrects a large portion of the quiescent errors and some due to multiple-access interference. The proposed scheme works particularly well in noisy situations ($P_e > 10^{-3}$), performing orders of magnitude better than the test pattern or the perfect side-information scheme.

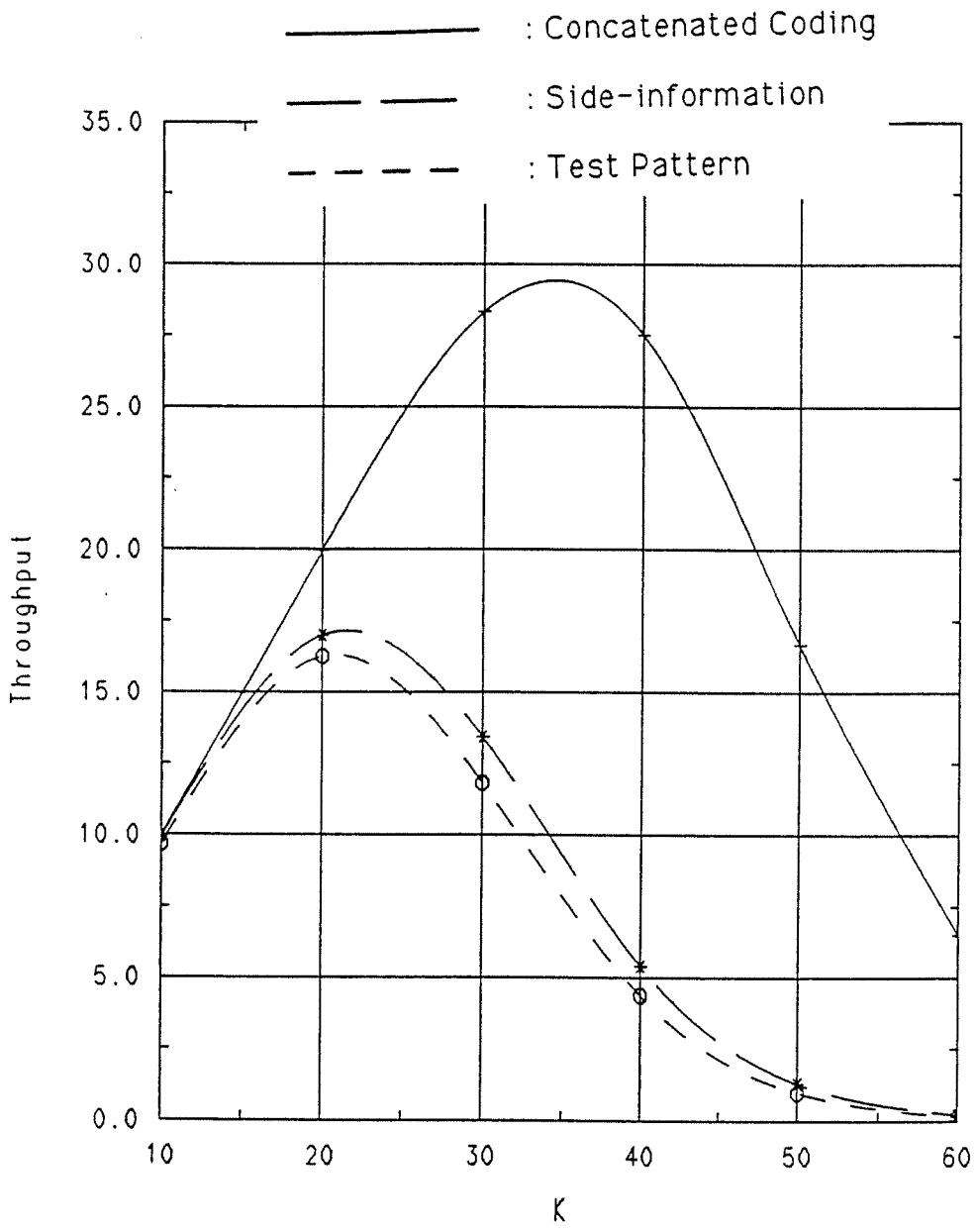

Figure 5.12: Unnormalized throughput *vs* the number of users in the network. $P_0 = 10^{-2}$.

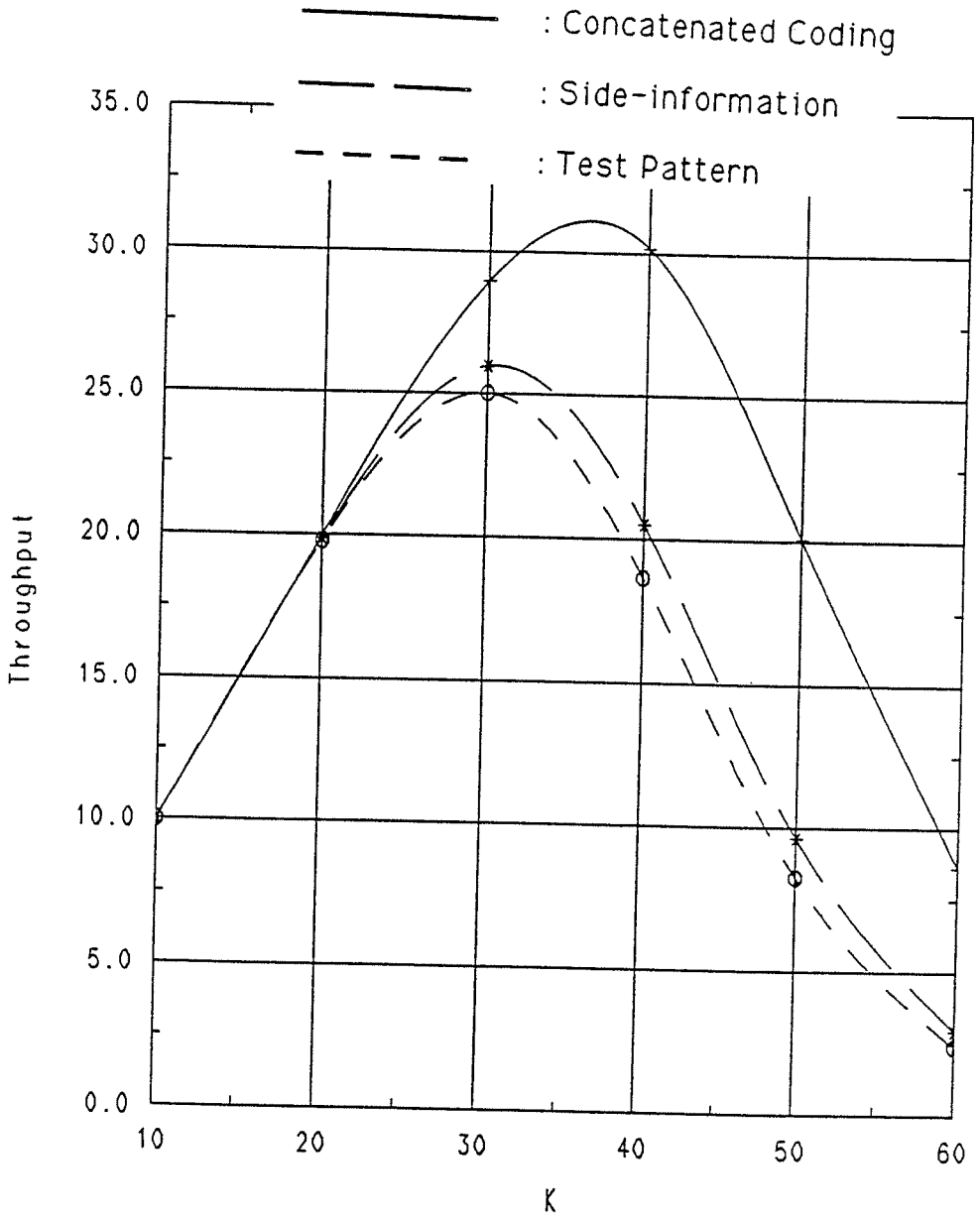

Figure 5.13: Unnormalized throughput *vs* the number of users in the network. $P_0 = 10^{-3}$.

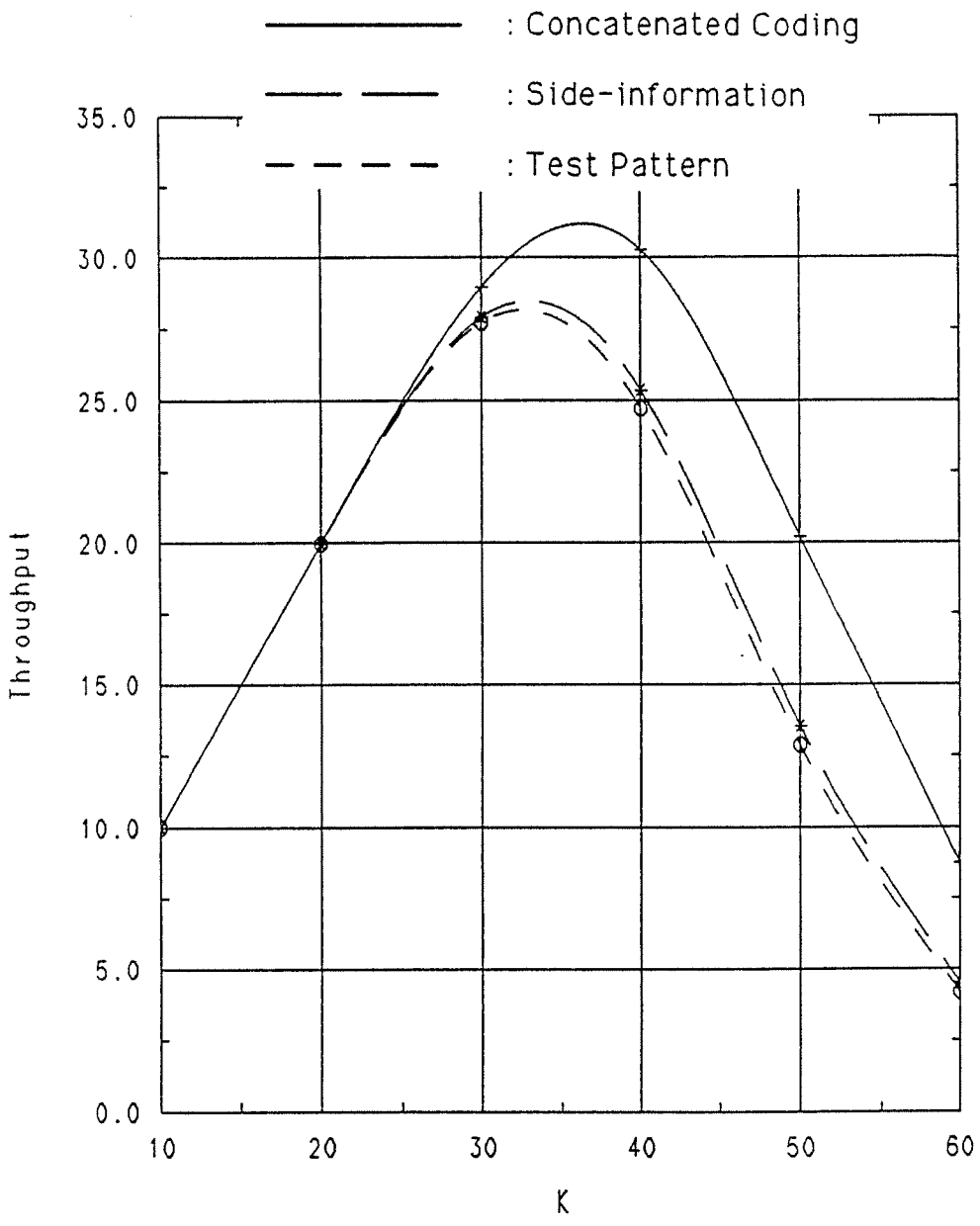

Figure 5.14: Unnormalized throughput *vs* the number of users in the network. $P_0 = 10^{-4}$.

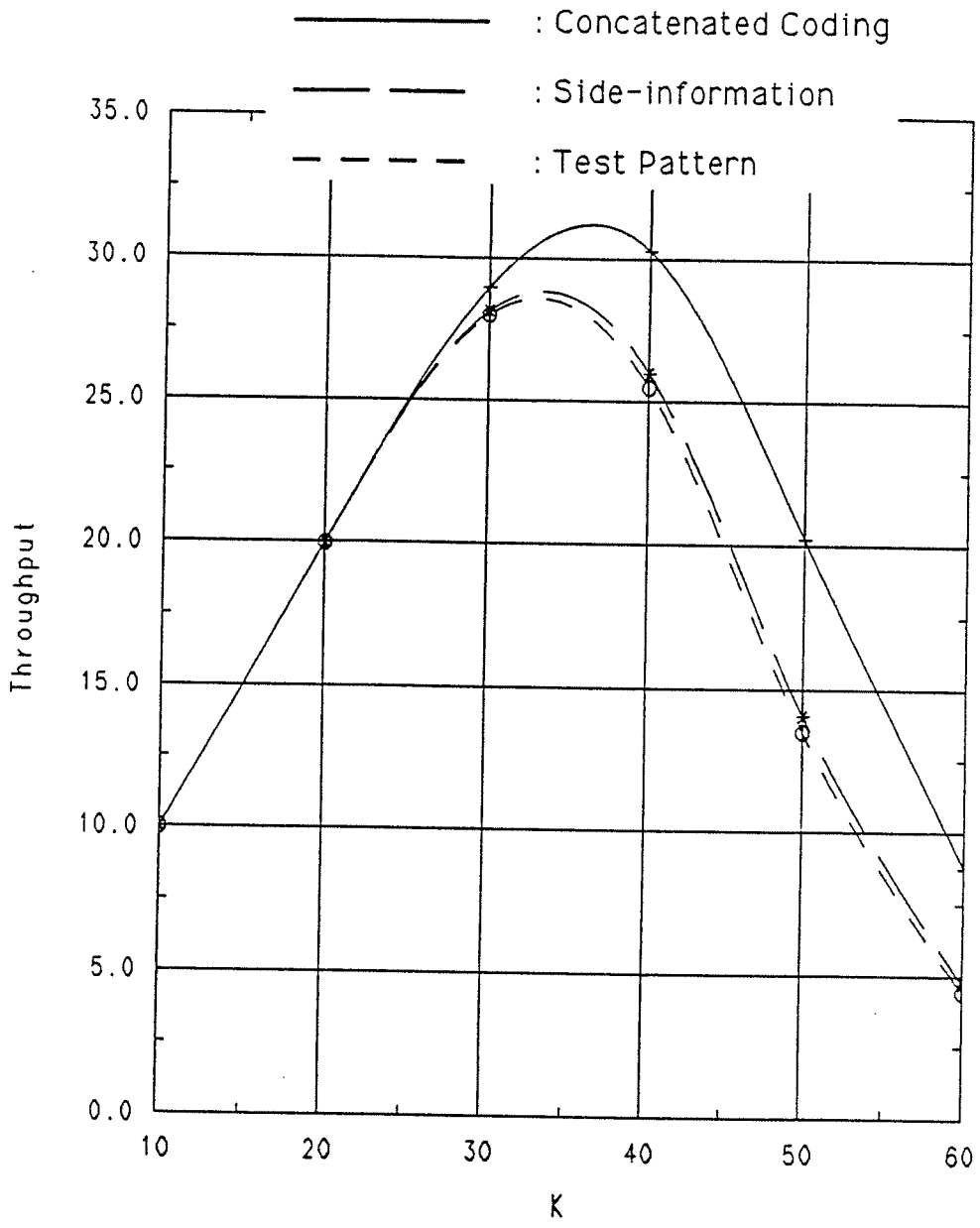

Figure 5.15: Unnormalized throughput *vs* the number of users in the network. $P_0 = 10^{-5}$.

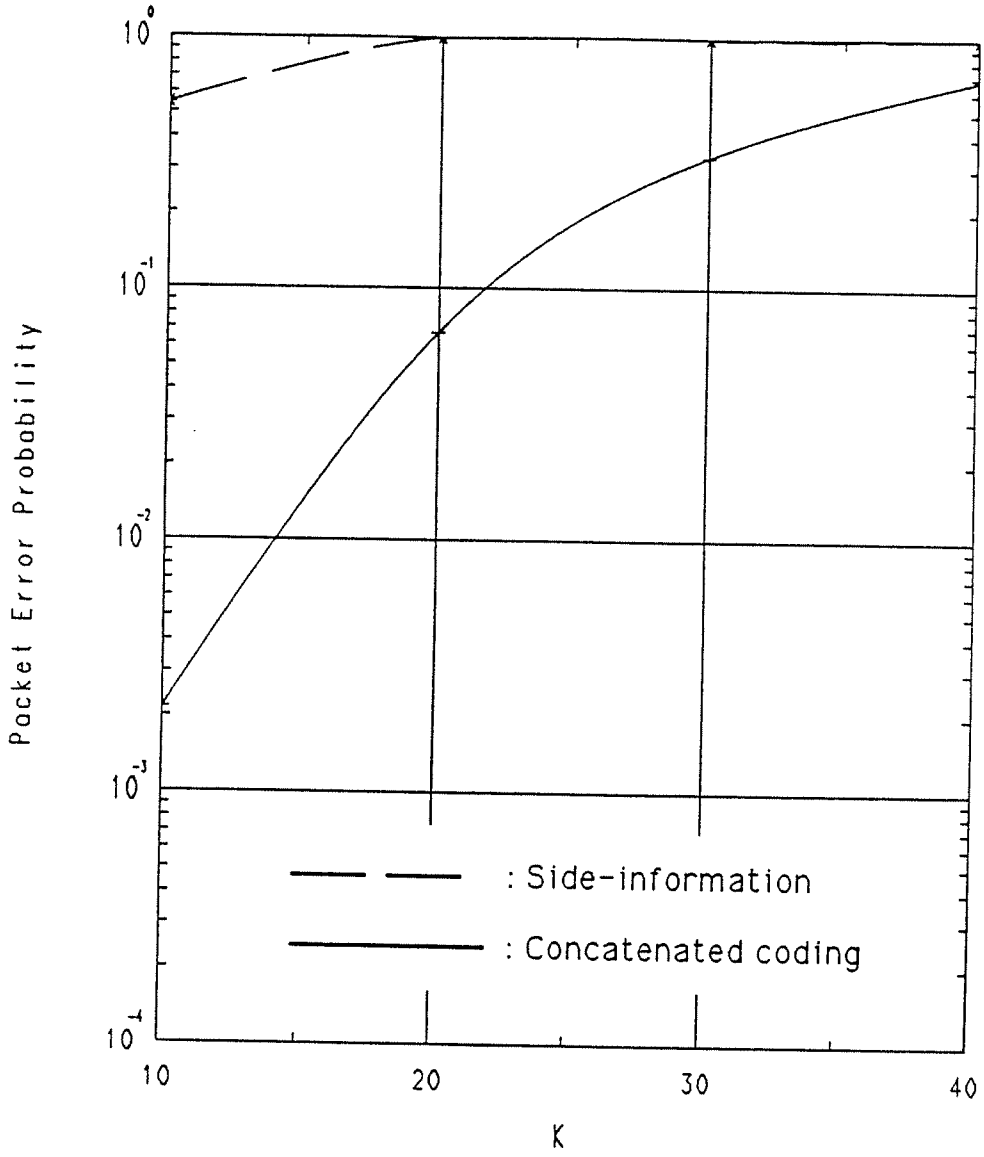

Figure 5.16: Packet error probability *vs* the number of users in the network with Rayleigh fading. $P_0 = 10^{-5}$.

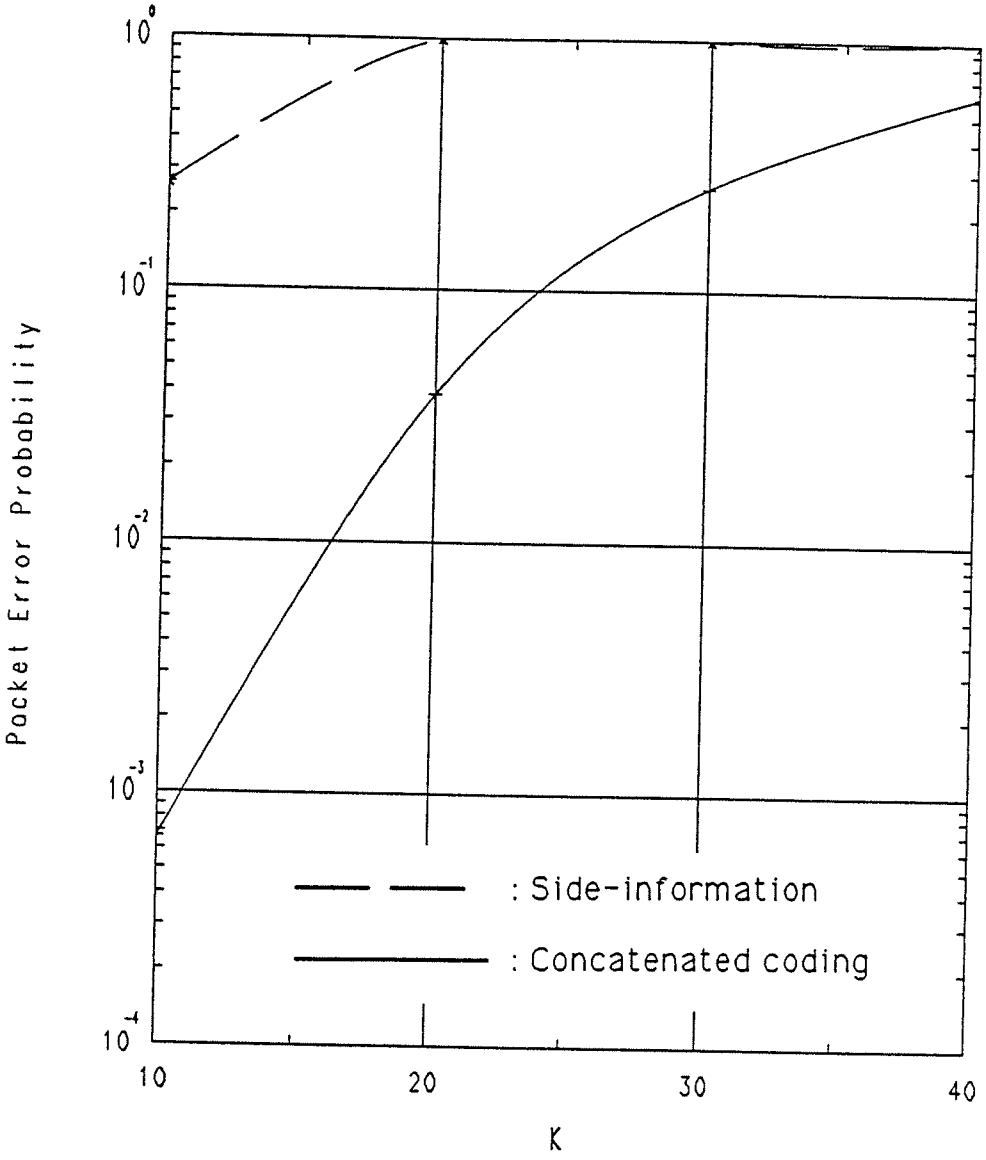

Figure 5.17: Packet error probability *vs* the number of users in the network with Rayleigh fading. $P_0 = 10^{-6}$.

CHAPTER VI

CONCLUSIONS AND EXTENTIONS

In this chapter, we will summarize the results obtained in this thesis on Asynchronous Frequency-Hop Spread-Spectrum Multiple-Access (AFHSS-MA) networks. We will also remark on generalizations and extentions on these results.

6.1 Conclusions

The first problem considered in this thesis is that of deriving an analytical expression for the probability of error in an AFHSS-MA network transmitting one Binary Frequency Keying (BFSK) modulated bit per hop. In most of the previous investigations, the probability of error whenever a hop is hit by multiple-access interference was assumed to be $\frac{1}{2}$ (the $\frac{1}{2}$-approximation.) In this thesis, we used the theory of spherically symmetric random vectors to derive an analytical expression for this probability when Markov hopping patterns are used. This expression is exact when standard orthogonal BFSK is employed and is an approximation when nonorthogonal BFSK is employed.

The fact that we assumed Markov hopping patterns greatly simplified the analysis and also the numerical computation. We showed that the numerical complexity is dominated by the computation of two expectations which are not a function of

the number of interfering users. Hence, once these expectations are computed, the computation of the probability of error for different number of interfering users can be done very easily.

We also showed that for practical values of the number of slots available in the network (q), the probability of error when independent hopping patterns are assumed can be accurately approximated by the probability of error when Markov hopping patterns are assumed.

The probability of error computed using the expressions developed in this thesis showed that the $\frac{1}{2}$-approximation is an excessively pessimistic assumption and thus analyses based on this assumption grossly underestimate the multiple-access capability of AFHSS-MA networks transmitting one bit per hop. It is also shown that the $\frac{1}{2}$-approximation has lead to misleading results. For example, it was previously believed that using perfect side-information to erase the hops that were hit by multiple-access interference leads to large improvements in performance over simple hard decisions. We showed that this is not the case. In fact, it turns out that a system employing simple hard decisions without side-information performs much better than a system using perfect side-information to erase the hops that were hit. This is a result of the fact that the probability of error when a hop is hit is, on the average, much smaller than $\frac{1}{2}$ and if all the hops that are hit are erased, many hops that could have been correctly demodulated would be discarded.

The expression developed for the probability of error also allowed us to consider the effects of different power levels of different users (near-far problem). Consideration of different power levels in the network is shown to an important issue.

The second problem considered in this thesis is the use of Viterbi Ratio Thresholding (VRT) in AFHSS-MA networks. The same technique used to derive the prob-

ability of error is used to derive the channel statistics when VRT is used. The Viterbi ratio thresholding is shown to offers significant improvements over hard decision at a small increase in system complexity. We also considered the use of binary convolutional codes with VRT in AFHSS-MA networks. It is shown that the usual bounds on the first event error probability and the packet error probability are very loose in the regions of interest and that simulations should be carried out to accurately estimate the performance of systems where convolutional coding is used.

The last problem considered is concerned with slow AFHSS-MA networks where $n > 1$ bits are transmitted per hop. The usual assumption is that whenever a hop is hit, all the symbols transmitted in that hop are hit. Here, we derived the probability that exactly l bits out of the n bits transmitted in a hop is hit given that a hop is hit by multiple-access interference. This is a very general result and can be used with various error models. We also propose a concatenated coding system with Reed-Solomon outer codes and binary (BCH) inner codes. The basic idea here is to encode the n bits transmitted in a hop with a BCH code to correct a small number of errors and detect a hit when the number of errors exceed a predetermined value. We showed that this scheme performs very well, especially when the signal-to-noise ratio is small or when there is fading in the channel.

6.2 Extentions

In this section, we discuss how the results obtained in this thesis can be extended. Also, we will look at other applications where the techniques developed in this thesis can be used.

In this thesis, we developed an expression for the bit error probability for an AFHSS-MA network where one binary symbol is transmitted per hop. It would be

both interesting and practically useful to extend this result to the case when one M-ary ($M > 2$) symbol is transmitted per hop. This would allow us to consider the performance of the popular Reed-Solomon codes. It is also probably not too difficult to extend the results to the case when there is Rayleigh fading in the channel.

The technique developed in this thesis can be applied to various other scenarios outside the spread-spectrum multiple-access field. For example it could be used to analyze the performance of a communications system under multi-component multipath. It could also be used to analyze the performance of spread-spectrum communications system under tone-jamming where the jammer has only a fuzzy knowledge of the band structure or the timing of the communications system.

In general the techniques developed in this thesis could find many applications in the analyses of communications systems when there is interference in the form of random tones.

BIBLIOGRAPHY

BIBLIOGRAPHY

[Abr 72] M. Abramowitz and I.A. Stegun, *Handbook of Mathematical Functions.* Dover Press. 1972.

[Bla 83] R.E. Blahut, *Theory and Practice of Error Control Coding*, Addison-Wesley, 1983.

[Bir 85] J.S. Bird, "Error performance of binary NCFSK in the presence of multiple tone interference and system noise," *IEEE Transactions on Communications,* Vol. COM-33, pp. 203-209, Mar. 1985.

[Che 88a] K. Cheun and W. Stark, "Performance of convolutional codes with diversity under worst case partial-band noise jamming," *Proceedings of the 1988 International Conference on Communications*

[Che 88b] K. Cheun and W.E. Stark, "Performance of convolutional codes with diversity under worst case partial-band noise jamming," *Proceedings of the IEEE International Conference on Communications 1988.*

[Cla 81] G.C. Clark JR. and J.B. Cain, *Error-Correcting Codes for Digital Communications*, Plenum Press, 1981.

[For 73] G.D. Forney, "The Viterbi Algorithm," *Proceeding of the IEEE,* vol. 61, pp.268-278, Mar. 1973.

[For 77] G.D. Forney *Concatenated Codes*, MIT research monograph No. 37, The MIT Press, Cambridge, Mass. 1966.

[Gal 68] R.G. Gallager, *Information Theory and Reliable Communications,* John Wiely & Sons, Inc.

[Ger 85] E.A. Geraniotis "Coherent hybrid DS-SFH spread-spectrum multiple-access communications," *IEEE Transactions on Communications,* Vol. SAC-3, pp. 695-705, Sept. 1985.

[Ger 82] E.A. Geraniotis and M.B. Pursley, "Error probabilities for slow-frequency-hop spread-spectrum multiple-access communications over fading channels," *IEEE Trans. Commun.*, vol. COM-30, pp.996-1009, May 1982.

[Ger 86b] E.A. Geraniotis, "Noncoherent hybrid DS/SFH spread-spectrum multiple-access communications," *IEEE Transactions on Communications*, vol. COM-34, pp.862-872, Sept. 1986.

[Ger 87] E.A. Geraniotis, "Coded FH/SS communications in the presence of combined partial-band noise jamming, Rician nonselective fading, and multiuser interference," *IEEE Journal on Selected Areas in Communications,* vol. SAC-5, No.2, pp.194-214, Feb. 1987.

[Ger 88] E.A. Geraniotis, "Frequency-hopped spread-spectrum systems have a larger multiple-access capability: The effect of unequal power levels," *Proceedings of the 1988 Conference on Information Sciences and Systems.*

[Has 88] A.A. Hassan, *Algorithms for Decoding Block Codes,* Ph.d. Thesis. University of Michigan, Ann Arbor. 1988.

[Heg 85] M. Hegde and W.E. Stark, "Multiple-access capability of frequecy hop spread-spectrum communications," *MILCOM '85 Conference Record,* pp.575-579.

[Heg 88] M. Hegde and W.E. Stark, "On the error probability of coded frequency-hopped spread-spectrum multiple-access systems," submitted to *IEEE Transactions on Communications.*

[Jah 45] E. Jahnke and F. Emde, *Tables of Functions with Formulae and Curves,* 4th ed. New York.

[Kel 88] C.M. Keller, "An exact analysis of hits in frequency-hopped spread-spectrum multiple-access communications," *Proceedings of the 1988 Conference on Information Sciences and Systems.*

[Kim 87] S. Kim, *Coding for spread-spectrum communication networks*, Ph.D. thesis, University of Michigan, Ann Arbor, 1987.

[Kim 89] S. Kim and W. Stark, "Optimum rate Reed-Solomon codes for frequency-hop spread-spectrum multiple-access communication system," *IEEE Transactions on Communications*, vol. COM-37, pp.138-144, Feb. 1989.

[Kuo 72] S. Kuo, *Computer Applications of Numerical Methods*, Addison Wesley, 1972.

[Lor 54] R.D. Lord, "The use of Hankel transforms in statistics," *Biometrika,* Vol. 41, pp. 44-45, 1954.

[Mad 88] U. Madhow and M.B. Pursley, "Limiting performance of frequency-hop random access," *Abstracts of Papers,* 1988 International Symposium on Information Theory. Kobe Japan. pp. 43

[Mce 84] R. McEliece and W. Stark, "Channels with blockj interference," *IEEE Transactions on Information Theory*, vol. IT-30, pp.44-53, Jan. 1984.

[Pro 83] J.G. Proakis, *Digital Communications,* McGraw-Hill, 1983.

[Pur 81] M.B. Pursley, "Spread-spectrum multiple-access communications," in *Multi-User Communication Systems,* G. Longo (editor), Springer-Verlag, Vienna and New York, pp.139-199, 1981.

[Pur 85] M.B. Pursley and D.J. Taipale, "Error probabilities for spread-spectrum packjet radio with convolutional codes with Viterbi decoding," IEEE Transactions on Communications, vol COM-35, No.1, pp.1-12, Jan, 1987.

[Pur 86] M.B. Pursley, "Frequency-hop transmission for satellite packet switching and terrestrial packet radio networks," *IEEE Transactions on Information Theory*, vol. IT-32, pp.652-667, Sept. 1986.

[Pur 87a] M.B. Pursley, "Tradeoffs between side information and code-rate in slow-frequency-hop packet radio networks," *Conference Record, IEEE International Conference on Communications*, June 1987.

[Pur 87b] M.B. Pursley, "The role of spread-spectrum in packet radio networks," *Proceedings of the IEEE,* vol.75, No.1, pp.116-134, Jan. 1987.

[Ray 81] D. Raychauduri, "Performance analysis of random access packet switched code division multiple access systems," IEEE Transactions on Communications, vol COM-29, No.6, pp.895-901, June, 1981.

[Sch 77] R.A. Scholtz, "The spread spectrum concept," *IEEE Transactions on Communications*, vol. COM-25, pp.748-755, Aug. 1977.

[Sim 85] M.K. Simon, J.K. Omura, R.A. Scholts and B.K. Levitt, *Spread spectrum communications Volume I, II, III*, Computer Science Press, 1985.

[Sho 88] R.T. Short and C.K. Rushforth, "Probability of error for noncoherent frequency-hop spread-spectrum multiple-access communications," submitted to *IEEE Transactions on Communications,*

[Vit 71] A.J. Viterbi, "Convolutional codes and their performance in communication systems," *IEEE Transactions on Communications,* vol COM-19, No.5, pp.751-772, Oct, 1971.

[Vit 79a] A.J. Viterbi and J.K. Omura, *Princeples of Digital Communications and Coding,* McGraw-Hill, Inc.

[Vit 79b] A.J. Viterbi, "Spread spectrum communications - myths and realities," *IEEE Communications Magazine,* pp.11-18, May, 1979.

[Vit 82] A.J. Viterbi, "A robust ratio-threshold technique to mitigate tone and partial-band jamming in coded MFSK systems," *MILCOM '82 Conference Record,* 1982

[Vit 85] A.J. Viterbi, "Robust decoding of jammed frequency hopped modulations," M/A-COM. INC. Mar. 1985.

[Wie 86] J.E. Wieselthier and A. Ephremides, "A distributed reservation-based CDMA protocol that does not require feedback information," *1986 IEEE International Symposium on Information Theory*, Ann Arbor, MI, Oct. 1986.